New considerations in predicting toxicity from partial irradiation of the lung

Nováková, Alena

NEW CONSIDERATIONS IN PREDICTING TOXICITY FROM PARTIAL IRRADIATION OF THE LUNG

ALENA NOVÁKOVÁ

NEW CONSIDERATIONS IN PREDICTING TOXICITY FROM PARTIAL IRRADIATION OF THE LUNG

ALENA NOVÁKOVÁ

STELLINGEN

behorende bij het proefschrift:

New considerations in predicting toxicity from partial irradiation of the lung

Alena Nováková

1. The risk of post-irradiation normal tissue toxicity is generally underestimated due to the lack of comprehensive accounting for multi-organ damage involving both lung and heart. Joint consideration of subclinical injury to both organs is necessary for an accurate prediction of acute and late respiratory complications after high-dose thoracic radiotherapy *(Holloway et al, 2004; this thesis)*.

2. Cardiotoxic effects of radiotherapy in lung cancer patients are currently obscured by comorbidities and competing risks. As the treatment of lung cancer improves, subclinical cardiac injury will acquire clinical relevance *(Prosnitz et al, 2005)*.

3. The syndrome of early radiation pneumonitis is not a single pathogenic unit. Instead, it consists of two distinct processes within lung tissue, the *vascular damage* and the *parenchymal inflammation* that have different dose thresholds and inverse outcomes in terms of late sequelae *(This thesis)*.

4. The pulmonary *vascular damage* occurring in low dose range will lead to serious hemodynamic consequences if spread over a large volume *(This thesis)*. It well explains the surprising observations of the strongest correlations between early pneumonitis and DVH parameters of lung volumes irradiated to very low total doses (V_{5-13}) *(Seppenwoolde et al, 2003; Yorke et al, 2005; Wang et al, 2006)*.

5. Intensity-modulated radiation therapy (IMRT) for lung cancer tends to deliver low yet damaging doses to larger volumes of normal lung. Proton treatment therefore is a better choice where high doses are needed for control of tumors surrounded by such critical organs and tissues.

6. Cancer research is a great thing, but in terms of numbers of saved lives, dedicating these financial resources to basic treatments and food in the developing world would be more efficient.

7. In work with experimental animals, besides anesthesia during procedures, more thought should be given to long-term analgesia afterwards.

8. One should never take for granted what has not been reproduced.

9. Mankind used its intellect to break free from regulatory principles of nature, and then was taken over by greed. Greed and overpopulation are at the core of today's global problems.

10. The gods had thought with some reason that there is no more dreadful punishment than futile and hopeless labor. But the struggle itself toward the heights is enough to fill a man's heart *(Albert Camus: The Myth of Sisyphus)*.

ISBN 978-90-367-3868-2
Printed by Drukkerij van Denderen B.V., Groningen, the Netherlands

The research presented in this thesis was conducted at the Department of Cell Biology, Section Radiation and Stress Cell Biology, University Medical Center Groningen (UMCG), University of Groningen (RUG), the Netherlands.

This research was financially supported by the Interuniversitary Institute for Radiopathology and Radiation Protection (IRS grant # 9.0.18) and by the Dutch Cancer Society (grant # RuG 2002-2673).

The publication of this thesis was financially supported by:
The Groningen University Institute for Drug Exploration (GUIDE), The Netherlands

CMB.

RIJKSUNIVERSITEIT GRONINGEN

NEW CONSIDERATIONS IN PREDICTING TOXICITY FROM PARTIAL IRRADIATION OF THE LUNG

Proefschrift

ter verkrijging van het doctoraat in de
Medische Wetenschappen
aan de Rijksuniversiteit Groningen
op gezag van de
Rector Magnificus, dr. F. Zwarts,
in het openbaar te verdedigen op
maandag 15 juni 2009
om 13.15 uur

door

Alena Nováková

geboren op 4 juni 1969
te Praag, Tsjechië

Promotor:	Prof. dr. H.H. Kampinga
Copromotor:	Dr. R.P. Coppes
Beoordelingscommissie:	Prof. dr. J.A. Langendijk
	Prof. dr. A.J. van der Kogel
	Prof. dr. P. Lambin

CONTENTS

CHAPTER 1: General introduction

Thoracic tumours are among the most common human malignancies. The treatment of choice is often radiation therapy. In some tumours like breast cancer or malignant lymphoma, good therapeutic results are achieved with intermediate doses of radiation and acceptable level of complications. In non-small cell lung carcinoma (NSCLC), the most common form of lung cancer, however, treatment results have been severely compromised by the proximity of critical normal structures and, namely, the risk of radiation-induced lung injury. NSCLC cure rates achieved with the conventional radiation doses (60-66 Gy) have been disappointingly low with 3-year overall survival of 20 – 55% for early disease (148) and 2-year overall survival ≤20% for locally advanced tumours (34,140,141). Yet, already those doses have been followed by symptoms of radiation-induced lung injury necessitating treatment in up to a fifth of patients (48,79,92,98,140). It has been calculated that doses close to 100 Gy, unthinkable with conventional radiotherapy, may be required to sterilize the size of tumours frequently treated in NSCLC (43). For over a decade, approaches are being investigated to surmount this obstacle. Efforts concentrate on increasing the accuracy and precision of dose delivery by implementing new techniques, namely three-dimensional conformal radiation therapy (3D-CRT) (6,9,10,16,20,56,75,129). With its use, tumour radiation doses of up to 100 Gy have been achieved in patients with smaller target volumes yielding favourable 3-year survival rates of 47-70% (16,75,129,155). This likely represents a ceiling for dose escalation using 3-D CRT because, at this dose level, late toxicities have been observed in more radioresistant tissues than lung tissue itself (7,16,101). Dose-escalation in patients with intermediate and large tumours is more challenging due to increased risk of complications. Doses of up to 84 Gy have been delivered with acceptable toxicity and, in some instances, survival benefits (2-y overall survival rates of 25-60%) have been reported (19,75,129,155,176). Nevertheless, the majority of patients with locally advanced NSCLC still die within 5 years of diagnosis from locoregional or distant progression of the disease (115). It is hoped that more aggressive strategies like concurrent chemoradiation therapy together with more refined 3-D CRT treatment planning will

improve outcomes for these patients (153). However, enhanced toxicity is the flip side of the coin. Thus, increasing the chances of lung cancer patients for long-term, complication-free survival requires further investigation and identification of factors determining the severity and probability of treatment side-effects. This work aimed at elucidation of relationship between irradiated region, irradiated volume, elicited cytokine response and occurrence of radiation-induced lung injury in clinical and experimental setting.

1.1 Interactions of ionizing radiation with living matter and biological consequences

Ionizing radiation represents a beam of fast moving particles (*particulate* radiation) or massless quanta of energy called *photons* (*electromagnetic* radiation) (52). When this beam hits an absorber, i.e. any material including living matter, the particles or photons transfer their energy to the atoms or molecules along their track. The term "ionizing" means that individual particles or photons of the radiation beam carry sufficient energy to eject orbital electrons from the energy-absorbing atoms or molecules and change their physical and chemical properties. Such event is termed *ionization*. In case of photon radiation, most ionizations are produced by *secondary electrons* with negative charge that were set in motion by the uncharged photons.

A living cell is for 80% composed of water. Water is an important target for action of photons, electrons and protons. Hydrolysis caused by ionization of a water molecule leads to the formation of highly reactive *free radicals* (also called *reactive oxygen species*, i.e. ROS) with an unpaired orbital electron. The most reactive is hydroxyl radical •OH with a lifetime of a few nanoseconds and a diffusion distance of a few nm (71,100). If a particle track passes close, generated radicals can reach critical targets within a cell like deoxyribonucleic acid (DNA) in the nucleus or phospholipid membranes in the cytoplasm. They break chemical bonds by abstracting hydrogen from the attacked molecules leaving behind carbohydrate residue with unpaired electron (R•). This residue subsequently reacts with oxygen forming nonrestorable organic peroxide. It is estimated that two thirds of biological damage from electromagnetic radiation arise through this oxygen-dependent *indirect* process rather than from a *direct* action of ionizing particles (52).

Such disruption of chemical bonds results in structural alterations in cellular macromolecules, e.g. DNA-strand breaks (51). Classically, genetic information

carrying DNA in *stem / progenitor cells*, the cell pool responsible for tissue regeneration, has been considered the most relevant target for radiation damage (104,122). Stem cells with misrepaired DNA breaks have been assumed to die while attempting mitosis (*mitotic failure / reproductive cell death*), failing to replenish the differentiated functional cell pool. In relation to a cell-type specific turnover time, radiation injury then becomes expressed as *hypoplasia* and acute and/or chronic malfunction of a tissue system (15).

More recently, evidence has been mounting that also cytoplasmic ionization events – through activation of plasma membrane-associated enzymes (e.g. sphingomyelinases) and/or through amplification by endogenous, metabolically generated reactive oxygen and nitrogen species (ROS/RNS) – can trigger signal transduction pathways (100), alter intercellular communication and lead to cell death by *apoptosis* (*programmed interphase cell death*) (2). Beside germinal and lymphatic tissues, apoptosis is generally not considered a significant contributor to the radiation-induced reproductive death of stem cells, and hence the permanent tissue damage (22). Nevertheless, it may play a role in certain tissues, for example fine vasculature. Recently, sphingomyelinase-mediated apoptosis of endothelia in irradiated intestinal mucosa has been causally linked to microvascular injury and gastrointestinal lethality in mice (112). Although the relevance of this mechanism of cell loss for the ultimate (late) effects remains under discussion, it could explain why certain tissue systems show acute dysfunction in much shorter post-irradiation times than would be expected from the turnover time of their cell populations. For example in lung and heart, the two organs in focus of this thesis, early ultrastructural damage to cellular organelles in the capillary endothelia has long been described (1,27,30,50,90,121) and has been implicated in an increase of capillary permeability and in capillary depletion observed within few days after irradiation (37,81,82,133,162,180). This is long before the post-irradiation *mitotic failure* of endothelia would be expected to occur in these organs judging from their long turnover times ranging between 100 and 400 days (30,82,144).

Apart from lethal effects on cells, radiation acts through yet another powerful mechanism. Nuclear and cytoplasmic radiation damage rapidly triggers a cascade of molecular events that, within hours of radiation exposure, lead to changes in gene expression in affected and also surrounding cells (142,143). This process, sustained for months after completion of RT, involves production of a number of inter-cellular

mediator proteins (*cytokines*) and extracellular matrix components that participate in determining the integrated tissue response throughout the latent, acute and chronic phases of radiation injury development (11,39,136,170).

1.2 Histology of the healthy lung

Over 40 types of cell make up the lung and most of them, like the ciliated epithelium lining the airways (from *bronchi* to *respiratory bronchioles*), are relatively radioresistant (30,133). Post-irradiation changes affect mostly the distal respiratory structures extending from the respiratory bronchioles – the alveolar ducts, sacs and alveoli where the actual gas exchange of oxygen and carbon dioxide between air and blood takes place. Cells found in this region can be distinguished only by electron microscopy. Over 90% of the alveolar wall is covered by postmitotic *type I epithelial cells* (*membranous pneumocytes*) (55). Those are very thin cells bound together by tight junctions. Their function is to facilitate gas transfer and, via active sodium transport, to remove fluid from the alveolar space. Much less numerous *type II epithelial cells* (*granular pneumocytes*) occupy corners of the alveolar walls. Those are round cells containing characteristic lamellar bodies involved with production and storage of *surfactant*, a phospholipid substance that covers the inner surface of alveoli lowering surface tension and preventing alveolar collapse at the end of expiration (55,137). Type II cells divide and serve as a progenitor cell population for type I cells (30,55). Fine alveolar walls (*septa*) contain a space termed *interstitium*. Interstitium is composed of mucopolysaccharide *extracellular matrix* (ECM) with reticular, elastic, collagen and fibronectin fibers supporting a highly anastomosing network of capillaries (55,123,133). Capillary lumina are delineated by *endothelial cells* resting on the basement membrane. In healthy lung, the interstitium is very thin and inconspicuous. It is virtually absent in places where capillaries and alveoli come into a contact. Here, the basement membranes of alveolar epithelium and capillary endothelium fuse together forming a less than 1 μm thick air-blood barrier (55). The interstitium also contains scattered connective tissue cells, i.e. *fibroblasts*, responsible for secretion of ECM macromolecules as well as proteases that degrade them. Fibroblasts are normally in a quiescent state but their proliferation, maturation and synthetic activity rise following tissue injury (123,127,135). Another lung cell with proliferative capacity is the *alveolar macrophage* (31,55). Macrophages likely originate from blood monocytes and can be found in the alveoli as well as in the

interstitium. They phagocyte bacteria and dust and play an important secretory role during inflammation. Finally, out of the cells implicated in post-irradiation response, pulmonary *mast cells* are ought to be mentioned. They are common in peribronchial tissue and alveoli but are rarely seen in formalin-fixed specimens as they degranulate (55). They release hypersensitivity mediator *histamin* that has also been shown to enhance collagen synthesis (28).

1.3 Histopathology and pathophysiology of radiation-induced lung injury

Classically, radiation-induced lung injury has been divided into two clinical syndromes - an cute *radiation pneumonitis* marked by an exudative inflammation 1-6 months after irradiation and a chronic *pulmonary fibrosis* steadily progressing from 4-6 months onwards (50,95,98,131,133,134,156,159). A *latent period* of several weeks would precede the onset of any symptoms (30,95,131,134). Indeed, after a radiation dose gets absorbed in pulmonary tissue, no changes are detectable by optical microscopy in the first few weeks post-irradiation (30,138). That is why this period has been traditionally termed *a latent phase*, a name no longer warranted in the light of current findings (39,136,170). Early ultrastructural changes can be found in virtually all cell types (50). Electron microscopic investigations of type I epithelial cells and endothelial cells have revealed vacuolization, blebbing, disruption of organelle membranes, separation from basement membrane and subendothelial oedema within hours to days following irradiation (1,90,121). Early alterations in structural proteins were proven immunohistochemically in these cellular types (66,67). Such changes are believed to contribute to an early increase in capillary permeability with interstitial and alveolar protein leak and edema, as well as to result in endothelial and epithelial cell death with denudation of basement membranes (30,37,50,83,133,162,174). Other studies emphasize immediate decrement in numbers of lamellar bodies in type II epithelial cells that correlate with increase of alveolar levels of surfactant (116,134,137,138). This suggests a degranulation in response to radiation injury sustained by the type II cells that may later negatively influence their ability to maintain sufficient levels of surfactant and to replace dying type I epithelial cells (138). Abrupt depletion of alveolar macrophages in the first two weeks post-irradiation demonstrates the radiosensitivity of their intrapulmonary proliferating pool (114,130,136). Their subsequent re-appearance in increased numbers and activated

state four weeks after the exposure has been linked to the onset of inflammation, upsurge in cytokine and ROS production and deepening of tissue hypoxia (42,136,169).

Currently, there is no general consensus as to what may be the primary lesion in development of radiation pneumopathy (30). Rather, the radiation response is viewed as a result of disruption of the balance and communication between the various cell populations of the pulmonary parenchyma (161). Alveolar macrophages and type II epithelial cells from irradiated rabbit lungs have been shown to respond rapidly (at 1 week) by production of cytokines that accelerated proliferation of septal fibroblasts (135). Starting immediately and sustained up to 26 weeks post-irradiation, increases in mRNA of proinflammatory cytokines (interleukin 1 = IL-1, tumour necrosis factor α = TNF-α) and profibrogenic cytokines (transforming growth factor β = TGF-β, platelet derived growth factor = PDGF) have been paralleled by acute inflammatory histopathologic changes as well as rise in collagen and fibronectin expression in the irradiated murine lung tissue (36,39,132,136). An early rise in TGF-β protein itself was detected immunohistochemically one hour (12) and one day (42) after the exposure in murine mammary gland and rat lung tissue, respectively. Up-regulated gene expression and/or direct activation of extracellular deposits of inactive cytokine precursor by ROS have been implicated in this rapid secretory response to radiation (11,97,170). A paracrine paradigm has been put forward that links the immediate molecular processes with chronic fibrotic sequelae appearing many ($\geq$6) months later (39,98,127,136,177). It involves prompt shifts in protein transcription resulting in cytokine release by cells that sustained radiation damage (i.e. alveolar macrophages and type II pneumocytes), this causing activation of target cells (i.e. septal fibroblasts) stimulating their proliferation, maturation and production of collagen and other ECM components, gradually leading to fibrosis. In other studies, both types of epithelial cells (type I and type II pneumocytes) have been shown to actively contribute to the remodeling process through protease and cytokine secretion (66). Additionally, tissue hypoxia (see paragraph 1.4), generating ROS and inducing profibrogenic and proangiogenic cytokines, has been described as a perpetuating force in the development of chronic fibroproductive radiation injury (42,95,169). The notion that gradual accumulation of connective tissue in lung interstitium commences long before the arbitrary 6-month timeline for the onset of fibrosis is in agreement

with reports of connective tissue fibrils and collagen deposition observed already within 1-2 months post-irradiation in both humans and rodents (133,174).

Similarly, the intervening acute phase (1-6 months) has been viewed as a consequence of proinflammatory cytokine release in combination with epithelial and endothelial injury (83,95,98,131,133,136,138). Through the compromised integrity of the alveolo-capillary barrier, exudation of plasma proteins and recruitment of inflammatory cells, these conditions constitute the basis for interstitial and intra-alveolar exudative inflammation characteristic of radiation pneumonitis (98,131,133,136,156,159).

Both conditions, the early exudative pneumonitis and the late fibrosis, through the thickening of interalveolar septa and the alveolo-capillary barrier, have the common outcome of loss of area available for gaseous exchange. These changes tend to be of non-uniform, focal nature in the early phases but become more widespread in the stages of advanced fibrosis (133,149,159,161). The clinical correlate of the compromised gas exchange is *dyspnoea* (laboured breathing and breathlessness) which, during the early phases, may be accompanied by fever and nonproductive cough (98).

1.4 Vascular changes

There is a consensus that endothelial injury with malfunction of fine vasculature plays an important role in the pathophysiology of the acute radiation pneumopathy bringing about the early increase in vascular permeability and intravascular protein exudation (30,37,50,83,95,98,131,133,174). Early mural and adventitial edema of arteriols and small arteries, vasculitis of arterioles and venules and perivascular cuffing have been reported (131,150,159).

Vascular injury in late phases evolves into arteriolo-capillary sclerosis, reduction of fine vasculature, intimal connective tissue proliferation, fibrinoid degeneration and hyalinization of the tunica media (131,133,150). Starting from arterioles and small arteries and gradually affecting also medium-sized and large arteries, those changes lead to an obliteration and reduction of lumens, thus forming the morphologic basis for increased pulmonary vascular resistance (pulmonary hypertension) with potentially severe circulatory consequences (150). Acute and/or chronic right cardiac hypertrophy and failure have been described in connection with

severe radiation-induced lung injury in experimental and clinical setting (50,98,150,175).

Another fallout from the loss of vasculature is an inadequate blood flow (chronic *ischemia*) associated with decreased oxygen delivery to tissues (*hypoxia*). It is interesting that damage progression from focal areas of ischemia/hypoxia was suggested to explain the initial focal nature of radiation-induced lung injury (61). Tissue hypoxia is known to promote macrophage accumulation, to induce generation of ROS and to activate proinflammatory, proangiogenic and profibrogenic transcription pathways in these cells (61,106). In turn, tissue hypoxia is further enhanced through increased oxygen consumption by activated proliferating cells in the inflamed terrain (106). It has been hypothesized that hypoxia may in fact be a driving force in the sustenance of cytokine over-production and development of chronic fibroproductive injury in the lung (42,95,169). However, a causal relationship between hypoxia and the radiation-induced tissue injury has not been established. It remains to be proven whether hypoxia is one of contributing pathogenetic factors, a mere consequence of reduced perfusion and intense metabolic activity in the wounded site or - possibly – a bit of both.

1.5 Consequentiality between early and late phases of radiation-induced lung injury

Many authors have addressed the issue of relation and consequentiality between the two manifestations of radiation-induced lung injury, acute (early) radiation pneumonitis and chronic (late) radiation fibrosis, as well as the question of target cell populations involved in those two processes, and came to many disparate conclusions. In one of the earliest morphological studies, it has been noted that mild, transient acute responses in the fine vasculature and connective tissue could be caused by relatively small doses, too low for effects on parenchymal cells, and that this kind of damage might subside leaving no evidence of chronic injury (133). Such interpretation would advocate a lower threshold for acute changes, at least those limited to pulmonary vasculature and connective tissue, which may not necessarily progress into late changes. Nonetheless, the authors offered a general paradigm of pathologic events following an organ irradiation that connected the latent, acute, subacute and chronic periods of injury with their varied clinical or subclinical (i.e. inapparent) manifestations into one continuous, progressive process (133). This

concept has been recently corroborated by studies that provided insight into the immediate and persistent molecular processes (i.e. cytokine and ECM gene expression cascades) taking place in irradiated lung (39,136,177) and other tissues (11,97).

In spite of that, accounts of dissociation between early and late effects in the lung have been common in literature. In reviews, the opinion that mild acute injury could reverse to normal without succession of chronic reaction has been voiced repeatedly, together with a claim that also lung fibrosis may develop *de novo* without a previous history of pneumonitis indicating that both entities may not be interrelated and may appear independently of each other (117,131,146,154). In contrast, acute damage appearing after lower doses than chronic damage or not followed by chronic damage has been reported in a histological study in mice (156) and a radiographic study in humans (161) suggesting a lower dose threshold for the acute pneumonitis. The opposite view that pneumonitis was always followed by fibrosis but fibrosis could in fact occur after lower doses without an evidence of early manifestations, has been advocated by a number of studies on mice. Those evaluated either mortality linked to early and late pulmonary toxicity (149), correlated early increases in surfactant secretion with late structural changes (118) or compared the extent of early protein exudation to the course of collagen biosynthesis (83). Yet another mouse study used breathing rate and mortality assays and showed sparing of early damage by fractionation without sparing of late damage, indicating the involvement of different cell or tissue compartments in the two phases of injury. The damage leading to late sequelae exhibited an independence of overall treatment time, while the acute responses appeared to be ameliorated by longer overall treatment times (35,157). Also in rats, accumulation of interstitial collagen after moderate radiation doses without antecedent alveolitis was described (174). The opinion that the dose to produce late fibrosis was always lower than that producing early pneumonitis, suggesting that imbalance in collagen metabolism could be elicited by doses subthreshold in terms of acute effects, has been discussed (39,134,136). A reconciliatory explanation has been offered stating that an acute phase of some degree was likely to precede in all cases the late phase even if it might not be recognized clinically due to lack of symptoms (98). A summary of the conclusions from reviewed literature is presented in Figure 1.

In addition, beside the classical radiation pneumonitis represented by the cytokine evoked inflammatory response, yet another mechanism has been implicated in the acute respiratory symptoms of radiotherapy patients – a hypersensitivity

pneumonitis (35,105,154). This claim has been based on reports of CD4+ T cell lymphocytosis found in bronchoalveolar lavage fluid from both lungs of symptomatic breast cancer patients 4-6 weeks after unilateral radiotherapy (105,125). Contrary to the classical pneumonitis terminating in fibrosis, this syndrome, termed "sporadic radiation pneumonitis", was shown to spontaneously resolve without long-term sequelae and should explain why some early effects do, while others do not, result in late effects.

To make the picture complete, yet another phase has been recognized on the transition between pneumonitis and fibrosis. It is the period when symptoms recede after the initial peak or gradually worsen towards the full-blown fibrosis. Histology examination reveals persisting acute exudative and inflammatory changes to merge and mix with advancing parenchymal fibrosis and arterio-capillary sclerosis (133) or reparative processes marked by presence of large foamy cells in the alveolar spaces (156,157,158). This period has been referred to as the *subacute* (133) or *intermediate* phase (98,136,156,157,158).

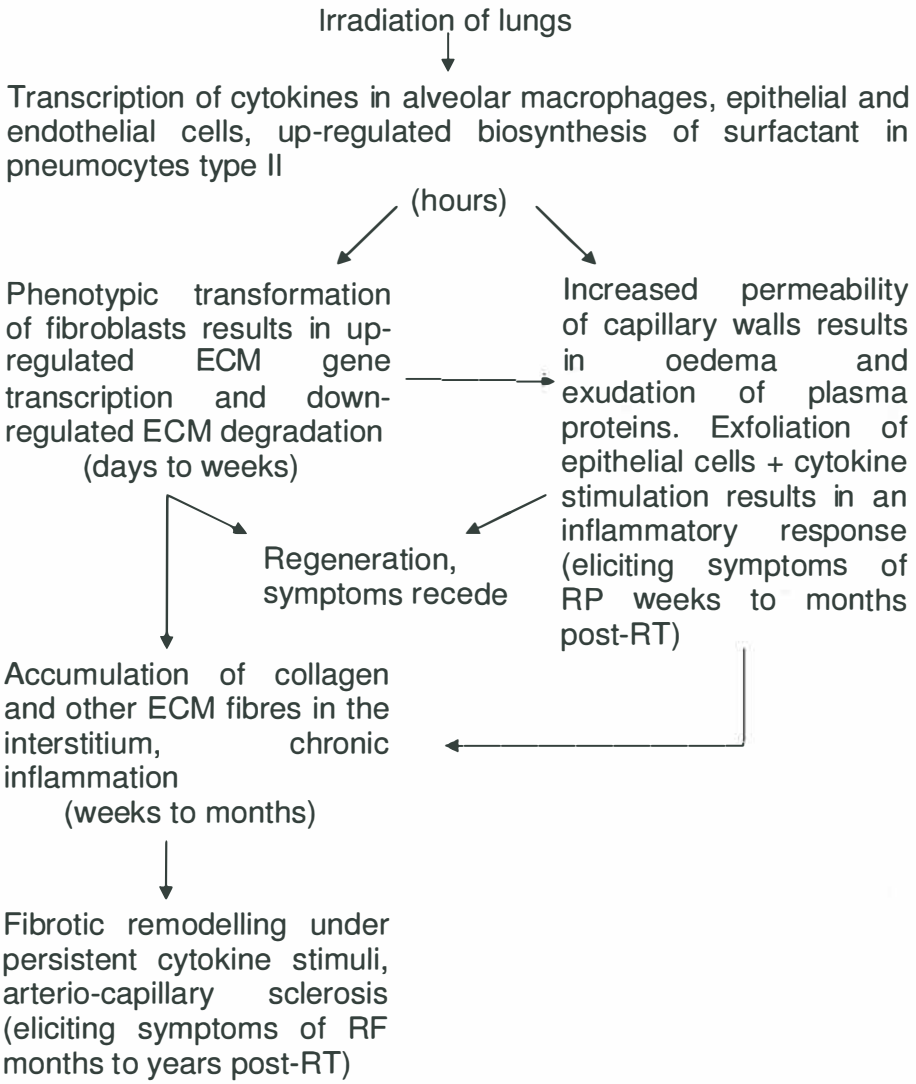

Figure 1: Pathogenesis summary of the pulmonary syndromes of radiation pneumonitis (RP) and radiation fibrosis (RF) based on literature: Rubin/Casarett 68; Roswit/White 77; Travis 80; Coggle et al 86; Rubin et al 92 (in ed. Perez/Brady); Ward et al 93; Finkelstein et al 94; Rubin et al 95; Rodemann/Bamberg 95; McDonald et al 1995; Stover/Kaner 01 (in ed. DeVita/ Hellman/ Rosenberg); Trott et al 04. See text for details.

1.6 Considerations in clinical application of lung irradiation

Doses relevant in terms of acute and late post-irradiation effects described above may arise from medical exposures of the lung to ionizing radiation during radiotherapy for malignant tumours. Thoracic tumours are most often treated with external beam irradiation where the radiation source is located outside a body and the radiation beam has to penetrate through (and gets partially absorbed in) healthy tissues before reaching a tumour. In order for radiation to be clinically useful, it has to be possible to achieve *tumour control*, i.e. to inflict sufficient radiation damage to sterilize all clonogenic tumour cells without exceeding the *normal tissue tolerance*, i.e. without causing a fatal failure of healthy organs and tissues around. Several approaches are being exploited to meet this precondition.

Firstly, the *dose distribution* is very important (152). By means of precise identification of the tumour localization, accurate positioning of a patient and arranging and weighing radiation fields (i.e. beams aimed at a tumour from different directions) the *tumour volume* has to be covered by a maximum dose. At the same time, as little dose should be given to as little *volume of normal tissues* as possible. More and more routinely used three-dimensional conformal radiation therapy (3D-CRT) has improved tumour targeting, permitted dose-escalation and yielded favourable local tumour control and survival rates among patients with NSCLC (84). Novel radiation techniques and modalities, like intensity modulated radiation therapy (IMRT) or proton radiation therapy, are being developed and introduced into clinical practice that should further improve the possibilities of an accurate dose delivery (23,24,99,107).

A second approach ensuring larger sparing of normal tissues than that of a tumour is *fractionation*. It is has been empirically established that dividing a treatment into multiple radiation doses (i.e. *fractions*) given over a period of a few weeks yields better curative results (i.e. improved tumour control for a given level of normal tissue toxicity) than a single large dose of radiation (53,152). This is due to more efficient recovery of healthy cells from radiation damage between fractions and due to the fact that the predominantly hypoxic (thus largely resistant to the free radicals mediated damage – see paragraph 1.1) tumour cells are disadvantaged by *reoxygenation* taking place in between fractions (53). A linear-quadratic model describing the relationship between the dose and its biologic effect can be used to compare expected efficacy and risk of complications after different fractionation schedules (62). For decades,

standard (*conventional*) radiotherapy regimen in NSCLC have been represented by 60 Gy total dose delivered in 2 Gy daily fractions in overall treatment time of 6 weeks (119,120). Recently, promising results have been achieved with *hyperfractionated - accelerated* schedules (i.e. 2-3 daily fractions of less than 2 Gy and shorter overall treatment time) that were designed to prevent tumour repopulation while maintaining acceptable levels of normal tissue toxicity. In inoperable stage I-III NSCLC patients, 3-year overall survival rates of 45% with 10% incidence of treatment requiring pulmonary or oesophageal toxicity have been reported (128).

Combination of radiotherapy with cytotoxic drugs (*chemoradiation therapy*) proved to be yet another useful approach to enhancement of treatment efficacy. Chemotherapy can be given prior to (induction / neoadjuvant), concurrently with (concurrent) or after (consolidation) the radiotherapy course and the interaction of the two modalities may be *additive* (chemotherapy acts on tumour cells outside the irradiation field or on different cell subpopulations within the tumour) or *synergistic* (a direct cellular interaction with stronger than just additive effect) (167). Chemotherapy may be given in full, systemically active dose or in a low "*radio-sensitizing*" dose. Favorable outcomes of clinical trials (4-year survival of 21% in stage II-III NSCLC) have led to the adoption of systemic-dose chemotherapy concurrent with irradiation to 60 Gy as the today's standard in treating locally advanced NSCLC patients with good performance status to withstand greater hematologic, oesophageal and pulmonary toxicity (19,32,99,153,168).

Combining radiotherapy with hypoxic cell sensitizers (64,111,153), normal tissue radioprotectors (95,99,153), antiangiogenic agents (168) and targeted molecular therapies (153) has yet to produce consistent therapeutic advantages in clinical trial setting and thus remains experimental.

1.7 Dosimetric factors influencing toxicity after lung irradiation

The impact of dose, volume and fractionation on the incidence and severity of pulmonary side-effects after radiotherapy has long been recognized. Human data of *whole lung exposure to single doses* were accumulated from total body irradiation and half body irradiation techniques used in conditioning regimens preceding bone marrow transplant. By relating the single doses to the recorded incidence of lethal radiation pneumonitis, a steep sigmoid dose-response curve has been generated indicating a sharp lethality increase from 0 to 90% just between 7 Gy and 11 Gy, 9.3

Gy being the *tolerance dose for 50% complication rate* (TD_{50}) (44,68,165). The data of *whole lung fractionated exposures* in children treated for Wilms' tumour demonstrated the clear protective effect of fractionation, yielding much higher tolerance doses: TD_5 (the tolerance dose for 5% lethality) = 26.5 Gy and TD_{50} = 30.5 Gy (173).

However, curative treatments for majority of solid tumours, including lung cancer, involve only partial lung exposures, rendering the estimation of complication probability after *fractionated partial lung irradiation* to be the major problem in clinical practice. Two levels of injury assessment have to be discerned when regarding this matter: the level of local (regional) effects assessed by means of histology, radiology or perfusion scans and the level of tolerance in terms of global lung function assessed by pulmonary function tests or by scoring of symptoms (59,146). While regional injury is commonly identifiable in patients who received lung doses in excess of 40 Gy, in a form of increased radiological density or reduced blood perfusion (the incidence being 70 and 90%, respectively), the impact of these changes on global lung function depends on the irradiated volume of lung tissue (89,92,98). This type of information is routinely provided by modern treatment planning techniques in a form of a *dose-volume histogram* (DVH). A DVH is a chart relating a locally absorbed dose on x-axis to a proportion of involved organ volume on y-axis, thus summing a three-dimensional (3D) dose distribution into a 2D plane. The inherent drawback of DVH's is that they discard all spatial information and regard all lung regions as equally sensitive and of equal functional importance (95). Even so, DVH's have been widely viewed as a tool that might aid in estimating the risk of post-irradiation pulmonary complications associated with an individual treatment plan prior to commencing a treatment. Several *dosimetric* (i.e. based on a dose distribution) parameters, that have been proposed as predictors of symptomatic radiation-induced lung injury, may be derived from DVHs (91,95,146,147). Those can be divided into simple parameters and more complex theoretical models estimating *normal tissue complication probability* (NTCP).

Simple parameters that were most frequently tested are mean lung dose and lung volume receiving ≥ 20 Gy or 30 Gy. The *mean lung dose* (MLD) represents a total dose absorbed within lung tissue averaged over the total lung volume. It may be corrected for effects of fractionation using the linear-quadratic model [the mean biological lung dose (79)] and take into account the varying pretreatment perfusion

across the lung [the mean perfused lung dose (33,86)]. The MLD showed significant correlation with increasing incidence of symptomatic radiation pneumonitis in several studies examining radiotherapy outcomes in patients with thoracic tumours (33,38,48,57,79,147,183). However, a parameter like the MLD was not considered to be appropriate where the dose distribution in the lungs varied widely, e.g. in a postoperative radiotherapy for breast cancer (46). Other popular simple parameters like volumes receiving 20 Gy and more (V_{20}) or 30 Gy and more (V_{30}), were found to be the best predictors for radiation pneumonitis in multivariate analyses published by Graham et al (48) and by Hernando et al (57), respectively.

When developing the theoretical models, authors have attempted to create mathematical function that would relate an irradiated volume and a dose delivered during a treatment schedule to the risk of radiation-induced lung injury and provide the best fit (retrospectively) to the available clinical data, i.e. give results similar to the observed incidence of symptomatic radiation pneumonitis. Two widely used models, the Lyman model and the critical-volume model, require reduction of the multi-step DVH (describing the inhomogeneous dose distribution) into a single-step DVH describing a uniform partial or whole organ irradiation that would lead to the same level of complications as the original, inhomogeneous treatment (78,80,146,147). From this single-step DVH, a single value is extracted (equivalent uniform dose = EUD) that is subsequently related to the NTCP.

For the reduction, the *Lyman model* (21,87) utilizes a power-law relationship between volume and dose and the model is characterized by 3 parameters: a volume exponent (n), a tolerance dose for 50% complication probability (TD_{50}) after irradiation to the reference volume and a steepness parameter (m) (21,80,146,147). By applying this model to various sets of clinical data, TD_{50} ranging from 24.5 to 30.8 Gy and n ranging from 0.87 to 1.0 (indicating a strong volume effect) have been determined for lung (21,48,57,93,96,110,147,183). The Lyman model is an empirical one - its function is not meant to represent any radiobiological theory. Most other models are mechanistic. They attempt to explain the measured effect by the structure of the organ or by the mechanism leading to the complication (166).

The *critical-volume (or parallel) model* (60,109,184) is based on the concept of functional subunits (FSU's). This concept introduced by Withers et al (178) implies that an organ consists of FSU's that can independently carry out organ function and can be repopulated from a single stem cell. The critical-volume model assumes that

the FSU's are arranged in parallel and their survival as a function of the locally applied dose is described by a sigmoid curve. The complication occurs only after the number/fraction of inactivated FSU's exceeds a critical threshold, also called *functional reserve*. The model is characterized by a local dose eliciting 50% effect on FSU survival (D_{50}) and a steepness parameter (k) of the FSU survival curve (60,109,146,147).

Another model that uses the concept of FSU's is the *relative seriality model* (46,65). This model assumes that an organ is formed by multiple fibers of FSU's. The fibers are organized in parallel but the FSU's in them are in series. The NTCP is calculated from the whole organ response that follows Poisson statistics (166). The model is characterized by 3 parameters: a dose giving 50% complication probability following uniform whole organ irradiation (D_{50}), a steepness parameter (γ) and a relative seriality factor (s) ranging from 0 to 1 for parallel and serial organization of an organ, respectively (65,146). For lung, factor s values of 0.01 (46) and 0.06 (147) have been determined indicating a strong parallel behavior.

Consistently, rates of radiation-induced lung injury have been reported to increase with both the simple dosimetric parameters and the NTCP estimates (38,48,57,79,96,110,147,183). It has not been possible to assess which of these parameters are superior. They are highly correlated with each other because relatively uniform radiation treatment techniques have been used in the individual studies (72,91,146). Unfortunately, despite their clear association with radiation-induced lung injury, dosimetric parameters are unable to optimally segregate patients into high- vs. low-risk groups. Too many low-risk patients develop complications while many high-risk patients do not (86,91).

It was postulated that the accuracy of prediction could improve if patients with poor pre-radiotherapy *global lung function* (assayed by pulmonary function tests) were excluded as they appear more likely to experience toxicity at low lung doses (86,91,93,126). Another way to strengthen the predictive power is to factor in pre-radiotherapy *regional lung function* represented by *perfusion*. Perfusion is assayed by means of single photon emission computed tomography (SPECT). Images of an organ from planning CT (computed tomography) with delineated 3D dose distribution are registered with SPECT images and functional dose-volume histogram (DVfH) (93,94) or dose-function (i.e. dose-SPECT count) histogram (DFH) (47,72,86) are created. SPECT – based functional parameters, analogical to the DVH – derived dosimetric

parameters, can be then determined from DVfH's or DFH's, for example the percent of perfused lung irradiated to ≥30 Gy (PV_{30}) or *mean perfused lung dose* (MpLD). MpLD and the sum of *predicted perfusion reduction* (PPR, OpRP) have shown significant correlation with post-radiotherapy decrements in pulmonary function tests (33). The same two parameters, each combined into a bidimensional model with metrics of pre-radiotherapy global lung function (i.e. pre-RT pulmonary function tests) improved prediction of symptomatic pneumonitis over single DVH-based parameters (86). However, the predictive power was still found insufficient for routine clinical use. This has been recently demonstrated in a joined study from Duke University Medical Center and the Netherlands Cancer Institute (72). A multi-parameter model taking into account values of MLD, OpRP and pre-radiotherapy pulmonary function tests failed to predict risk of radiation pneumonitis when applied prospectively to a diverse population of patients. The actual observed incidence of pneumonitis was, indeed, higher in the high-risk group but the difference in the incidence rates did not reach statistical significance. As a result, there are currently no validated means of predicting an individual patient's risk of developing pulmonary toxicity (72). It is generally agreed that not only dosimetric and functional information, but also information on biologic determinants of radiosensitivity should be included in multi-parameter models and tested on larger patient populations in the future (72,86).

1.8 Biological determinants of radiation-induced pulmonary toxicity – patient related characteristics

Traditionally, patient's age (29), sex (126), performance status (103,126), preexisting lung comorbidity (103), tobacco history (57,103) and pre-radiotherapy lung function assessed by pulmonary function tests (93,103,126) fell into this category. Also the use and timing of chemotherapy have been reported to influence an individual patient's response to radiation treatment (88,99). Such determinants have shown relations to the development of radiation pneumonitis in some studies (references above) while in others they did not (47,48,57,58,99,163,179,183). With the exception of pre-radiotherapy lung function and concurrent chemotherapy, their importance seems to be overridden by the impact of dosimetric parameters.

Recently, a promising area of research has been the modulation of normal tissue radiation response by the patient's individual *cytokine background* (41). In the

forefront of this research effort stands the pivotal regulator of tissue repair, cytokine *transforming growth factor β* (TGF-β). It exerts effects on cell proliferation, differentiation, apoptosis, modulates inflammation and has a prominent role in the extracellular matrix (ECM) remodeling following mechanical or cytotoxic insult (11,69,97,171). Three TGF-β isoforms (TGF-β1,2,3) with largely overlapping spectrum of biological activities exist in mammals (18,69). TGF-β1 is the predominant isoform found in human plasma (49,172) and it has been most frequently implicated in fibroproliferative diseases (18,97). TGF-β is secreted as a latent precursor by many cell types and deposited in the ECM. *In vivo*, the most common activation mechanism is through proteases such as plasmin, which is positively regulated by increased expression of tissue-type plasminogen activator following irradiation (11,40,45). Beside this path, using a model of murine mammary gland, a direct, rapid redox-mediated activation of latent TGF-β by ionizing radiation has been observed (11,12,13). TGF-β activation and dose-dependent local expression in irradiated lung tissue has been linked to the initiation and promotion of post-irradiation lung injury in experimental studies on mice and rats (36,39,132,136,181). Also in men, sustained dysregulation of TGF-β activity is believed to produce non-healing inflammatory and fibroproductive response in the irradiated lung gradually obliterating tissue architecture and impairing lung function (41,177). It was noted with an interest that many cancer patients (e.g. 50% of lung cancer patients) present with elevated latent TGF-β levels in their plasma prior to treatment (4,14,63,73,74,76,77,108), the most likely source of the cytokine being their tumours (124,151) or tumour stroma (4,74). Further, a strong correlation was observed between the elevated pre-treatment TGF-β plasma level and risk of veno-occlusive and pulmonary complications following high-dose chemotherapy for advanced breast cancer (8). The authors continued their investigation on 73 patients with NSCLC undergoing weekly TGF-β1 sampling throughout the course of curative radiotherapy. They found that TGF-β1 plasma dynamics during the treatment, i.e. the ratio of the end-radiotherapy over the pre-radiotherapy plasma concentration being < 1 identified patients who did not subsequently develop symptomatic pneumonitis with 90% sensitivity and predictive value (3). A hypothesis was formulated that plasma TGF-β1 levels during a treatment reflected the balance between decreasing production by shrinking tumour and increasing expression at the site of normal tissue injury. Further so, that the excess circulating TGF-β1 could be up-taken and activated at the site of

injury where it would be expected, in an *endocrine* mode of action, to enhance the pathologic process and therefore predispose the patient to manifestation of symptomatic pneumonitis (4,5). Based on their encouraging data, the authors proposed to use serial plasma TGF-β1 measurements during the radiotherapy for lung cancer as an indicator of risk of development of radiation-induced lung injury and for selecting patients who were likely to benefit from more aggressive dose-escalation treatment without an unacceptable increase in toxicity (3). Among other researchers, we embraced the challenge of testing the predictive power of this highly promising biological parameter against new, independent sets of clinical data – which is a focus of **Chapter 2** in current thesis.

A number of other biomarkers found in plasma have been investigated in limited clinical trials with noteworthy results. Elevated pre-treatment, end-treatment and post-treatment plasma levels of pro-inflammatory cytokines *interleukin Iα* and *interleukin 6* (IL-1α, IL-6) correlated with symptomatic pneumonitis following radiotherapy for thoracic malignancies (25,26). Rising plasma concentrations of *mucin-like glycoprotein antigen* (KL-6) found on pneumocytes and bronchiolar epithelial cells or of specific epithelial proteins *surfactant proteins A* and *D* during the radiotherapy course were indicative of radiation pneumonitis (41,99). However, those results are not consistently reproduced and need to be validated in prospective studies on larger numbers of patients (54).

Biomarker profiles should reflect inter-patient phenotypic variations that influence the susceptibility to radiation-induced normal tissue injury, i.e. *intrinsic radiosensitivity*. Not surprisingly, some effort has been aimed towards direct gene expression profiling. A detailed review has been recently published (17). Initially, optimism was raised by reports on the possible prognostic value of *in vitro* radiosensitivity of normal human skin fibroblasts for late effects of radiotherapy. However, significance of such relationship disappeared when assessed in two larger and more rigorous confirmatory studies (113,139). Nowadays, single nucleotide polymorphisms, immunohistochemical markers and DNA microarray gene signatures represent assays that show promise in radiation oncology applications. However, those techniques are still a long way from clinically usable assays of individual radiation sensitivity.

In summary, investigations on biologic determinants of radiation-induced normal tissue injury hold a great promise for patients undergoing thoracic

radiotherapy, especially because no one single dosimetric predictor is capable to optimally separate these patients into low- vs. high-risk groups in terms of pulmonary toxicity of the treatment. A combination of multiple biologic and dosimetric parameters will be needed to generate a normal tissue injury risk profile allowing to tailor the treatment to the needs of an individual patient (6,72,93,99). An ongoing research has to address a selection of appropriate indices and their incorporation into multi-parameter predictive models that will be reliable enough for clinical decision-making.

1.9 Biological determinants of radiation-induced pulmonary toxicity – regional variations in lung sensitivity

Regional variations in radiosensitivity of the lung gained an attention after it was shown in mice that irradiation of a given subvolume in the pulmonary base produced higher toxicity in terms of breathing rate increases and mortality 22-28 weeks after the exposure than irradiation of the identical subvolume in the apex (85,160). Those accounts of higher radiation sensitivity of lung base compared to lung apex were explained either by a non-uniform distribution of target cells, i.e. cells within alveolar parenchyma involved in the actual gas exchange (164) or by direction-dependent *in-field* and *out-of-field* effects mediated most likely by circulating cytokines and induced reactive oxygen and nitrogen species (ROS/RNS) production (70,102). Subsequently, it was noted in clinical studies that although majority of tumours is typically located in the upper lung region, the incidence of symptomatic pneumonitis is significantly higher among patients with lower lung tumours than with upper lung tumours (48,58,145,179,182,183). Moreover, the incidence of symptomatic pneumonitis within 6 months from the radiotherapy course correlated significantly with dosimetric indices (mean regional dose and Lyman model NTCP) derived from dose distributions in the lower lung but not the upper lung (145,182,183). Also, the introduction of a parameter describing tumour location led to an improved power of prediction of complications over models that lacked spatial information (58). Such results seemed to indicate that radiation injury to the lower lung was more causative in terms of respiratory dysfunction than injury to the upper lung. Beside the non-uniform distribution of target cells and out-of-field effects mentioned above, mechanisms underlying this phenomenon were further suggested to include better perfusion/ventilation and thus bigger physiological importance of lower

lung than upper lung in upright position in humans (58,183). Alternatively, the extent of respiratory motion that is greater in the lower lung was pointed out as a cause for more functional lung tissue being irradiated when tumours in the lung base were treated (58,145,183). In experimental studies on a rat model, we identified yet another - extrapulmonary - factor that could possibly account for the higher incidence of symptomatic pneumonitis following lower lung irradiation in men, as well as for the functional hypersensitivity of upper lung region observed in rats during our investigation. This work is described in **Chapters 3** and **4** of this thesis.

Notwithstanding the controversy regarding the underlying mechanisms, the importance of *regional* (*spatial*) *effects* for determination of the likelihood of pulmonary complications following thoracic irradiation is widely acknowledged (91,95,99). As a consequence, unraveling of the causes and finding ways how to incorporate these effects into multi-parameter predictive models have become one of the priorities of the current radiobiological research.

1.10 Aim and outline of the thesis

The purpose of this work was to identify and characterize new factors that influence radiosensitivity of normal lung tissue during radiation treatment of thoracic malignancies. This is needed to improve the predictive power of clinically tested models for pre-treatment assessment of risk of symptomatic radiation-induced lung injury developing as a side-effect of the treatment. Initially, the investigation concentrated on the immuno-modulatory, pro-fibrotic cytokine TGF-β. Clinical evaluation of its alleged endocrine action was carried out in a group of NSCLC patients undergoing curative RT (**Chapter 2**).

All further research was performed in an experimental setting using a rat animal model. The impact of in-homogeneous alveolar density in the lung on the severity of morphological and functional impairment resulting from irradiation of different lung regions, as well as the interaction with subclinical damage to the heart, were assessed in a study entailing 50% total lung volume irradiation (X-ray) targeted to six different lung regions (**Chapter 3**). In contrast to the traditional concept of the heart as a late-responding organ, the contribution of cardiac irradiation to the development of an acute respiratory dysfunction following thoracic irradiation was confirmed in a proton irradiation study (**Chapter 4**). The study presented under Chapter 3 also provided an opportunity to determine the correlation between the

functional and structural changes assessed by non-invasive means of computer tomography (**Chapter 5**). Finally, dose-volume-effect relations regarding the morphological and functional endpoints were investigated following X-ray irradiation of varying lung volumes (**Chapter 6**).

References

1. Adamson, I.Y., Bowden, D.H., and Wyatt, J.P. A pathway to pulmonary fibrosis: an ultrastructural study of mouse and rat following radiation to the whole body and hemithorax. Am J Pathol 1970; 58: 481-498.
2. Albanese, J. and Dainiak, N. Modulation of intercellular communication mediated at the cell surface and on extracellular, plasma membrane-derived vesicles by ionizing radiation. Exp Hematol 2003; 31: 455-464.
3. Anscher, M.S., Kong, F.M., Andrews, K., Clough, R., Marks, L.B., Bentel, G., and Jirtle, R.L. Plasma transforming growth factor beta1 as a predictor of radiation pneumonitis. Int J Radiat Oncol Biol Phys 1998; 41: 1029-1035.
4. Anscher, M.S., Kong, F.M., and Jirtle, R.L. The relevance of transforming growth factor beta 1 in pulmonary injury after radiation therapy. Lung Cancer 1998; 19: 109-120.
5. Anscher, M.S., Kong, F.M., Murase, T., and Jirtle, R.L. Short communication: normal tissue injury after cancer therapy is a local response exacerbated by an endocrine effect of TGF beta. Br J Radiol 1995; 68: 331-333.
6. Anscher, M.S., Marks, L.B., Shafman, T.D., Clough, R., Huang, H., Tisch, A., Munley, M., Herndon, J.E., Garst, J., Crawford, J., and Jirtle, R.L. Using plasma transforming growth factor beta-1 during radiotherapy to select patients for dose escalation. J Clin Oncol 2001; 19: 3758-3765.
7. Anscher, M.S., Marks, L.B., Shafman, T.D., Clough, R., Huang, H., Tisch, A., Munley, M., Herndon, J.E., Garst, J., Crawford, J., and Jirtle, R.L. Risk of long-term complications after TFG-beta1-guided very-high-dose thoracic radiotherapy. Int J Radiat Oncol Biol Phys 2003; 56: 988-995.
8. Anscher, M.S., Peters, W.P., Reisenbichler, H., Petros, W.P., and Jirtle, R.L. Transforming growth factor beta as a predictor of liver and lung fibrosis after autologous bone marrow transplantation for advanced breast cancer. N Engl J Med 1993; 328: 1592-1598.
9. Armstrong, J., Raben, A., Zelefsky, M., Burt, M., Leibel, S., Burman, C., Kutcher, G., Harrison, L., Hahn, C., Ginsberg, R., Rusch, V., Kris, M., and Fuks, Z. Promising survival with three-dimensional conformal radiation therapy for non-small cell lung cancer. Radiother Oncol 1997; 44: 17-22.
10. Armstrong, J.G., Burman, C., Leibel, S., Fontenla, D., Kutcher, G., Zelefsky, M., and Fuks, Z. Three-dimensional conformal radiation therapy may improve the therapeutic ratio of high dose radiation therapy for lung cancer. Int J Radiat Oncol Biol Phys 1993; 26: 685-689.
11. Barcellos-Hoff, M.H. How do tissues respond to damage at the cellular level? The role of cytokines in irradiated tissues. Radiat Res 1998; 150: S109-S120.
12. Barcellos-Hoff, M.H., Derynck, R., Tsang, M.L., and Weatherbee, J.A. Transforming growth factor-beta activation in irradiated murine mammary gland. J Clin Invest 1994; 93: 892-899.
13. Barcellos-Hoff, M.H. and Dix, T.A. Redox-mediated activation of latent transforming growth factor-beta 1. Mol Endocrinol 1996; 10: 1077-1083.
14. Barthelemy-Brichant, N., David, J.L., Bosquee, L., Bury, T., Seidel, L., Albert, A., Bartsch, P., Baugnet-Mahieu, L., and Deneufbourg, J.M. Increased TGFbeta1 plasma level in patients with lung cancer: potential mechanisms. Eur J Clin Invest 2002; 32: 193-198.

15. Bedford, J.S., Mitchell, J.B., Griggs, H.G., and Bender, M.A. Radiation-induced cellular reproductive death and chromosome aberrations. Radiat Res 1978; 76: 573-586.
16. Belderbos, J.S., Heemsbergen, W.D., De Jaeger, K., Baas, P., and Lebesque, J.V. Final results of a Phase I/II dose escalation trial in non-small-cell lung cancer using three-dimensional conformal radiotherapy. Int J Radiat Oncol Biol Phys 2006; 66: 126-134.
17. Bentzen, S.M. From cellular to high-throughput predictive assays in radiation oncology: challenges and opportunities. Semin Radiat Oncol 2008; 18: 75-88.
18. Border, W.A. and Noble, N.A. Transforming growth factor beta in tissue fibrosis. N Engl J Med 1994; 331: 1286-1292.
19. Bradley, J. A review of radiation dose escalation trials for non-small cell lung cancer within the Radiation Therapy Oncology Group. Semin Oncol 2005; 32: S111-S113.
20. Bradley, J., Graham, M.V., Winter, K., Purdy, J.A., Komaki, R., Roa, W.H., Ryu, J.K., Bosch, W., and Emami, B. Toxicity and outcome results of RTOG 9311: a phase I-II dose-escalation study using three-dimensional conformal radiotherapy in patients with inoperable non-small-cell lung carcinoma. Int J Radiat Oncol Biol Phys 2005; 61: 318-328.
21. Burman, C., Kutcher, G.J., Emami, B., and Goitein, M. Fitting of normal tissue tolerance data to an analytic function. Int J Radiat Oncol Biol Phys 1991; 21: 123-135.
22. Ch'ang, H.J., Maj, J.G., Paris, F., Xing, H.R., Zhang, J., Truman, J.P., Cardon-Cardo, C., Haimovitz-Friedman, A., Kolesnick, R., and Fuks, Z. ATM regulates target switching to escalating doses of radiation in the intestines. Nat Med 2005; 11: 484-490.
23. Chang, J.Y., Liu, H.H., and Komaki, R. Intensity modulated radiation therapy and proton radiotherapy for non-small cell lung cancer. Curr Oncol Rep 2005; 7: 255-259.
24. Chang, J.Y., Zhang, X., Wang, X., Kang, Y., Riley, B., Bilton, S., Mohan, R., Komaki, R., and Cox, J.D. Significant reduction of normal tissue dose by proton radiotherapy compared with three-dimensional conformal or intensity-modulated radiation therapy in Stage I or Stage III non-small-cell lung cancer. Int J Radiat Oncol Biol Phys 2006; 65: 1087-1096.
25. Chen, Y., Hyrien, O., Williams, J., Okunieff, P., Smudzin, T., and Rubin, P. Interleukin (IL)-1A and IL-6: applications to the predictive diagnostic testing of radiation pneumonitis. Int J Radiat Oncol Biol Phys 2005; 62: 260-266.
26. Chen, Y., Williams, J., Ding, I., Hernady, E., Liu, W., Smudzin, T., Finkelstein, J.N., Rubin, P., and Okunieff, P. Radiation pneumonitis and early circulatory cytokine markers. Semin Radiat Oncol 2002; 12: 26-33.
27. Cilliers, G.D., Harper, I.S., and Lochner, A. Radiation-induced changes in the ultrastructure and mechanical function of the rat heart. Radiother Oncol 1989; 16: 311-326.
28. Clark, R.A. Cutaneous tissue repair: basic biologic considerations. I. J Am Acad Dermatol 1985; 13: 701-725.
29. Claude, L., Perol, D., Ginestet, C., Falchero, L., Arpin, D., Vincent, M., Martel, I., Hominal, S., Cordier, J.F., and Carrie, C. A prospective study on radiation pneumonitis following conformal radiation therapy in non-small-cell lung cancer: clinical and dosimetric factors analysis. Radiother Oncol 2004; 71: 175-181.

30. Coggle, J.E., Lambert, B.E., and Moores, S.R. Radiation effects in the lung. Environ Health Perspect 1986; 70: 261-291.
31. Coggle, J.E. and Tarling, J.D. The proliferation kinetics of pulmonary alveolar macrophages. J Leukoc Biol 1984; 35: 317-327.
32. Curran, W., Scott, C., Langer, C., and et al. Lon-term benefit is observed in a phase III comparison of sequential vs concurrent chemo-radiation for patients with unresectable NSCLC: RTOG 9410. Proc Am Soc Clin Oncol 2003; 22: abstract 2499a, p.621a.
33. De Jaeger, K., Seppenwoolde, Y., Boersma, L.J., Muller, S.H., Baas, P., Belderbos, J.S., and Lebesque, J.V. Pulmonary function following high-dose radiotherapy of non-small-cell lung cancer. Int J Radiat Oncol Biol Phys 2003; 55: 1331-1340.
34. Dillman, R.O., Herndon, J., Seagren, S.L., Eaton, W.L., Jr., and Green, M.R. Improved survival in stage III non-small-cell lung cancer: seven-year follow-up of cancer and leukemia group B (CALGB) 8433 trial. J Natl Cancer Inst 1996; 88: 1210-1215.
35. Dorr, W., Baumann, M., and Herrmann, T. Radiation-induced lung damage: a challenge for radiation biology, experimental and clinical radiotherapy. Int J Radiat Biol 2000; 76: 443-446.
36. Epperly, M.W., Travis, E.L., Sikora, C., and Greenberger, J.S. Manganese [correction of Magnesium] superoxide dismutase (MnSOD) plasmid/liposome pulmonary radioprotective gene therapy: modulation of irradiation-induced mRNA for IL-I, TNF-alpha, and TGF-beta correlates with delay of organizing alveolitis/fibrosis. Biol Blood Marrow Transplant 1999; 5: 204-214.
37. Evans, M.L., Graham, M.M., Mahler, P.A., and Rasey, J.S. Changes in vascular permeability following thorax irradiation in the rat. Radiat Res 1986; 107: 262-271.
38. Fay, M., Tan, A., Fisher, R., Mac, M.M., Wirth, A., and Ball, D. Dose-volume histogram analysis as predictor of radiation pneumonitis in primary lung cancer patients treated with radiotherapy. Int J Radiat Oncol Biol Phys 2005; 61: 1355-1363.
39. Finkelstein, J.N., Johnston, C.J., Baggs, R., and Rubin, P. Early alterations in extracellular matrix and transforming growth factor beta gene expression in mouse lung indicative of late radiation fibrosis. Int J Radiat Oncol Biol Phys 1994; 28: 621-631.
40. Flaumenhaft, R., Abe, M., Mignatti, P., and Rifkin, D.B. Basic fibroblast growth factor-induced activation of latent transforming growth factor beta in endothelial cells: regulation of plasminogen activator activity. J Cell Biol 1992; 118: 901-909.
41. Fleckenstein, K., Gauter-Fleckenstein, B., Jackson, I.L., Rabbani, Z., Anscher, M., and Vujaskovic, Z. Using biological markers to predict risk of radiation injury. Semin Radiat Oncol 2007; 17: 89-98.
42. Fleckenstein, K., Zgonjanin, L., Chen, L., Rabbani, Z., Jackson, I.L., Thrasher, B., Kirkpatrick, J., Foster, W.M., and Vujaskovic, Z. Temporal onset of hypoxia and oxidative stress after pulmonary irradiation. Int J Radiat Oncol Biol Phys 2007; 68: 196-204.
43. Fletcher, G.H. Clinical dose-response curves of human malignant epithelial tumours. Br J Radiol 1973; 46: 1-12.

44. Fryer, C.J., Fitzpatrick, P.J., Rider, W.D., and Poon, P. Radiation pneumonitis: experience following a large single dose of radiation. Int J Radiat Oncol Biol Phys 1978; 4: 931-936.
45. Fukunaga, N., Burrows, H.L., Meyers, M., Schea, R.A., and Boothman, D.A. Enhanced induction of tissue-type plasminogen activator in normal human cells compared to cancer-prone cells following ionizing radiation. Int J Radiat Oncol Biol Phys 1992; 24: 949-957.
46. Gagliardi, G., Bjohle, J., Lax, I., Ottolenghi, A., Eriksson, F., Liedberg, A., Lind, P., and Rutqvist, L.E. Radiation pneumonitis after breast cancer irradiation: analysis of the complication probability using the relative seriality model. Int J Radiat Oncol Biol Phys 2000; 46: 373-381.
47. Garipagaoglu, M., Munley, M.T., Hollis, D., Poulson, J.M., Bentel, G.C., Sibley, G., Anscher, M.S., Fan, M., Jaszczak, R.J., Coleman, R.E., and Marks, L.B. The effect of patient-specific factors on radiation-induced regional lung injury. Int J Radiat Oncol Biol Phys 1999; 45: 331-338.
48. Graham, M.V., Purdy, J.A., Emami, B., Harms, W., Bosch, W., Lockett, M.A., and Perez, C.A. Clinical dose-volume histogram analysis for pneumonitis after 3D treatment for non-small cell lung cancer (NSCLC). Int J Radiat Oncol Biol Phys 1999; 45: 323-329.
49. Grainger, D.J., Mosedale, D.E., and Metcalfe, J.C. TGF-beta in blood: a complex problem. Cytokine Growth Factor Rev 2000; 11: 133-145.
50. Gross, N.J. The pathogenesis of radiation-induced lung damage. Lung 1981; 159: 115-125.
51. Hall, E.J. DNA strand breaks and chromosomal aberrations. In: Hall, E.J. Radiobiology for the radiologist; Philadelphia 1994: 15-27.
52. Hall, E.J. The physics and chemistry of radiation absorption. In: Hall, E.J. Radiobiology for the radiologist; Philadelphia 1994: 1-13.
53. Hall, E.J. Time, dose and fractionation in radiotherapy. In: Hall, E.J. Radiobiology for the radiologist; Philadelphia 1994: 211-229.
54. Hart, J.P., Broadwater, G., Rabbani, Z., Moeller, B.J., Clough, R., Huang, D., Sempowski, G.A., Dewhirst, M., Pizzo, S.V., Vujaskovic, Z., and Anscher, M.S. Cytokine profiling for prediction of symptomatic radiation-induced lung injury. Int J Radiat Oncol Biol Phys 2005; 63: 1448-1454.
55. Hasleton, P.S. Anatomy of the lung. In: Hasleton, P.S., editor. Spencer's pathology of the lung; New York 1996.
56. Hayman, J.A., Martel, M.K., Ten Haken, R.K., Normolle, D.P., Todd, R.F., III, Littles, J.F., Sullivan, M.A., Possert, P.W., Turrisi, A.T., and Lichter, A.S. Dose escalation in non-small-cell lung cancer using three-dimensional conformal radiation therapy: update of a phase I trial. J Clin Oncol 2001; 19: 127-136.
57. Hernando, M.L., Marks, L.B., Bentel, G.C., Zhou, S.M., Hollis, D., Das, S.K., Fan, M., Munley, M.T., Shafman, T.D., Anscher, M.S., and Lind, P.A. Radiation-induced pulmonary toxicity: a dose-volume histogram analysis in 201 patients with lung cancer. Int J Radiat Oncol Biol Phys 2001; 51: 650-659.
58. Hope, A.J., Lindsay, P.E., El, N., I, Alaly, J.R., Vicic, M., Bradley, J.D., and Deasy, J.O. Modeling radiation pneumonitis risk with clinical, dosimetric, and spatial parameters. Int J Radiat Oncol Biol Phys 2006; 65: 112-124.
59. Hopewell, J.W. The volume effect in radiotherapy--its biological significance. Br J Radiol 1997; 70 Spec No: S32-S40.

60. Jackson, A., Kutcher, G.J., and Yorke, E.D. Probability of radiation-induced complications for normal tissues with parallel architecture subject to non-uniform irradiation. Med Phys 1993; 20: 613-625.
61. Jackson, I.L., Chen, L., Batinic-Haberle, I., and Vujaskovic, Z. Superoxide dismutase mimetic reduces hypoxia-induced O2*-, TGF-beta, and VEGF production by macrophages. Free Radic Res 2007; 41: 8-14.
62. Joiner, M.C. and van der Kogel, A.J. The linear-quadratic approach to fractionation and calculation of isoeffect relationships. In: Steel, G.G., editor. Basic clinical radiobiology; London 1997: 106-122.
63. Junker, U., Knoefel, B., Nuske, K., Rebstock, K., Steiner, T., Wunderlich, H., Junker, K., and Reinhold, D. Transforming growth factor beta 1 is significantly elevated in plasma of patients suffering from renal cell carcinoma. Cytokine 1996; 8: 794-798.
64. Kaanders, J.H., Bussink, J., and van der Kogel, A.J. Clinical studies of hypoxia modification in radiotherapy. Semin Radiat Oncol 2004; 14: 233-240.
65. Kallman, P., Agren, A., and Brahme, A. Tumour and normal tissue responses to fractionated non-uniform dose delivery. Int J Radiat Biol 1992; 62: 249-262.
66. Kasper, M. and Haroske, G. Alterations in the alveolar epithelium after injury leading to pulmonary fibrosis. Histol Histopathol 1996; 11: 463-483.
67. Kasper, M., Reimann, T., Hempel, U., Wenzel, K.W., Bierhaus, A., Schuh, D., Dimmer, V., Haroske, G., and Muller, M. Loss of caveolin expression in type I pneumocytes as an indicator of subcellular alterations during lung fibrogenesis. Histochem Cell Biol 1998; 109: 41-48.
68. Keane, T.J., Van Dyk, J., and Rider, W.D. Idiopathic interstitial pneumonia following bone marrow transplantation: the relationship with total body irradiation. Int J Radiat Oncol Biol Phys 1981; 7: 1365-1370.
69. Kelley, J. Transforming growth factor-beta. In: Kelley, J., editor. Cytokines of the lung; New York 1993: 101-137.
70. Khan, M.A., Van Dyk, J., Yeung, I.W., and Hill, R.P. Partial volume rat lung irradiation; assessment of early DNA damage in different lung regions and effect of radical scavengers. Radiother Oncol 2003; 66: 95-102.
71. Kim, G.J., Chandrasekaran, K., and Morgan, W.F. Mitochondrial dysfunction, persistently elevated levels of reactive oxygen species and radiation-induced genomic instability: a review. Mutagenesis 2006; 21: 361-367.
72. Kocak, Z., Borst, G.R., Zeng, J., Zhou, S., Hollis, D.R., Zhang, J., Evans, E.S., Folz, R.J., Wong, T., Kahn, D., Belderbos, J.S., Lebesque, J.V., and Marks, L.B. Prospective assessment of dosimetric/physiologic-based models for predicting radiation pneumonitis. Int J Radiat Oncol Biol Phys 2007; 67: 178-186.
73. Kong, F., Jirtle, R.L., Huang, D.H., Clough, R.W., and Anscher, M.S. Plasma transforming growth factor-beta1 level before radiotherapy correlates with long term outcome of patients with lung carcinoma. Cancer 1999; 86: 1712-1719.
74. Kong, F.M., Anscher, M.S., Murase, T., Abbott, B.D., Iglehart, J.D., and Jirtle, R.L. Elevated plasma transforming growth factor-beta 1 levels in breast cancer patients decrease after surgical removal of the tumor. Ann Surg 1995; 222: 155-162.
75. Kong, F.M., Ten Haken, R.K., Schipper, M.J., Sullivan, M.A., Chen, M., Lopez, C., Kalemkerian, G.P., and Hayman, J.A. High-dose radiation

improved local tumor control and overall survival in patients with inoperable/unresectable non-small-cell lung cancer: long-term results of a radiation dose escalation study. Int J Radiat Oncol Biol Phys 2005; 63: 324-333.
76. Kong, F.M., Washington, M.K., Jirtle, R.L., and Anscher, M.S. Plasma transforming growth factor-beta 1 reflects disease status in patients with lung cancer after radiotherapy: a possible tumor marker. Lung Cancer 1996; 16: 47-59.
77. Krasagakis, K., Tholke, D., Farthmann, B., Eberle, J., Mansmann, U., and Orfanos, C.E. Elevated plasma levels of transforming growth factor (TGF)-beta1 and TGF-beta2 in patients with disseminated malignant melanoma. Br J Cancer 1998; 77: 1492-1494.
78. Kutcher, G.J. and Burman, C. Calculation of complication probability factors for non-uniform normal tissue irradiation: the effective volume method. Int J Radiat Oncol Biol Phys 1989; 16: 1623-1630.
79. Kwa, S.L., Lebesque, J.V., Theuws, J.C., Marks, L.B., Munley, M.T., Bentel, G., Oetzel, D., Spahn, U., Graham, M.V., Drzymala, R.E., Purdy, J.A., Lichter, A.S., Martel, M.K., and Ten Haken, R.K. Radiation pneumonitis as a function of mean lung dose: an analysis of pooled data of 540 patients. Int J Radiat Oncol Biol Phys 1998; 42: 1-9.
80. Kwa, S.L., Theuws, J.C., Wagenaar, A., Damen, E.M., Boersma, L.J., Baas, P., Muller, S.H., and Lebesque, J.V. Evaluation of two dose-volume histogram reduction models for the prediction of radiation pneumonitis. Radiother Oncol 1998; 48: 61-69.
81. Lauk, S. Endothelial alkaline phosphatase activity loss as an early stage in the development of radiation-induced heart disease in rats. Radiat Res 1987; 110: 118-128.
82. Lauk, S. and Trott, K.R. Endothelial cell proliferation in the rat heart following local heart irradiation. Int J Radiat Biol 1990; 57: 1017-1030.
83. Law, M.P. and Ahier, R.G. Vascular and epithelial damage in the lung of the mouse after X rays or neutrons. Radiat Res 1989; 117: 128-144.
84. Lee, C.B., Stinchcombe, T.E., Rosenman, J.G., and Socinski, M.A. Therapeutic advances in local-regional therapy for stage III non-small-cell lung cancer: evolving role of dose-escalated conformal (3-dimensional) radiation therapy. Clin Lung Cancer 2006; 8: 195-202.
85. Liao, Z.X., Travis, E.L., and Tucker, S.L. Damage and morbidity from pneumonitis after irradiation of partial volumes of mouse lung. Int J Radiat Oncol Biol Phys 1995; 32: 1359-1370.
86. Lind, P.A., Marks, L.B., Hollis, D., Fan, M., Zhou, S.M., Munley, M.T., Shafman, T.D., Jaszczak, R.J., and Coleman, R.E. Receiver operating characteristic curves to assess predictors of radiation-induced symptomatic lung injury. Int J Radiat Oncol Biol Phys 2002; 54: 340-347.
87. Lyman, J.T. Complication probability as assessed from dose-volume histograms. Radiat Res Suppl 1985; 8: S13-S19.
88. Mah, K., Keane, T.J., Van Dyk, J., Braban, L.E., Poon, P.Y., and Hao, Y. Quantitative effect of combined chemotherapy and fractionated radiotherapy on the incidence of radiation-induced lung damage: a prospective clinical study. Int J Radiat Oncol Biol Phys 1994; 28: 563-574.

89. Mah, K., Van Dyk, J., Keane, T., and Poon, P.Y. Acute radiation-induced pulmonary damage: a clinical study on the response to fractionated radiation therapy. Int J Radiat Oncol Biol Phys 1987; 13: 179-188.
90. Maisin, J.R. The ultrastructure of the lung of mice exposed to a supra-lethal dose of ionizing radiation on the thorax. Radiat Res 1970; 44: 545-564.
91. Marks, L.B. Dosimetric predictors of radiation-induced lung injury. Int J Radiat Oncol Biol Phys 2002; 54: 313-316.
92. Marks, L.B., Fan, M., Clough, R., Munley, M., Bentel, G., Coleman, R.E., Jaszczak, R., Hollis, D., and Anscher, M. Radiation-induced pulmonary injury: symptomatic versus subclinical endpoints. Int J Radiat Biol 2000; 76: 469-475.
93. Marks, L.B., Munley, M.T., Bentel, G.C., Zhou, S.M., Hollis, D., Scarfone, C., Sibley, G.S., Kong, F.M., Jirtle, R., Jaszczak, R., Coleman, R.E., Tapson, V., and Anscher, M. Physical and biological predictors of changes in whole-lung function following thoracic irradiation. Int J Radiat Oncol Biol Phys 1997; 39: 563-570.
94. Marks, L.B., Spencer, D.P., Sherouse, G.W., Bentel, G., Clough, R., Vann, K., Jaszczak, R., Coleman, R.E., and Prosnitz, L.R. The role of three dimensional functional lung imaging in radiation treatment planning: the functional dose-volume histogram. Int J Radiat Oncol Biol Phys 1995; 33: 65-75.
95. Marks, L.B., Yu, X., Vujaskovic, Z., Small, W., Jr., Folz, R., and Anscher, M.S. Radiation-induced lung injury. Semin Radiat Oncol 2003; 13: 333-345.
96. Martel, M.K., Ten Haken, R.K., Hazuka, M.B., Turrisi, A.T., Fraass, B.A., and Lichter, A.S. Dose-volume histogram and 3-D treatment planning evaluation of patients with pneumonitis. Int J Radiat Oncol Biol Phys 1994; 28: 575-581.
97. Martin, M., Lefaix, J., and Delanian, S. TGF-beta1 and radiation fibrosis: a master switch and a specific therapeutic target? Int J Radiat Oncol Biol Phys 2000; 47: 277-290.
98. McDonald, S., Rubin, P., Phillips, T.L., and Marks, L.B. Injury to the lung from cancer therapy: clinical syndromes, measurable endpoints, and potential scoring systems. Int J Radiat Oncol Biol Phys 1995; 31: 1187-1203.
99. Mehta, V. Radiation pneumonitis and pulmonary fibrosis in non-small-cell lung cancer: pulmonary function, prediction, and prevention. Int J Radiat Oncol Biol Phys 2005; 63: 5-24.
100. Mikkelsen, R.B. and Wardman, P. Biological chemistry of reactive oxygen and nitrogen and radiation-induced signal transduction mechanisms. Oncogene 2003; 22: 5734-5754.
101. Miller, K.L., Shafman, T.D., Anscher, M.S., Zhou, S.M., Clough, R.W., Garst, J.L., Crawford, J., Rosenman, J., Socinski, M.A., Blackstock, W., Sibley, G.S., and Marks, L.B. Bronchial stenosis: an underreported complication of high-dose external beam radiotherapy for lung cancer? Int J Radiat Oncol Biol Phys 2005; 61: 64-69.
102. Moiseenko, V.V., Battista, J.J., Hill, R.P., Travis, E.L., and Van Dyk, J. In-field and out-of-field effects in partial volume lung irradiation in rodents: possible correlation between early dna damage and functional endpoints. Int J Radiat Oncol Biol Phys 2000; 48: 1539-1548.
103. Monson, J.M., Stark, P., Reilly, J.J., Sugarbaker, D.J., Strauss, G.M., Swanson, S.J., Decamp, M.M., Mentzer, S.J., and Baldini, E.H. Clinical

radiation pneumonitis and radiographic changes after thoracic radiation therapy for lung carcinoma. Cancer 1998; 82: 842-850.
104. Moore, J.V., Hendry, J.H., and Hunter, R.D. Dose-incidence curves for tumour control and normal tissue injury, in relation to the response of clonogenic cells. Radiother Oncol 1983; 1: 143-157.
105. Morgan, G.W. and Breit, S.N. Radiation and the lung: a reevaluation of the mechanisms mediating pulmonary injury. Int J Radiat Oncol Biol Phys 1995; 31: 361-369.
106. Murdoch, C., Muthana, M., and Lewis, C.E. Hypoxia regulates macrophage functions in inflammation. J Immunol 2005; 175: 6257-6263.
107. Murshed, H., Liu, H.H., Liao, Z., Barker, J.L., Wang, X., Tucker, S.L., Chandra, A., Guerrero, T., Stevens, C., Chang, J.Y., Jeter, M., Cox, J.D., Komaki, R., and Mohan, R. Dose and volume reduction for normal lung using intensity-modulated radiotherapy for advanced-stage non-small-cell lung cancer. Int J Radiat Oncol Biol Phys 2004; 58: 1258-1267.
108. Narai, S., Watanabe, M., Hasegawa, H., Nishibori, H., Endo, T., Kubota, T., and Kitajima, M. Significance of transforming growth factor beta1 as a new tumor marker for colorectal cancer. Int J Cancer 2002; 97: 508-511.
109. Niemierko, A. and Goitein, M. Modeling of normal tissue response to radiation: the critical volume model. Int J Radiat Oncol Biol Phys 1993; 25: 135-145.
110. Oetzel, D., Schraube, P., Hensley, F., Sroka-Perez, G., Menke, M., and Flentje, M. Estimation of pneumonitis risk in three-dimensional treatment planning using dose-volume histogram analysis. Int J Radiat Oncol Biol Phys 1995; 33: 455-460.
111. Overgaard, J. and Horsman, M.R. Overcoming hypoxic cell radioresistance. In: Steel, G.G., editor. Basic clinical radiobiology; London 1997: 141-151.
112. Paris, F., Fuks, Z., Kang, A., Capodieci, P., Juan, G., Ehleiter, D., Haimovitz-Friedman, A., Cordon-Cardo, C., and Kolesnick, R. Endothelial apoptosis as the primary lesion initiating intestinal radiation damage in mice. Science 2001; 293: 293-297.
113. Peacock, J., Ashton, A., Bliss, J., Bush, C., Eady, J., Jackson, C., Owen, R., Regan, J., and Yarnold, J. Cellular radiosensitivity and complication risk after curative radiotherapy. Radiother Oncol 2000; 55: 173-178.
114. Peel, D.M. and Coggle, J.E. The effect of X irradiation on alveolar macrophages in mice. Radiat Res 1980; 81: 10-19.
115. Penland, S.K. and Socinski, M.A. Management of unresectable stage III non-small cell lung cancer: the role of combined chemoradiation. Semin Radiat Oncol 2004; 14: 326-334.
116. Penney, D.P. and Rubin, P. Specific early fine structural changes in the lung irradiation. Int J Radiat Oncol Biol Phys 1977; 2: 1123-1132.
117. Penney, D.P., Siemann, D.W., Rubin, P., Shapiro, D.L., Finkelstein, J., and Cooper, R.A., Jr. Morphologic changes reflecting early and late effects of irradiation of the distal lung of the mouse: a review. Scan Electron Microsc 1982; 413-425.
118. Penney, D.P., Van Houtte, P., Siemann, D.W., Rosenkrans, W.A., Jr., Rubin, P., and Cooper, R.A., Jr. Long term effects of radiation and combined modalities on mouse lung. Scan Electron Microsc 1986; 221-228.
119. Perez, C.A., Pajak, T.F., Rubin, P., Simpson, J.R., Mohiuddin, M., Brady, L.W., Perez-Tamayo, R., and Rotman, M. Long-term observations of the

patterns of failure in patients with unresectable non-oat cell carcinoma of the lung treated with definitive radiotherapy. Report by the Radiation Therapy Oncology Group. Cancer 1987; 59: 1874-1881.
120. Perez, C.A., Stanley, K., Rubin, P., Kramer, S., Brady, L., Perez-Tamayo, R., Brown, G.S., Concannon, J., Rotman, M., and Seydel, H.G. A prospective randomized study of various irradiation doses and fractionation schedules in the treatment of inoperable non-oat-cell carcinoma of the lung. Preliminary report by the Radiation Therapy Oncology Group. Cancer 1980; 45: 2744-2753.
121. Phillips, T.L. An ultrastructural study of the development of radiation injury in the lung. Radiology 1966; 87: 49-54.
122. Puck, T.T. and MARCUS, P.I. Action of x-rays on mammalian cells. J Exp Med 1956; 103: 653-666.
123. Raghu, G. and Kinsella, M. Cytokine effects on extracellular matrix. In: Kelley, J., editor. Cytokines of the lung; New York 1993: 491-543.
124. Roberts, A.B., Thompson, N.L., Heine, U., Flanders, C., and Sporn, M.B. Transforming growth factor-beta: possible roles in carcinogenesis. Br J Cancer 1988; 57: 594-600.
125. Roberts, C.M., Foulcher, E., Zaunders, J.J., Bryant, D.H., Freund, J., Cairns, D., Penny, R., Morgan, G.W., and Breit, S.N. Radiation pneumonitis: a possible lymphocyte-mediated hypersensitivity reaction. Ann Intern Med 1993; 118: 696-700.
126. Robnett, T.J., Machtay, M., Vines, E.F., McKenna, M.G., Algazy, K.M., and McKenna, W.G. Factors predicting severe radiation pneumonitis in patients receiving definitive chemoradiation for lung cancer. Int J Radiat Oncol Biol Phys 2000; 48: 89-94.
127. Rodemann, H.P. and Bamberg, M. Cellular basis of radiation-induced fibrosis. Radiother Oncol 1995; 35: 83-90.
128. Rojas, A.M., Lyn, B.E., Wilson, E.M., Williams, F.J., Shah, N., Dickson, J., and Saunders, M.I. Toxicity and outcome of a phase II trial of taxane-based neoadjuvant chemotherapy and 3-dimensional, conformal, accelerated radiotherapy in locally advanced nonsmall cell lung cancer. Cancer 2006; 107: 1321-1330.
129. Rosenzweig, K.E., Fox, J.L., Yorke, E., Amols, H., Jackson, A., Rusch, V., Kris, M.G., Ling, C.C., and Leibel, S.A. Results of a phase I dose-escalation study using three-dimensional conformal radiotherapy in the treatment of inoperable nonsmall cell lung carcinoma. Cancer 2005; 103: 2118-2127.
130. Rosiello, R.A., Merrill, W.W., Rockwell, S., Carter, D., Cooper, J.A., Jr., Care, S., and Amento, E.P. Radiation pneumonitis. Bronchoalveolar lavage assessment and modulation by a recombinant cytokine. Am Rev Respir Dis 1993; 148: 1671-1676.
131. Roswit, B. and White, D.C. Severe radiation injuries of the lung. AJR Am J Roentgenol 1977; 129: 127-136.
132. Rube, C.E., Uthe, D., Schmid, K.W., Richter, K.D., Wessel, J., Schuck, A., Willich, N., and Rube, C. Dose-dependent induction of transforming growth factor beta (TGF-beta) in the lung tissue of fibrosis-prone mice after thoracic irradiation. Int J Radiat Oncol Biol Phys 2000; 47: 1033-1042.
133. Rubin, P. and Casarett, G.W. Radiation effects on fine vasculature. Respiratory system. In: Rubin, P. and Casarett, G.W. Clinical radiation pathology; Philadelphia 1968: pp. 43-51 and 423-470.

134. Rubin, P., Constine, L.S., and Nelson, D.F. Late effects of cancer treatment. In: Perez, C.A., Brady, L.W., editors. Principles and practice of radiation oncology; Philadelphia 1992: 124-161.
135. Rubin, P., Finkelstein, J., and Shapiro, D. Molecular biology mechanisms in the radiation induction of pulmonary injury syndromes: interrelationship between the alveolar macrophage and the septal fibroblast. Int J Radiat Oncol Biol Phys 1992; 24: 93-101.
136. Rubin, P., Johnston, C.J., Williams, J.P., McDonald, S., and Finkelstein, J.N. A perpetual cascade of cytokines postirradiation leads to pulmonary fibrosis. Int J Radiat Oncol Biol Phys 1995; 33: 99-109.
137. Rubin, P., Shapiro, D.L., Finklestein, J.N., and Penney, D.P. The early release of surfactant following lung irradiation of alveolar type II cells. Int J Radiat Oncol Biol Phys 1980; 6: 75-77.
138. Rubin, P., Siemann, D.W., Shapiro, D.L., Finkelstein, J.N., and Penney, D.P. Surfactant release as an early measure of radiation pneumonitis. Int J Radiat Oncol Biol Phys 1983; 9: 1669-1673.
139. Russell, N.S., Grummels, A., Hart, A.A., Smolders, I.J., Borger, J., Bartelink, H., and Begg, A.C. Low predictive value of intrinsic fibroblast radiosensitivity for fibrosis development following radiotherapy for breast cancer. Int J Radiat Biol 1998; 73: 661-670.
140. Saunders, M., Dische, S., Barrett, A., Harvey, A., Griffiths, G., and Palmar, M. Continuous, hyperfractionated, accelerated radiotherapy (CHART) versus conventional radiotherapy in non-small cell lung cancer: mature data from the randomised multicentre trial. CHART Steering committee. Radiother Oncol 1999; 52: 137-148.
141. Sause, W., Kolesar, P., Taylor S IV, Johnson, D., Livingston, R., Komaki, R., Emami, B., Curran, W., Jr., Byhardt, R., Dar, A.R., and Turrisi, A., III. Final results of phase III trial in regionally advanced unresectable non-small cell lung cancer: Radiation Therapy Oncology Group, Eastern Cooperative Oncology Group, and Southwest Oncology Group. Chest 2000; 117: 358-364.
142. Schmidt-Ullrich, R.K. Molecular targets in radiation oncology. Oncogene 2003; 22: 5730-5733.
143. Schmidt-Ullrich, R.K., Dent, P., Grant, S., Mikkelsen, R.B., and Valerie, K. Signal transduction and cellular radiation responses. Radiat Res 2000; 153: 245-257.
144. Schultz-Hector, S. Radiation-induced heart disease: review of experimental data on dose response and pathogenesis. Int J Radiat Biol 1992; 61: 149-160.
145. Seppenwoolde, Y., De Jaeger, K., Boersma, L.J., Belderbos, J.S., and Lebesque, J.V. Regional differences in lung radiosensitivity after radiotherapy for non-small-cell lung cancer. Int J Radiat Oncol Biol Phys 2004; 60: 748-758.
146. Seppenwoolde, Y. and Lebesque, J.V. Partial irradiation of the lung. Semin Radiat Oncol 2001; 11: 247-258.
147. Seppenwoolde, Y., Lebesque, J.V., De Jaeger, K., Belderbos, J.S., Boersma, L.J., Schilstra, C., Henning, G.T., Hayman, J.A., Martel, M.K., and Ten Haken, R.K. Comparing different NTCP models that predict the incidence of radiation pneumonitis. Normal tissue complication probability. Int J Radiat Oncol Biol Phys 2003; 55: 724-735.

148. Sibley, G.S. Radiotherapy for patients with medically inoperable Stage I nonsmall cell lung carcinoma: smaller volumes and higher doses--a review. Cancer 1998; 82: 433-438.
149. Siemann, D.W., Hill, R.P., and Penney, D.P. Early and late pulmonary toxicity in mice evaluated 180 and 420 days following localized lung irradiation. Radiat Res 1982; 89: 396-407.
150. Slauson, D.O., Hahn, F.F., and Chiffelle, T.L. The pulmonary vascular pathology of experimental radiation pneumonitis. Am J Pathol 1977; 88: 635-654.
151. Stander, M., Naumann, U., Wick, W., and Weller, M. Transforming growth factor-beta and p-21: multiple molecular targets of decorin-mediated suppression of neoplastic growth. Cell Tissue Res 1999; 296: 221-227.
152. Steel, G.G. Introduction: The significance of radiobiology for radiotherapy. In: Steel, G.G., editor. Basic clinical radiobiology; London 1997: 1-7.
153. Stinchcombe, T.E., Fried, D., Morris, D.E., and Socinski, M.A. Combined modality therapy for stage III non-small cell lung cancer. Oncologist 2006; 11: 809-823.
154. Stover, D.E. and Kaner, R.J. Adverse effects of treatment: Pulmonary toxicity. In: De Vita, V.T., Hellman, S., Rosenberg, S.A., editors. Cancer - Principles and practice of oncology; Philadelphia 2001: 2894-2904.
155. Sura, S., Yorke, E., Jackson, A., and Rosenzweig, K.E. High-dose radiotherapy for the treatment of inoperable non-small cell lung cancer. Cancer J 2007; 13: 238-242.
156. Travis, E.L. The sequence of histological changes in mouse lungs after single doses of x-rays. Int J Radiat Oncol Biol Phys 1980; 6: 345-347.
157. Travis, E.L. and Down, J.D. Repair in mouse lung after split doses of X rays. Radiat Res 1981; 87: 166-174.
158. Travis, E.L., Down, J.D., Holmes, S.J., and Hobson, B. Radiation pneumonitis and fibrosis in mouse lung assayed by respiratory frequency and histology. Radiat Res 1980; 84: 133-143.
159. Travis, E.L., Harley, R.A., Fenn, J.O., Klobukowski, C.J., and Hargrove, H.B. Pathologic changes in the lung following single and multi-fraction irradiation. Int J Radiat Oncol Biol Phys 1977; 2: 475-490.
160. Travis, E.L., Liao, Z.X., and Tucker, S.L. Spatial heterogeneity of the volume effect for radiation pneumonitis in mouse lung. Int J Radiat Oncol Biol Phys 1997; 38: 1045-1054.
161. Trott, K.R., Herrmann, T., and Kasper, M. Target cells in radiation pneumopathy. Int J Radiat Oncol Biol Phys 2004; 58: 463-469.
162. Ts'ao, C.H., Ward, W.F., and Port, C.D. Radiation injury in rat lung. I. Prostacyclin (PGI2) production, arterial perfusion, and ultrastructure. Radiat Res 1983; 96: 284-293.
163. Tsujino, K., Hirota, S., Endo, M., Obayashi, K., Kotani, Y., Satouchi, M., Kado, T., and Takada, Y. Predictive value of dose-volume histogram parameters for predicting radiation pneumonitis after concurrent chemoradiation for lung cancer. Int J Radiat Oncol Biol Phys 2003; 55: 110-115.
164. Tucker, S.L., Liao, Z.X., and Travis, E.L. Estimation of the spatial distribution of target cells for radiation pneumonitis in mouse lung. Int J Radiat Oncol Biol Phys 1997; 38: 1055-1066.

165. Van Dyk, J., Keane, T.J., Kan, S., Rider, W.D., and Fryer, C.J. Radiation pneumonitis following large single dose irradiation: a re-evaluation based on absolute dose to lung. Int J Radiat Oncol Biol Phys 1981; 7: 461-467.
166. van Luijk, P. Dose-volume effects in rat spinal cord irradiated with protons. Chapter 6: Modeling. Thesis; Groningen, The Netherlands 2003.
167. Vokes, E.E. Interactions of chemotherapy and radiation. Semin Oncol 1993; 20: 70-79.
168. Vokes, E.E., Crawford, J., Bogart, J., Socinski, M.A., Clamon, G., and Green, M.R. Concurrent chemoradiotherapy for unresectable stage III non-small cell lung cancer. Clin Cancer Res 2005; 11: 5045s-5050s.
169. Vujaskovic, Z., Anscher, M.S., Feng, Q.F., Rabbani, Z.N., Amin, K., Samulski, T.S., Dewhirst, M.W., and Haroon, Z.A. Radiation-induced hypoxia may perpetuate late normal tissue injury. Int J Radiat Oncol Biol Phys 2001; 50: 851-855.
170. Vujaskovic, Z., Marks, L.B., and Anscher, M.S. The physical parameters and molecular events associated with radiation-induced lung toxicity. Semin Radiat Oncol 2000; 10: 296-307.
171. Wahl, S.M. Transforming growth factor beta (TGF-beta) in inflammation: a cause and a cure. J Clin Immunol 1992; 12: 61-74.
172. Wakefield, L.M., Letterio, J.J., Chen, T., Danielpour, D., Allison, R.S., Pai, L.H., Denicoff, A.M., Noone, M.H., Cowan, K.H., O'Shaughnessy, J.A., and . Transforming growth factor-beta1 circulates in normal human plasma and is unchanged in advanced metastatic breast cancer. Clin Cancer Res 1995; 1: 129-136.
173. Wara, W.M., Phillips, T.L., Margolis, L.W., and Smith, V. Radiation pneumonitis: a new approach to the derivation of time-dose factors. Cancer 1973; 32: 547-552.
174. Ward, H.E., Kemsley, L., Davies, L., Holecek, M., and Berend, N. The pulmonary response to sublethal thoracic irradiation in the rat. Radiat Res 1993; 136: 15-21.
175. Ward, W.F., Molteni, A., Ts'ao, C.H., and Solliday, N.H. Pulmonary endothelial dysfunction induced by unilateral as compared to bilateral thoracic irradiation in rats. Radiat Res 1987; 111: 101-106.
176. Werner-Wasik, M., Swann, R.S., Bradley, J., Graham, M., Emami, B., Purdy, J., and Sause, W. Increasing tumor volume is predictive of poor overall and progression-free survival: secondary analysis of the Radiation Therapy Oncology Group 93-11 phase I-II radiation dose-escalation study in patients with inoperable non-small-cell lung cancer. Int J Radiat Oncol Biol Phys 2008; 70: 385-390.
177. Williams, J., Chen, Y., Rubin, P., Finkelstein, J., and Okunieff, P. The biological basis of a comprehensive grading system for the adverse effects of cancer treatment. Semin Radiat Oncol 2003; 13: 182-188.
178. Withers, H.R., Taylor, J.M., and Maciejewski, B. Treatment volume and tissue tolerance. Int J Radiat Oncol Biol Phys 1988; 14: 751-759.
179. Yamada, M., Kudoh, S., Hirata, K., Nakajima, T., and Yoshikawa, J. Risk factors of pneumonitis following chemoradiotherapy for lung cancer. Eur J Cancer 1998; 34: 71-75.
180. Yeung, T.K., Lauk, S., Simmonds, R.H., Hopewell, J.W., and Trott, K.R. Morphological and functional changes in the rat heart after X irradiation: strain differences. Radiat Res 1989; 119: 489-499.

181. Yi, E.S., Bedoya, A., Lee, H., Chin, E., Saunders, W., Kim, S.J., Danielpour, D., Remick, D.G., Yin, S., and Ulich, T.R. Radiation-induced lung injury in vivo: expression of transforming growth factor-beta precedes fibrosis. Inflammation 1996; 20: 339-352.
182. Yorke, E.D., Jackson, A., Rosenzweig, K.E., Braban, L., Leibel, S.A., and Ling, C.C. Correlation of dosimetric factors and radiation pneumonitis for non-small-cell lung cancer patients in a recently completed dose escalation study. Int J Radiat Oncol Biol Phys 2005; 63: 672-682.
183. Yorke, E.D., Jackson, A., Rosenzweig, K.E., Merrick, S.A., Gabrys, D., Venkatraman, E.S., Burman, C.M., Leibel, S.A., and Ling, C.C. Dose-volume factors contributing to the incidence of radiation pneumonitis in non-small-cell lung cancer patients treated with three-dimensional conformal radiation therapy. Int J Radiat Oncol Biol Phys 2002; 54: 329-339.
184. Yorke, E.D., Kutcher, G.J., Jackson, A., and Ling, C.C. Probability of radiation-induced complications in normal tissues with parallel architecture under conditions of uniform whole or partial organ irradiation. Radiother Oncol 1993; 26: 226-237.

CHAPTER 2: Transforming growth factor – β plasma dynamics and post-irradiation lung injury in lung cancer patients

Alena Novakova-Jiresova[a], Mieke M. van Gameren[b], Rob P. Coppes[a/b], Harm H. Kampinga[a], Harry J.M. Groen[c]

[a] Department of Cell Biology, section Radiation and Stress Cell Biology

[b] Department of Radiation Oncology

[c] Department of Pulmonary Diseases

University Medical Center Groningen, University of Groningen, The Netherlands

Radiotherapy and Oncology 2004; 71: 183-189.

Abstract

Purpose: To investigate the relevance of transforming growth factor-β (TGF-β) dynamics in plasma for identification of patients at low risk for developing pneumonitis as a complication of thoracic radiotherapy (RT).

Patients and methods: Non-small cell lung cancer patients undergoing conventional RT were included in the prospective study. Concentrations of TGF-β were measured in the patients' plasma prior to and weekly during 6 weeks of RT. The incidence of symptoms of early post-irradiation lung injury, i.e. symptomatic radiation pneumonitis, was correlated with TGF-β parameters.

Results: 46 patients were included in the study. 11 patients (24%) developed symptomatic radiation pneumonitis. Absolute TGF-β plasma levels did not differ between the groups of patients without or with pneumonitis. However, patients who developed pneumonitis tended to show increases in TGF-β levels in the middle of the RT course relative to their pre-treatment levels while TGF-β plasma levels of patients who did not develop pneumonitis tended to decrease over the RT treatment. The

difference in the relative TGF-β dynamics between the groups reached marginal significance in the 3rd week of the treatment (p=0.055) but weakened towards the end of the RT course. The utility of TGF-β testing was evaluated at each RT week based on the test's ability to yield more accurate estimate of complication probability in an individual patient compared to empirically expected probability in similar group of patients. The ratio of TGF-β level at week 3/week 0 being < 1 showed an ability to improve the prediction of freedom from pneumonitis, yet with a large degree of uncertainty (wide confidence intervals). The accuracy of prediction deteriorated at later time points (weeks 4, 5 and 6) rendering the end-RT ratios without predictive power.

Conclusions: We observed a trend of plasma TGF-β concentration to decrease below the pre-treatment value during the RT treatment in patients who did not develop pulmonary complications after the RT treatment. However, this trend was not consistent enough to warrant safe decision-making in clinical setting.

2.1 Introduction

A failure to maintain local control after the curative RT for non-small cell lung cancer (NSCLC) remains to be an important cause of poor survival in inoperable lung cancer patients [4]. It has been long accepted that the prescribed radiation doses in the range of 60-70 Gy delivered in the conventional RT are insufficient for eradicating the tumour [18]. The more recent estimates placed the dose required for achieving a significant probability of durable tumour control in the vicinity of 84 Gy [34]. Yet, already the conventional doses cause respiratory complications in as many as 20 % of the treated patients [17,23,39]. A sub-acute, inflammatory phase of lung tissue injury, radiation pneumonitis, followed by chronic progressive fibrosis poses a great threat to the patient and limits the dose that can be safely delivered to the target volume. The possible approaches how to obviate this obstacle include improvements of the physical parameters of the dose-delivery (IMRT, image guided radiotherapy) as well as biological optimisation of the treatment planning. An intensive search for biological variables that would identify patients suitable for dose-escalation at the end of the conventional treatment is ongoing. With regard to this, pre-RT pulmonary function tests [23,32,33], SPECT-based treatment planning [33] as well as cytokine effects [3,4,5,6,9,13,15,19,33,41,42] have been amply discussed in the literature.

The cytokine TGF-β has been implicated in the development and perpetuation of the post-irradiation injury in various tissues, including the lung [35,38]. TGF-β is known to be upregulated in normal tissues damaged by radiation [2,36,38] as well as to be overproduced by tumours [14,25]. Although the basis for its autocrine and paracrine mode of action is well established, the endocrine effects have been debated. TGF-β is secreted as an inactive, latent complex with non-covalently bound latency associated peptide. This bond must be cleaved by proteolytic enzymes or presence of free radicals to enable signalling through the TGF-β membrane receptors on target cells [10,31]. Physiologically, TGF-β circulates in blood in its latent form or complexed with plasma proteins, the likely source being thrombocytes, white blood cells [22] or bone matrix [43]. Out of the three known isoforms, TGF-β1 is the predominant isoform in human plasma, TGF-β2 and β3 accounting for less than 5% of its total plasma concentration in healthy subjects [43]. Plasma TGF-β1 is also the most extensively studied isoform in cancer patients although, occasionally, elevations in the two other isoforms have also been detected [28,29,43]. Regarding the activity,

increases in both, latent and active TGF-β1, have been reported in plasma of cancer patients [11,24,25,26,27,37]. While the 25 kD active TGF-β1 molecule has a plasma half-life of only 2-3 min and is rapidly sequestrated by and degraded in the liver [44], the evidence for ability of the large latent complex to cross the vascular endothelium in any direction is lacking [22]. However, a hypothesis has been put forward that damaged vasculature at the site of post-irradiation tissue injury or in a tumour stroma could allow leakage of the latent TGF-β1 between plasma and tissues providing a basis for its endocrine action [4].

In clinical setting, about half of the patients with NSCLC presents with elevated plasma TGF-β1 levels before treatment, most likely due to the TGF-β1 over-production by their tumours [3,26,27]. A normalisation of plasma TGF-β1 level by the end of RT has been linked to a lower risk of pulmonary complications after the treatment in several clinical trials [3,5,9,19,41]. Dynamics of TGF-β1 in plasma were suggested as a marker of RT-induced normal tissue injury as well as tumour response. It was proposed that this marker might be utilised in clinic for selecting patients at low risk of complications suitable for RT dose-escalation [3,7,8].

In this study, we assessed the value of TGF-β measurements in predicting freedom from symptomatic radiation pneumonitis in a group of NSCLC patients treated with conventional thoracic RT. A preliminary analysis of the subset of our data has been already published [41].

2.2 Patients and methods

Patient eligibility: Lung cancer patients from an outpatient clinic of the Department of Pulmonary Diseases at the University Hospital of Groningen, the Netherlands, were included in the prospective study. They had to fulfil the following criteria: age ≤ 76 years, locally unresectable stage IIIA or IIIB NSCLC proven either by mediastionoscopy, explorative thoracotomy, or clinically by involvement of the phrenic or recurrent nerve, Eastern Cooperative Oncology Group (ECOG) performance score ≤ 2, weight loss < 10%, serum creatinine ≤ 120 μmol/l or creatinine clearence ≥ 60 ml/min, serum bilirubin ≤ 2.0 mg/dl, leukocytes ≥ 3.0×10^9/l and thrombocytes ≥ 100×10^9/l. Ineligible were patients with prior chemo- or radiotherapy. Pulmonary function tests (PFT) including total lung capacity (TLC), vital capacity (VC), forced expiratory volume in 1 second (FEV_1), CO diffusing

capacity corrected for alveolar volume (K_{CO}), pulmonary capillary blood volume (Vcap) and membrane diffusing factor (D_M) were obtained before RT. The measured values were expressed as per cent of predicted value. Written informed consent was obtained from all patients. The study was approved by the Medical Ethical Committee of the University Hospital of Groningen.

Treatment: Curative conventional thoracic RT was delivered using a linear accelerator (6 MV photons) in 2 Gy daily fractions, 5 fractions a week, over a total treatment time of 6 weeks. The initial planning target volume (PTV1) encompassed all visible local and regional disease with a 2 cm margin based on the thoracic CT scan prior to the start of the treatment. Further, PTV1 included the mediastinum from 2 cm above the suprasternal notch to 5 cm below the carina, extending 2 cm across the midline. The reduced planning target volume (PTV2) contained only the local and regional disease with a 1cm margin. The PTV1 and PTV2 received total doses of 40 Gy and 60 Gy, respectively. The area of the initial anterior-posterior irradiation portal (till 40 Gy) minus blocks in cm^2 and the PTV2 volume in cm^3 were calculated for each patient.

Endpoint: The clinical evaluation of patients was performed weekly during the course of RT, 6 weeks after completion of RT, then every 3 months during the 1^{st} year, every 6 months during the 2^{nd} and 3^{rd} year and once a year thereafter. The endpoint of the study was the development of symptomatic radiation pneumonitis. The scoring system of the National Cancer Institute Common Toxicity Criteria (CTC) version 2 was used. Scoring was performed without a knowledge of the TGF-β levels in plasma.

Patient characteristics: 46 subsequent patients were included. All were tobacco smokers. In 30 patients, carboplatinum (Carboplatin, Bristol Meyers Squibb) was administered concurrently with radiotherapy as a radiosensitizer in a total dose of 860 mg/m^2 in a continuous infusion over 6 weeks. 11 patients developed radiation pneumonitis and 35 showed no symptoms. The patient and treatment related characteristics of the two patient groups are presented in Table 1. None of the featured variables differed significantly between the groups.

Plasma TGF-β quantification: Blood samples were collected from patients prior to and then weekly during the 6 weeks of RT. Blood was drawn without placing a tourniquet on a patient's arm to prevent thrombocyte degranulation. Blood was

collected in tubes containing 7.5% K_3 EDTA and immediately placed on ice. The samples were centrifuged at 4°C for 30 min at 1000g within 1 h upon collection. The plasma for TGF-β determination was withdrawn from the middle of the plasma column avoiding the platelet interface. It was stored at –80°C until analysis. TGF-β concentration in plasma was measured in a bioassay with mink lung epithelial cells (MLEC) permanently transfected with a reporter gene construct, plasminogen activator inhibitor-1 (PAI-1) promoter fused to the firefly luciferase gene [1,40]. This bioassay is based on the ability of TGF-β to specifically induce PAI-1 expression. The binding of TGF-β to the MLEC cells results in a dose-dependent increase in luciferase activity in the cell lysate. The assay can not distinguish between the three TGF-β isoforms [1]. Therefore, we use the term TGF-β without the numeric index in our study although TGF-β1 is expected to account for the vast majority of the measured TGF-β concentration [40]. Since an acid-activation step was performed at the start of the assay, only total TGF-β (active + latent form) was detected. The detection limit was 0.1 ng/ml. All sequential samples from one particular patient were analysed simultaneously in one multi-well plate to ensure identical conditions of the assay procedure. The control group used for determination of the physiologic plasma TGF-β value consisted of healthy volunteers described earlier [40]. The mean control plasma TGF-β value in our study was 7,2 ± SD 2,8 ng / ml. The mean control value + 2 SD (= 12.8 ng/ml) was regarded as a cut-off between normal and pathologically elevated TGF-β levels. The TGF-β levels in plasma of each individual patient were expressed both as absolute concentration (ng/ml) and as relative parameters, i.e. ratios of a value from a particular week of RT divided by the pre-RT value (w1/0, w2/0 etc.). The ratios were available only in 33 patients as 13 patients lacked week 0 value due to logistic reasons. The number of patients evaluable at each particular time-point is given in Table 2.

Statistical analysis: Univariate and multivariate methods were applied to study the relation between the pneumonitis incidence (as binary variable) and various potentially predictive variables. We used the non-parametric Mann-Whitney U-test for the univariate evaluation of continuous predictive variables (age, pre-RT PFT, initial radiation field area, PTV2, absolute TGF-β levels and TGF-β ratios at each individual time point) and the Pearson chi-squared test for the univariate evaluation of categorical predictive variables (PS, stage, carboplatinum administration). The

Table 1

Patient characteristics

Variable	Without pneumonitis	With pneumonitis
	n = 35	n = 11
Median age (years)	62 (range 45 – 76)	65 (range 44 – 76)
Sex (male / female)	34 / 1	10 / 1
PS (= 0 / 1 / 2)	14 / 18 / 3	4 / 7 / 0
Stage (IIIA / IIIB)	15 / 20	7 / 4
Histology SSC / AC / LCC	16 / 8 / 11	7 / 3 / 1
Mean TLC (± SD)	88.7 (± 15.4)	84.9 (±10.9)
Mean VC (± SD)	89.7 (± 20.5)	81.6 (± 14.8)
Mean FEV_1 (± SD)	69.7 (± 17.5)	61.8 (± 17.2)
Mean K_{CO} (± SD)	112.1 (± 18.5)	107.8 (± 37.1)
Mean Vcap (± SD)	74.1 (± 19.7)	64.8 (± 13.8)
Mean D_M (± SD)	87.2 (± 20.4)	72.6 (± 17.2)
Carboplatinum	22	8
Mean field area (cm^2)	236 (range 104 – 352)	227 (range 176 – 293)
Mean PTV2 (cm^3)	776 (range 198 – 4445)	570 (range 161 – 1028)

PS = performance score.
SCC = sqaumous cell carcinoma, AC = adenocarcinoma, LCC = large cell carcinoma.
Mean TLC, VC, FEV_1, K_{CO}, Vcap, D_M = mean percent predicted values of PFT prior to RT.
Mean field area = the area of the initial anterior-posterior irradiation portal (till 40 Gy) minus blocks.

combined effects of the predictive variables were evaluated in multivariate analysis (multiple logistic regression). The number of cases included in the regression varied from analysis to analysis depending on the missing values of TGF-β parameters and thus its results are to be viewed as explorative. We used 5% as the nominal level of statistical significance. Exact P-values were calculated where appropriate. Calculations were performed in the SPSS software package version 10.0. Further, to describe the predictive properties of the plasma TGF-β dynamics (i.e. the ratios being ≥ 1 or < 1 and presence or absence of pneumonitis), we calculated sensitivity,

specificity, positive and negative predictive values and the corresponding 95% confidence intervals separately for each week of the RT treatment. The 95% confidence intervals (95% CI) were calculated by the exact method.

2.3 Results

Of the 46 included patients, 11 (24%) developed radiation pneumonitis within 6 months after RT. The severity of pneumonitis was of grade 1 in 5 patients, grade 2 in 3 patients and grade 3 in 3 patients. The median follow-up was 51 weeks (range 11 to 230+ weeks). The pre-RT TGF-β level in plasma was elevated above the cut-off in 30 (91%) out of 33 measured patients.

The TGF-β variables compared between the groups of patients not developing or developing pneumonitis are summarised in Table 2. Regarding the absolute TGF-β plasma levels from week 0 to 6 (only w.0, w.3 and w.6 values shown in the table), there were no significant differences between the groups. Also, most of the relative TGF-β parameters did not differ with an exception of week 3 / week 0 ratio (w3/0) that was borderline significantly higher in the pneumonitis group (p=0.055, Mann-Whitney U-test).

The dynamics in relative TGF-β changes are visualised in Figure 1. A striking observation was the large variability of the ratio values in the pneumonitis group. Between weeks 1 and 5, the 75^{th} and the 97.5^{th} percentiles of the pneumonitis group encompassed higher ratio values than the same percentiles in the group without symptoms. This suggested that the plasma TGF-β concentrations in patients subsequently developing pneumonitis tended to rise above the pre-RT value during the first 5 weeks of the treatment, while patients not developing pneumonitis had much narrower spread of the ratio values fluctuating around or just below 1. The difference disappeared at 6 weeks. Nevertheless, due to the large variability, the difference between the groups reached only borderline significance and that only at week 3 (Table 2).

Therefore we tested the clinical utility of the relative TGF-β parameters for detection of patients at low risk of radiation pneumonitis in our set of patients. Ratios from w3/0 to w6/0 were assessed separately (Table 3). Patients were considered to be a true positive if their ratio was ≥ 1 and they developed pneumonitis. They were considered a true negative if their ratio was < 1 and they did not develop pneumonitis.

Table 2

TGF-β variables – comparison between patients developing or not developing pneumonitis

Variable	Without pneumonitis	With pneumonitis	p value
Median absolute TGF-β concentration (with range) from *n* evaluable patients			
w0	39.9 (7.1-85.7) *n=24*	45.8 (10.6-106.4) *n= 9*	0.65
w3	40.9 (2.2-118.5) *n=30*	36.1 (13.1-147.0) *n= 9*	0.88
w6	36.6 (10.4-115.1) *n=15*	38.2 (7.3-74.7) *n= 6*	0.97
Median TGF-β ratio (with range) from *n* evaluable patients			
w1/0	0.98 (0.38-3.27) *n=21*	1.12 (0.16-2.91) *n= 8*	0.76
w2/0	1.01 (0.18-4.03) *n=20*	1.38 (0.25-1.86) *n= 7*	0.31
w3/0	1.02 (0.09-1.65) *n=20*	1.41 (0.32-3.45) *n= 7*	0.055
w4/0	0.91 (0.19-1.76) *n=20*	0.95 (0.24-4.17) *n= 7*	0.73
w5/0	0.88 (0.07-1.42) *n=18*	0.98 (0.13-6.49) *n= 7*	0.66
w6/0	0.73 (0.32-1.71) *n= 8*	0.61 (0.18-3.29) *n= 5*	0.72

w0, w3, w6 = median absolute pre-, mid- and end-RT concentrations of TGF-β in plasma (ng/ml); w1/0 - w6/0 = median ratios of the TGF-β plasma concentration at a particular week relative to the pre-RT concentration.
P-value (exact) obtained from a comparison by the Mann-Whitney U-test.

It is apparent from Table 3 that the best prediction of freedom from pneumonitis was achieved when using the mid-RT parameter (the ratio of w3/0) as documented by the negative predictive value = 91%. However, a large uncertainty was associated with this value (95% CI ranging from 59 to 100%). Thus, if the overall pneumonitis probability in this set of patients was 24%, the negative test outcome at the 3rd week of the RT treatment could revise the probability to 9% (i.e. 100 minus 91), or perhaps to 41% or 0% (i.e. 100 minus 59 or 100). The accuracy of the prediction diminished further at the later time points (weeks 4, 5 and 6). This confirmed the observation made already in Table 2 and Figure 1: that only the w3/0 TGF-β ratio was able to make some distinction between patients developing or not developing pneumonitis.

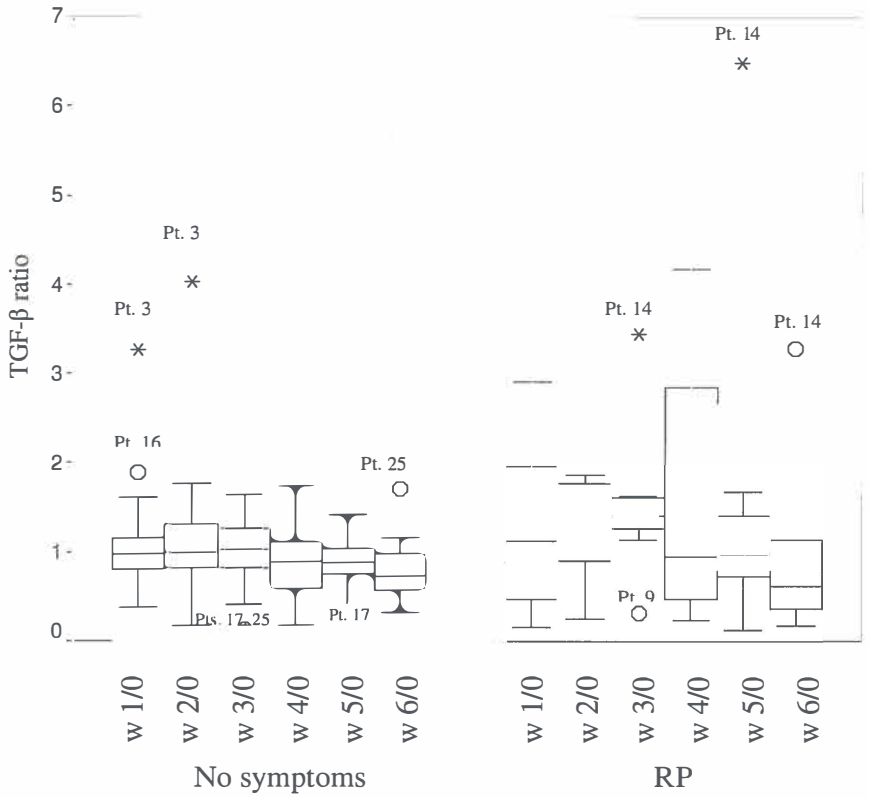

Figure 1: Plasma TGF-β levels during 6 weeks of radiotherapy relative to the pretreatment TGF-β level expressed as ratios of the value at a particular week over the pre-RT value (i.e. w1/0 – w6/0). The ratios were plotted separately for the group without pneumonitis ("No symptoms") and with pneumonitis ("RP"). The boxes indicate the 25th and the 75th percentile (the lower and upper edge, respectively), the central line represents the median. Median numeric values and numbers of patients evaluable at each time point can be found in Table 2. The points at the ends of the whiskers are the 2.5th and the 97.5th percentiles. Outliers (circles) and extreme values (stars) are plotted individually with a patient serial number. The difference between the groups was borderline significant (p=0.055, Man-Whitney U-test) only for the ratio w3/0 (dashed boxes).

Table 3
Test-performance characteristics of the TGF-β ratios in relation to radiation pneumonitis

Ratio	w3/0	w4/0	w5/0	w6/0
n evaluable patients	n=27	n=27	n=25	n=13
Sensitivity	86 %	43 %	43 %	40 %
Specificity	50 %	55 %	72 %	75 %
Positive predictive value	38 %	25 %	38 %	50 %
(with 95% CI)	(15 - 65%)	(5 - 57%)	(9 - 76%)	(7 - 93%)
Negative predictive value	91 %	73 %	77 %	67 %
(with 95% CI)	(59 - 100%)	(45 - 92%)	(50 - 93%)	(30 - 93%)

Numbers were rounded up.

Finally, the relationship between pneumonitis incidence and variables presented in tables 1 and 2 (age, PS, stage, pre-RT PFT, initial radiation field area till 40Gy, PTV2, absolute plasma concentrations of TGF-β and TGF-β ratios from all weeks) was evaluated in multivariate analysis. None of the results reached statistical significance.

In conclusion, the transience and weakness of the observed link between plasma TGF-β and pulmonary symptoms in this set of patients would imply that the power of TGF-β dynamics to predict radiation pneumonitis (or freedom from it) is rather low. Moreover, closer examination of the only time point that demonstrated some predictive power revealed more reasons for caution. Three patients with the highest w3/0 ratios (> 1.5) in the pneumonitis group tended to have a low pre-treatment TGF-β values (w0 = 10.6, 16.9 and 11.7 ng/ml) below or close to the cut-off of 12.8 ng/ml. In contrast, the pre-treatment values were generally elevated in remaining patients from both groups (only 2 more patients had initial TGF-β < 20 ng/ml). Thus, the three highest ratios in the pneumonitis group at week 3 were, in fact, result of only minor absolute increases in plasma TGF-β concentration in two out of three cases. This questions the mechanism behind the putative association between the pneumonitis risk and relative increases in TGF-β plasma levels.

2.4 Discussion

Many efforts in radiotherapy focus on the determination of clinically useful indicators that would discriminate between patients with high or low risk of pulmonary complications after RT treatment of thoracic tumours. This would allow selection of patients in whom the radiation dose to the tumour could be safely escalated to ensure a cure.

TGF-β1 is a ubiquitous immunomodulatory and profibrotic cytokine that plays a major role in tissue responses to irradiation. A link between rising plasma TGF-β1 level during the thoracic RT treatment and the subsequent development of radiation pneumonitis has been presented in the literature [4,42]. Two possible sources of rising plasma TGF-β1 have been suggested by these authors. First, the tumour stroma could be a source. When a tumour would not respond to therapy, its stroma would keep on producing increasing amounts of the cytokine. Second, the gradually accumulating normal tissue damage within the irradiation field would be expected to launch TGF-β1 production in the injured site. Under physiological circumstances, the locally produced TGF-β1 would not be likely to transit into the circulation [22]. However, the vasculature is often defective in both the tumours and normal tissue damaged by radiation. Therefore, it is believed to be possible for the excessive TGF-β1 to leak into the circulation and to be detected in plasma as a possible marker of tumour response and normal tissue injury [4,42]. At the same time, the TGF-β1 is believed to leak back to the site of the injury, become activated and augment local processes leading later to the manifestation of radiation pneumonitis and fibrosis. This hypothesis is based on clinically observed association between rising plasma TGF-β1 levels towards the end of thoracic RT and increased incidence of pulmonary complications in several studies involving mostly lung cancer patients [3,5,9,19,41]. Also for radiation-induced fibrosis of the breast, an association with high TGF-β1 levels in plasma (pre-treatment) was reported [30].

Our current data, however, do not support the notion that TGF-β values in plasma could be used to identify patients at low risk for developing radiation pneumonitis. Although we found a mid-treatment rise in the relative plasma TGF-β values in patients who developed pneumonitis and not in those who did not develop symptoms of pulmonary injury, the predictive power of this observation was rather low. Further, no relation was detected between pneumonitis and absolute pre-

treatment TGF-β values or other than mid-treatment relative changes. Especially the end/pre-RT TGF-β ratio was suggested as the most reliable identifier of patients at low risk of radiation-induced pulmonary symptoms in earlier studies [3,5,7,8,9,19]. Our finding that we particularly lose significant relationship at these end/pre-RT ratios rises questions about the importance of the timing of TGF-β dynamics assessment that would ensure clinical reliability of the parameter.

Our study is in agreement with studies of Marks et al [33] and Chen et al [13] that also failed to find relationship between TGF-β parameters and radiation-induced pulmonary symptoms. Whereas the data by Chen et al [13] may have been confounded by the use of heparin as an anticoagulant in blood collection tubes, with a higher risk of platelet degranulation [40,43], this can not explain the negative results of Marks et al [33] or ourselves. Lack of association between plasma TGF-β1 levels and late morbidity following radiotherapy for stage I-III cervical carcinoma [16] or abnormal wound healing in skin [12] further questions the power of this parameter to discriminate between patients at risk or not at risk of radiation-induced complications.

So, what could be the reason for the conflicting results with regards to the TGF-β plasma levels and radiation-induced complications? We can only speculate. First, for the time point of week 3 of the RT treatment where we found a weak association, the results were dominated by patients with low pre-treatment values. Here, even small changes in absolute TGF-β concentration could have spuriously large effects on ratio calculations. So far, the notion that a minimal rise in plasma TGF-β level predisposed some patients to pneumonitis while massively elevated but persistent levels had no consequences in other patients lacks a pathophysiological explanation. Secondly, in case of respiratory function, the clinical outcome may be influenced by treatment related dysfunction of other organs (e.g. the heart) on which TGF-β plasma levels might have less impact. In that aspect, selecting patients for dose-escalation based on one sole parameter like TGF-β dynamics might be dangerously simplistic approach. Finally, as mentioned above, changes in plasma levels of TGF-β can be caused by two, partly counteractive, mechanisms. On one hand, plasma levels may decrease due to the death of the TGF-β producing tumour stromal cells following radiation. On the other hand, radiation may increase the plasma TGF-β pool due to elevated production of the cytokine by cells in injured normal tissues from which leakage to the circulating system may occur depending on the level of damage to the endothelium. With respect to the latter, a recent dose

escalation study for lung cancer by de Jaeger et al [15] is worth mentioning. Like in the current study, no relation between changes in circulating TGF-β1 and the development of symptomatic radiation pneumonitis was found. However, a clear relation between mean lung dose and plasma TGF-β1 levels at the end of radiotherapy was detected. The increases in the cytokine concentration could be linked only to the radiation-induced normal tissue injury as patients with non-responding tumours ("progressive disease") were excluded from the study. Such a finding corroborates our conclusion that, although the extent of radiation-induced pulmonary injury may be reflected in rising plasma TGF-β levels, the strength of the association is too variable to serve as a reliable predictor of manifestation of symptoms.

We could not evaluate the influence of radiation dose because all patients were treated to a constant total dose of 60 Gy. However, the irradiated volume ranged considerably. Despite that, no relationship between irradiated volume and incidence of pneumonitis was detected in this study. This may be a consequence of unavailability of 3D dosimetry data.

In conclusion, we report a weak predictive association between mid-treatment plasma TGF-β dynamics and low risk of symptomatic radiation pneumonitis in the set of lung cancer patients treated by conventional RT. However, together with the existing conflicting data from the literature, we feel it is justified to conclude that the predictive power of the sole TGF-β parameter is too unstable to warrant a reliable use in clinical decision-making.

Acknowledgements

The authors thank Dr. Vaclav Fidler for his indispensable advice regarding the statistical analysis of the data and Mrs. M.A.W.H. van Waarde and Mrs. A.J. van Assen for an excellent technical support.

References

[1] Abe M, Harpel JG, Metz CN, Nunes I, Loskutoff DJ and Rifkin DB. An assay for transforming growth factor-beta using cells transfected with a plasminogen activator inhibitor-1 promoter-luciferase construct. Anal. Biochem. 1994;216:276-284.

[2] Anscher MS, Crocker IR and Jirtle RL. Transforming growth factor-β1 expression in irradiated liver. Radiat. Res. 1990;122:77-85.

[3] Anscher MS, Kong F-M, Andrews K et al. Plasma transforming growth factor β1 as a predictor of radiation pneumonitis. Int. J. Radiat. Oncol. Biol. Phys. 1998;41:1029-1035.

[4] Anscher MS, Kong F-M and Jirtle RL. The relevance of transforming growth factor β1 in pulmonary injury after radiation therapy. Lung Cancer 1998;19:109-120.

[5] Anscher MS, Kong F-M, Marks LB, Bentel GC and Jirtle RL. Changes in plasma transforming growth factor beta during radiotherapy and the risk of symptomatic radiation-induced pneumonitis. Int. J. Radiat. Oncol. Biol. Phys. 1997;37:253-258.

[6] Anscher MS, Kong F-M, Murase T and Jirtle RL. Short communication: Normal tissue injury after cancer therapy is a local response exacerbated by an endocrine effect of TGFβ. Br. J. Radiol. 1995;68:331-333.

[7] Anscher MS, Marks LB, Shafman TD et al. Using plasma transforming growth factor beta-1 during radiotherapy to select patients for dose escalation. J. Clin. Oncol. 2001;19: 3758-3765.

[8] Anscher MS, Marks LB, Shafman TD et al. Risk of long-term complications after TFG-beta1-guided very-high-dose thoracic radiotherapy. Int. J. Radiat. Oncol. Biol. Phys. 2003;56: 988-995.

[9] Anscher MS, Murase T, Prescott DM et al. Changes in plasma TGFβ levels during pulmonary radiotherapy as a predictor of the risk of developing radiation pneumonitis. Int. J. Radiat. Oncol. Biol. Phys. 1994;30:671-676.

[10] Barcellos-Hoff MH, Derynck R, Tsang ML-S and Weatherbee JA. Transforming growth factor-β activation in irradiated murine mammary gland. J. Clin. Invest. 1994;93:892-899.

[11] Barthelemy-Brichant N, David JL, Bosquee L et al. Increased TGFbeta1 plasma level in patients with lung cancer: potential mechanisms. Eur. J. Clin. Invest. 2002; 32: 193-198.

[12] Bayat A, Bock O, Mrowietz U, Ollier WE and Ferguson MW. Genetic susceptibility to keloid disease and hypertrophic scarring: transforming growth factor beta1 common polymorphisms and plasma levels. Plast. Reconstr. Surg. 2003;111:535-543.

[13] Chen Y, Williams J, Ding I et al. Radiation pneumonitis and early circulatory cytokine markers. Semin. Radiat. Oncol. 2002;12:26-33.

[14] de Caestecker MP, Piek E and Roberts AB. Role of transforming growth factor-β signaling in cancer. J. Natl. Cancer Inst. 2000;92:1388-1402.

[15] de Jaeger K, Seppenwoolde Y, Kampinga HH, Boersma LJ, Belderbos JSA and Lebesque JV. Significance of plasma transforming growth factor-β levels for radiotherapy of non-small cell lung cancer. Int. J. Radiat. Oncol. Biol. Phys. (in press)

[16] Dickson J, Davidson SE, Hunter RD and West CM. Pretreatment plasma TGF beta 1 levels are prognostic for survival but not morbidity following radiation therapy of carcinoma of the cervix. Int. J. Radiat. Oncol. Biol. Phys. 2000;48:991-995.

[17] Emami B and Perez CA. Lung. In: Perez CA, Brady LW, editors. Principles and Practice of Radiation Oncology. 2nd Edition, Philadelphia: J. B. Lippincott Company. 1992;p.829.

[18] Fletcher GH. Clinical dose-response curves of human malignant epithelial tumours. Br. J. Radiol. 1973;46:1-12.

[19] Fu X-L, Huang H, Bentel G et al. Predicting the risk of symptomatic radiation-induced lung injury using both the physical and biologic parameters V_{30} and transforming growth factor β. Int. J. Radiat. Oncol. Biol. Phys. 2001;50:899-908.

[20] Gallagher EJ. Clinical utility of likelihood ratios. Ann. Emerg. Med. 1998;31:391-397.

[21] Giard RW and Hermans J. The diagnostic information of tests for the detection of cancer: the usefulness of the likelihood ratio concept. Eur. J. Cancer 1996;32A:2042-2048.

[22] Grainger DJ, Mosedale DE and Metcalfe JC. TGF-β in blood: a complex problem. Cytokine Growth Factor Rev. 2000;11:133-145.

[23] Hernando ML, Marks LB, Bentel GC et al. Radiation-induced pulmonary toxicity: a dose-volume histogram analysis in 201 patients with lung cancer. Int. J. Radiat. Oncol. Biol. Phys. 2001;51:650-659.

[24] Junker U, Knoefel B, Nuske K et al. Transforming growth factor beta 1 is significantly elevated in plasma of patients suffering from renal cell carcinoma. Cytokine 1996;8:794-798.

[25] Kong F-M, Anscher MS, Murase T, Abbott BD, Iglehart JD and Jirtle RL. Elevated plasma transforming growth factor-β_1 levels in breast cancer patients decrease after surgical removal of the tumor. Ann. Surg. 1995;222:155-162.

[26] Kong F, Jirtle RL, Huang DH, Clough RW and Anscher MS. Plasma transforming growth factor-beta1 level before radiotherapy correlates with long term outcome of patients with lung carcinoma. Cancer 1999;86:1712-1719.

[27] Kong F-M, Washington MK, Jirtle RL and Anscher MS. Plasma transforming growth factor-β1 reflects disease status in patients with lung cancer after radiotherapy: a possible tumor marker. Lung Cancer 1996;16:47-59.

[28] Krasagakis K, Tholke D, Farthmann B, Eberle J, Mansmann U and Orfanos CE. Elevated plasma levels of transforming growth factor (TGF)-beta1 and TGF-beta2 in patients with disseminated malignant melanoma. Br. J. Cancer 1998;77:1492-1494.

[29] Li C, Wang J, Wilson PB et al. Role of transforming growth factor beta3 in lymphatic
metastasis in breast cancer. Int. J. Cancer 1998;79:455-459.

[30] Li C, Wilson PB, Levine E, Barber J, Stewart AL and Kumar S. TGF-beta1 levels in pre-treatment plasma identify breast cancer patients at risk of developing post-radiotherapy fibrosis. Int. J. Cancer 1999;84:155-159.

[31] Lyons RM, Gentry LE, Purchio AF and Moses HL. Mechanism of activation of latent recombinant transforming growth factor β1 by plasmin. J. Cell Biol. 1990;110:1361-1367.

[32] Marks LB, Fan M, Clough R et al. Radiation-induced pulmonary injury: symptomatic versus subclinical endpoints. Int. J. Radiat. Biol. 2000;76:469-475.

[33] Marks LB, Munley MT, Bentel GC et al. Physical and biological predictors of changes in whole-lung function following thoracic irradiation. Int. J. Radiat. Oncol. Biol. Phys. 1997;39:563-570.

[34] Martel MK, Ten Haken RK, Hazuka MB et al. Estimation of tumor control probability model parameters from 3-D dose distributions of non-small cell lung cancer patients. Lung Cancer 1999;24:31-37.

[35] Martin M, Lefaix J-L and Delanian S. TGF-β1 and radiation fibrosis: a master switch and a specific therapeutic target? Int. J. Radiat. Oncol. Biol. Phys. 2000;47:277-290.

[36] Martin M, Lefaix J-L, Pinton P, Crechet F and Daburon F. Temporal modulation of TGF-β1 and β-actin gene expression in pig skin and muscular fibrosis after ionizing radiation. Radiat. Res. 1993;134:63-70.

[37] Narai S, Watanabe M, Hasegawa H et al. Significance of transforming growth factor beta1 as a new tumor marker for colorectal cancer. Int. J. Cancer 2002;97:508-511.

[38] Rubin P, Johnston CJ, Williams JP, McDonald S and Finkelstein JN. A perpetual cascade of cytokines postirradiation leads to pulmonary fibrosis. Int. J. Radiat. Oncol. Biol. Phys. 1995;33:99-109.

[39] Saunders M, Dische S, Barrett A, Harvey A, Griffiths G and Parmar M (on behalf of the CHART Steering committee). Continuous, hyperfractionated, accelerated radiotherapy (CHART) versus conventional radiotherapy in non-small cell lung cancer: mature data from the randomised multicentre trial. Radiother. Oncol. 1999;52:137-148.

[40] van Waarde MAWH, van Assen AJ, Kampinga HH, Konings AWT and Vujaskovic Z. Quantification of transforming growth factor-β in biological material using cells transfected with a plasminogen activator inhibitor-1 promoter-luciferase construct. Anal. Biochem. 1997;247:45-51.

[41] Vujaskovic Z and Groen HJM. TGF-β, radiation-induced pulmonary injury and lung cancer. Int. J. Radiat. Biol. 2000;76:511-516.

[42] Vujaskovic Z, Marks LB and Anscher MS. The physical parameters and molecular events associated with radiation-induced lung toxicity. Semin. Radiat. Oncol. 2000;10:296-307.

[43] Wakefield LM, Letterio JJ, Chen T et al. Transforming growth factor-beta1 circulates in normal human plasma and is unchanged in advanced metastatic breast cancer. Clin. Cancer Res. 1995;1:129-136.

[44] Wakefield LM, Winokur TS, Hollands RS, Christopherson K, Levinson AD and Sporn MB. Recombinant latent transforming growth factor beta 1 has a longer plasma half-life in rats than active transforming growth factor beta 1, and a different tissue distribution. J. Clin. Invest. 1990;86:1976-1984.

CHAPTER 3: Pulmonary radiation injury: Identification of risk factors associated with regional hypersensitivity

Alena Novakova-Jiresova[1], Peter van Luijk[2], Harry van Goor[3], Harm H. Kampinga[1], Rob P. Coppes[1,2]

[1] Department of Cell Biology, section Radiation and Stress Cell Biology

[2] Department of Radiation Oncology

[3] Department of Pathology

University Medical Center Groningen, University of Groningen, The Netherlands

Cancer Research 2005; 65 (9): 3568 – 3576.

Abstract

Purpose: Effective radiation treatment of thoracic tumors is often limited by radiosensitivity of surrounding tissues. Several experimental studies have suggested variations in radiosensitivity of different pulmonary regions. Mice and rat studies in part contradict each other and urged for a more detailed analysis. This study was designed to obtain a more comprehensive insight in radiation injury development, expression and its regional heterogeneity in lung. The latter is obviously highly critical for optimization of radiotherapy treatment plans and may shed light on the mechanisms of lung dysfunction after irradiation.

Methods and Results: Six different but volume-equal regions in rat lung were irradiated. Whereas the severity of damage, as seen in histological analysis, was comparable in all regions, the degree of lung dysfunction, measured as breathing rates, largely varied. During the *pneumonitic* phase (*early:* 6-12 weeks), the most sensitive regions contained a substantial part of alveolar lung parenchyma. Also, a trend for hypersensitivity was observed when the heart lay in the irradiation field. In

the *fibrotic* phase (*late:* 34-38 weeks), lung parenchyma and heart encompassing regions were the most sensitive. No impact of the heart was observed during the *intermediate* phase (16-28 weeks).

Conclusions: The severity of respiratory dysfunction after partial thoracic irradiation is likely governed by an interaction between pulmonary and cardiac functional deficits. As a repercussion, more severe acute and delayed toxicity should be expected after combined lung and heart irradiation. This should be considered in the process of radiotherapy treatment planning of thoracic malignancies.

3.1 Introduction

As the most frequent malignant tumours routinely treated by radiation occur in a thoracic region, reducing the risk of radiation injury to adjacent healthy organs is a crucial issue in clinical radiotherapy and radiation biology. The lung is a very radiosensitive, vital organ, damage to which can lead to complications in up to one fifth of the patients undergoing radiotherapy (1-6). The sequelae come typically in two phases: acute inflammatory pneumonitis and late pulmonary fibrosis (3,4,7-10). Both pathologic processes, i.e. the inflammatory infiltration, congestion and endothelial damage in the former and replacement of functional parenchyma by connective tissue in the latter, lead to compromised lung perfusion, increased vascular resistance, reduced gas-exchange inter-phase between air and blood, and sub-optimal blood oxygenation. Clinical symptoms range from dyspnoea on effort to respiratory failure, right heart failure, and possibly death (4,6,8).

As curative radiotherapy in the thoracic region is generally delivered using external radiation beams, the irradiation of normal tissues is an inevitable side-effect of achieving tumoricidal dose within a tumour surrounded by those tissues. Modern treatment planning technology allows comparison between dose-distributions of several treatment alternatives in patients prior to commencing the treatment and thus provides a margin for clinical decision-making. Therefore, efforts are aimed at creating clinically applicable routine strategies enabling precise treatment tailoring in each individual patient, maximizing the dose-delivery to a tumour while preventing severe toxicity risks. Such tailoring requires thorough knowledge of factors determining the risk of normal tissue complications.

The role of physical dosimetric factors such as total radiation dose, irradiated volume (1,2,7,11,12) and dose per fraction (5,7) has received considerable attention. Although those factors are clearly relevant, several lines of evidence suggest that they alone are insufficient for an accurate estimation of complication probabilities (13,14). Therefore, the attention turned towards an investigation of possible biological determinants. Beside inhomogeneous lung perfusion (15,16) and cytokine effects (17,18), the location of the irradiated sub-volume within the lung is likely to play an important role.

In humans, regional heterogeneity in response to lung irradiation was suggested in a prospective trial of lung cancer patients, where the middle or lower lung location of an irradiated sub-volume was related to a higher risk of complications

than the upper lung location (1). This, however, was only significant in univariate but not multivariate analysis, likely due to limitations of clinical studies where matching identical irradiated volumes in different locations is a difficult task. In that aspect, the main emphasis lies with experimental studies. A pioneering work has been done in mice. Here, the lung base appeared to be the most sensitive in terms of higher morbidity (breathing rate elevation) and lethality after irradiation of similar sub-volumes compared to lung apex or mid-region (19,20). The authors linked this regionally heterogeneous response to differences in the proportion of gas-exchange structures (alveoli) within the entire organ inherent to the anatomical architecture of tracheo-bronchial tree. It was proposed that the location of the sub-volume along the vertical axis, i.e. the apical, mid-region or basal location has to be taken into account when predicting an impact of lung injury (21).

To obtain a more comprehensive insight in radiation injury development, expression and its dependence on regional heterogeneity in lung, we used a rat model of partial lung irradiation expanded to more clinically relevant regions and allowing higher accuracy of dose delivery than previous studies thanks to the larger size of rat thorax (22). Our preliminary studies confirmed the importance of the location of the irradiated sub-volume but, at the same time, yielded first estimates of sensitivity that were partially contradictory to the mice data of the Travis group (22,23). This required testing an alternative hypothesis that the bronchial tree layout and alveolar density, being similar in rats and mice, might not be the only determinants of the regionally heterogeneous radiation response. Our current study addressed this issue by investigating the outcome of targeted irradiation of 50% sub-volumes in the right, left, apical, basal, mediastinal (central) and lateral (peripheral) lung regions. We demonstrate differences in radiation response between these regions in terms of the lung function (breathing rate elevation) and show that these differences fluctuate in relation to the time elapsed from irradiation. Using a histopathological evaluation, we document that those regional differences are not due to selective radiosensitivity of the regions as such. Rather, the data suggest that alveolar density in the affected lung regions and an additional, external factor of heart irradiation interact over a time and jointly determine the global outcome of the thoracic irradiation in terms of respiratory function.

3.2 Materials and Methods

Animals: Adult male albino Wistar rats (n=232) of the Hsd/Cpb:WU strain bread in a specific pathogen free colony (Harlan-CPB, Rijswijk, The Netherlands) were used in the experiments. They were housed five to a cage under a 12 h light - 12 h dark cycle and fed rodent chow (RMH-B, Hope Farms, Woerden, The Netherlands) and water ad libitum. The experiments were performed in agreement with the Netherlands Experiments on Animals Act (1977) and the European Convention for the Protection of Vertebrate Animals Used for Experimental Purposes (Strasbourg, 18.III.1986).

Collimator design: Three-millimeter lead collimators were constructed for anterior-posterior and posterior-anterior irradiations targeted to six different lung regions: right, left, apical, basal, mediastinal or lateral. Based on thoracic computed tomography (CT) scans of five non-irradiated rats weighing 300-340g, the borders of the collimators were calculated to expose precisely 50% (± 5%) of total lung volume (including both the alveolar parenchyma and bronchial structures encompassed within). Details of the procedure have been published earlier (22,24). Simulator images (anterior-posterior) of resulting irradiation portals are shown in Fig. 1. The alveoli essential for the gas exchange are not homogeneously distributed over the whole lung as certain parts contain more large bronchi (21). Based on literature and the anatomy as observed during the extirpation of rat lungs it was noted that the mediastinal region, in contrast to the lateral region, contained more large bronchi and blood vessels and, as a result, less functional parenchyma. For the right, left, apical and basal regions no differences were observed. CT-based analysis of pulmonary density revealed similar patterns.

Heart irradiation: The irradiation portals as designed for this study also involved the heart. The volume of the heart in the irradiation fields was for the right region 25 ± 5%, left 75 ± 5%, apical 99 ± 1%, basal 1 ± 1%, mediastinal 97 ± 3% and for the lateral region 3 ± 3% (see Fig. 1).

Irradiation procedure: Positioning of the animals and dosimetry were adapted from procedures used previously for parotid gland irradiations in this laboratory (24). Rats weighing 280 – 320 g were anaesthetized with intraperitoneal injection of ketamin (40 mg kg^{-1}) and xylazin (6 mg kg^{-1}) and positioned in a polymethylmethacrylate holder hanging vertically by their upper incisor teeth fitted in a groove of a positioning rod just behind an appropriate collimator. The hanging

position did not influence the density distribution in the lung tissue as determined by CT-density measurements. The thorax outside the irradiation field as well as the rest of the body were shielded by 3-mm lead plate. One of the six lung regions (Fig. 1) was irradiated from two parallel opposing anterior-posterior / posterior-anterior irradiation fields using an orthovoltage X-ray machine (Mueller MG 300, Philips, Eindhoven, The Netherlands) operated at 200 kV and 15 mA (0.5 mm Cu and Al filters, HVL_1 = 1.05 mm Cu). Two separate positioning holders were needed for the anterior-posterior and posterior-anterior irradiations that followed immediately one another. The total doses were delivered within 20 minutes in each animal. At a focus-skin distance of 21.3 cm, the midplane dose rate was determined using the average of the entrance and exit dose rates. The entrance and exit dose rates were determined by means of thermoluminiscent dosimetry on live shaved rats and checked against tabulated percentage dose distributions. The difference in collimator size was included in the dose rate, using tabulated back-scatter factors and the percentage dose distributions. The nominal dose rate was 2.68 – 2.90 $Gymin^{-1}$. It was verified from the percentage dose distributions and by a radiochromic film (GafChromic, type MD-55, ISP Technologies Inc., Wayne, New Jersey) exposure in a wax phantom with a rat equivalent diameter of 35 mm that the dose inhomogeneity across the thorax in the beams direction was $\leq 7\%$. Using dose profile-films, the 15% and 10% iso-doses were found to extend not more than 4.5 and 10 mm beyond the edge of the shield, respectively. We assumed those doses negligible in terms of "in field" effects. "In-beam" monitoring of the X- ray tube output was performed during the irradiations using an ionisation chamber (PTW "Farmer", B30001, Freiburg, Germany). Within each of the six region cohorts (right, left, apical etc.), four dose groups were irradiated by a single dose either of 16, 18, 20 or 22 Gy. Control animals were anaesthetized and sham irradiated.

Follow-up and morbidity: 232 animals were inspected for a minimum of twice a week for general health and weighed biweekly. The irradiation did not lead to major alterations in food intake although the animals from 18-22 Gy dose groups lagged mildly behind controls in their weight gain (data not shown). We encountered 13 cases of unplanned sacrifice or death due to anaesthesia overdose (4), sanguineous nasal frothing (2), purulent bronchopneumonia (1), > 10% weight loss (1), spinal paralysis (1) and causes unrelated to the experimental procedure (4). We did not observe any morbidity among controls. The numbers of animals per dose group

reduced during the follow-up due to sacrifices for histology: they were 9, 7 and 5 between 0-8, 10-26 and 28-38 weeks, respectively. The control group consisted of 14, 10 and 7 animals in these periods.

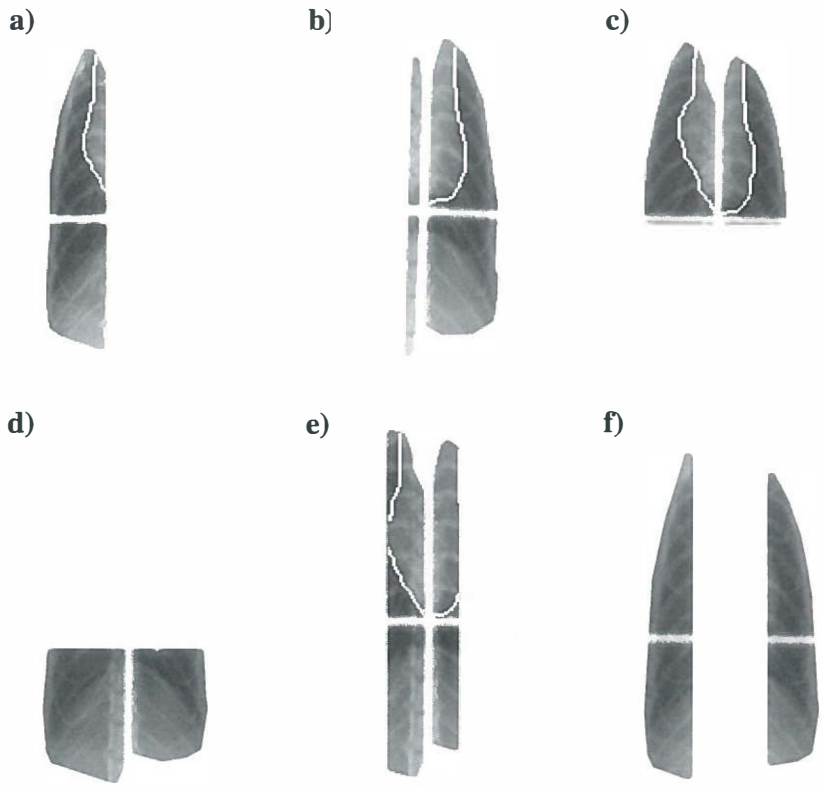

Figure 1: Simulator films of the AP irradiation portals for the 50% right (**a**), left (**b**), apical (**c**), basal (**d**), mediastinal (**e**) and lateral (**f**) lung regions. Note the heart contour in the left, apical and mediastinal fields.

Breathing rate assay: Breathing rate assay is an established method for evaluation of respiratory function in rodents (25,26). After two training sessions, a breathing rate (BR) at rest was recorded for each rat less than a week before the irradiation and then every two weeks till 38 weeks post-irradiation. As described earlier (22,27), an unrestrained animal was placed in a 1500ml air-tight but transparent tube of a whole-body plethysmograph connected to a pressure transducer. The frequency of pressure changes inside the tube was recorded and displayed on a calibrated chart as breaths per minute (bpm). A mean BR of an animal was then calculated from minimum of 4 steady regions of the recording lasting ≥ 15 seconds. If the measurement required more than 5 minutes to obtain, the animal was let out of the tube and rested to prevent anxiety as well as drop of oxygen inside the tube. A mean BR of a dose group (bpm) with its standard error (SEM) was calculated from the means of individual animals at each time point.

Histology: Two rats per dose group and three to four controls were selected at random and sacrificed by an intraperitoneal pentobarbital overdose at 8, 26 and 38 weeks post-irradiation. While the heart was still beating, the animals were heparinized, the thoracic cavity exposed and pulmonary and systemic circulation perfused *in situ* by phosphate buffer saline (PBS, pH 7.3) via the right ventricle and liver incision. The lungs were then removed and inflated by intratracheal infusion of 4% formaldehyde in PBS (pH 7.3) under a hydrostatic pressure of 20cm H_2O. The trachea was tied and the entire specimen was immersed in 4% buffered formaldehyde for overnight fixation. A clear margin between the damaged and normal tissue was macroscopically distinguishable forming the expected shape of the irradiation portal. The damaged (presumably irradiated) parts of every specimen were separated; standardized tissue samples were excised from each affected lobe and embedded in paraffin. Three-micrometer serial sections were mounted on slides, stained with haematoxylin and eosin (H&E) or Masson's trichrome (MT) stain for collagen fibres (bluish-green) and examined by light microscopy. The defining pathology in the irradiated lung parenchyma was a focal lesion distinguished by inflammatory infiltrate, interstitial and/or intra-alveolar edema, and fibrotic obliteration of alveoli (see Fig. 2). The severity of focal lesions on each slide was assessed using a semi-quantitative scoring system: no foci present = score 0; small foci present (focus < ½ of 100x magnification field) = score 1; medium foci present (focus ≤ 100x field) = score 2; large foci present (focus ≤ 40x field) and total affected area ≤ 50% of the total

tissue cross-section = score 3; confluent foci present (focus exceeds 40x field) and total affected area > 50% of the total tissue cross-section = score 4. One H&E and one MT slide per rat was examined and assigned a joint score.

Statistical analysis: The comparison of BR values among the six region cohorts was done in three distinct periods of BR dynamics: *early* phase (6-12 weeks), *intermediate* phase (16-28 weeks) and *late* phase (34-38 weeks). Within these periods, the BR values of individual animals from 18 to 22 Gy dose groups belonging to one region cohort (Tab. 1), or to one or two region cohorts (Fig. 4), were pooled together and compared with the BR values of other cohorts. Because the values were not Normally distributed, non-parametric tests (Mann – Whitney *U*-test and Kruskal – Wallis test, the SPSS software package version 11.0) were used. The Mann Whitney p-values were adjusted according to the Bonferroni correction for multiple comparisons. The nominal level of statistical significance (after the adjustment) was 5%. The same tests were used for comparison of histological scores among the six region cohorts. The scores of 6 rats from 18 to 22 Gy dose groups of one region cohort sacrificed at one time point (8, 26 or 38 weeks) were pooled together and compared with the scores of other cohorts (Tab. 1). Odds ratios (OR) that were used for analysis of BR data were derived from 2x2 tables and their 90% confidence intervals (CI) were calculated using the standard error of the logarithm of the appropriate OR. The 90% CI were chosen (rather than 95% CI) to assess the 5% significance only in the lower tail area (i.e. to assess the 5% probability that the OR is not higher than 1).

3.3 Results

3.3.1 Pathology and histopathology

The perfused and inflated lung specimens were examined macroscopically on autopsy. At 8 weeks post-irradiation, the irradiated regions were darker (hyperaemic) than the shielded regions. They contained small whitish patches apparent through the darkened pleural surface. No obvious shrinkage was visible. However, severe shrinkage of the irradiated regions was observed at the higher doses (≥20Gy) from 26 weeks onwards. Thus, the macroscopic pathology was initially dominated by signs of inflammation (8 weeks) and later by fibrotic retraction (26 and 38 weeks).

At microscopic evaluation, a delicate structure of alveolar tissue was apparent in non-irradiated controls at all time points (Fig. 2 a - f). At 8 weeks after irradiation, a dose dependent increase in inflammatory foci dispersed throughout normally looking parenchyma was observed in the irradiated lungs, ranging from <10 to >50% of the total tissue cross-section on a slide. Within these foci, interstitial and, at higher doses, intra-alveolar oedema (exudate) occurred. The alveolar spaces were filled by inflammatory infiltrate consisting mainly of alveolar macrophages and occasionally a few neutrophils (Fig. 2 g, j). A variable degree of collagen deposition (none to moderate) accompanied the inflammatory process (Fig. 2 j).

At later times after radiation (26 and 38 weeks), the foci acquired a fibrous character. Dose-dependent build-up of interstitial collagen led from focal septal thickening to complete obliteration of vast areas of alveolar spaces. Where alveoli disappeared, only lumina of bronchi and hypertrophic vessels gaped in compact connective tissue (Fig. 2 h, k, i,, l). Mononuclear inflammatory infiltration was still present in remaining alveoli and mainly in the interstitium. The intra-alveolar exudate was rare at 26 and not observed at 38 weeks. Together, these findings indicate resorption of the acute exudative inflammation and its replacement by a chronic interstitial inflammation with fibro-production and progressive collagen accumulation from 26 weeks onwards (Fig. 2 m).

Figure 2 (next page): Histological changes in lung parenchyma at 8 weeks (**a,d** control; **g,j** right lung after 22Gy), 26 weeks (**b,e** control; **h,k** left lung after 22Gy) and 38 weeks (**c,f** control; **i,l** lateral region after 22Gy). Serial sections were stained with H&E (upper) and Masson's trichrome stain (lower). In control tissue (**a - f**), normal parenchyma with thin alveolar septa (*1*) and collagen deposits (green) limited to the adventitia of bronchi (*2*) or vessels (*3*) could be seen at all time points. Findings 8 weeks after irradiation (**g,j**) revealed an acute exudative inflammation. The alveoli were filled with inflammatory infiltrate (*1*) and eosin-stained exudate (*2*). Atypical type II pneumocytes (*3*) were observed. Alveolar septa were edematous and infiltrated (*4*). Initial collagen deposition (green) appeared occasionally (*5*). Chronic productive inflammation dominated at 26 (**h,k**) and 38 (**i,l**) weeks. Alveolar spaces (rudiments = *4*) were obliterated by a connective tissue with diffuse collagen deposits (green *5*) engulfing lumina of bronchi (*2*) and hypertrophic vessels (*3*). Persisting inflammatory infiltration (*1*). Time pattern of the changes is shown in the scheme (**m**).

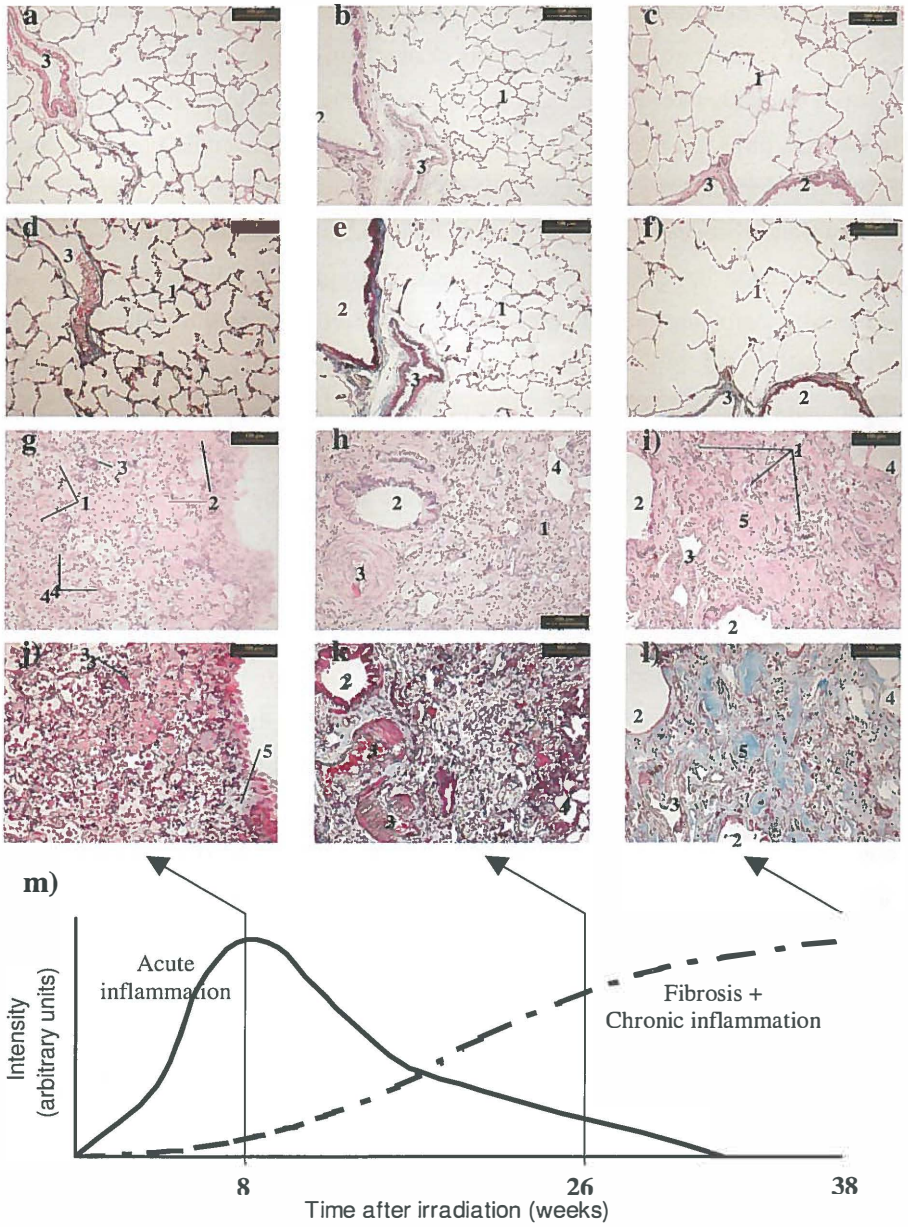
a
b
c
d
e
f
g
h
i
j
k
l
m)
Acute
inflammation
Fibrosis +
Chronic inflammation
Intensity
(arbitrary units)
8
26
38
Time after irradiation (weeks)

Figure 2

3.3.2 Respiratory function

To investigate radiation-induced changes in pulmonary function, BRs were assayed biweekly over 38 weeks post-irradiation (Fig. 3). A dose-dependent increase in BR was observed after ≥ 18 Gy in all cohorts (typical example Fig. 3 a). Similar time-dependent changes were observed for all regions (Fig. 3 b). The first increase in BR appeared between 6 and 12 weeks, followed by a decrease and a subsequent second increase between 16 and 28 weeks. Beyond 30 weeks, a second recovery occurred. Combining this BR dynamics with histology data, three phases could be distinguished (Fig. 2 m; Fig. 3 b): an *early* phase (week 6-12) of an acute exudative inflammation paralleled by the first BR peak; an *intermediate* phase (week 16-28) and a *late* phase (week 34-38), both characterized by a chronic fibro-productive inflammation with either a generalized increase in BR (the *intermediate* phase) or a variable BR recovery (the *late* phase).

3.3.3 Regional variations

Despite the general similarities in terms of the dynamics of the respiratory response, the magnitude of the response varied between the regions. Table 1 shows the six region cohorts ordered according to the severity of the respiratory dysfunction (represented by the mean bpm) in each of the three phases. This functional rating is compared with the semi-quantitative histopathology score (i.e. morphology). It appears that morphology failed to explain the clear-cut variations in dysfunction.

Figure 3 (next page): Mean BR after 50% lung volume irradiation. **a**) Dose-dependent BR increases in time – an example of the 50% lateral irradiation cohort: 16 Gy (◇), 18 Gy (□), 20 Gy (Δ) and 22 Gy (○). Data points represent mean BR in breaths per minute (bpm) within a dose group of 9 (week 0-8), 7 (week 10-26) or 4 to 5 animals (week 28-38), with SEM bars. Baseline BR (●) fluctuates around 163.7 ± 0.7 bpm. **b**) BR increases seen in 22 Gy dose groups of right (◆), left (□), apical (■), basal (Δ), mediastinal (▲) and lateral (○) irradiation cohorts. Data points represent mean BR in breaths per minute (bpm) within a group, with SEM bars. Three phases of BR dynamics can be distinguished and are marked between 6 and 12 weeks (*early* phase: the first BR elevation), 16 and 28 weeks (*intermediate* phase: generalized BR elevation) and 34 to 38 weeks (*late* phase: sub-optimal recovery). Baseline BR (●) fluctuates around 163.7 ± 0.7 bpm throughout the follow-up.

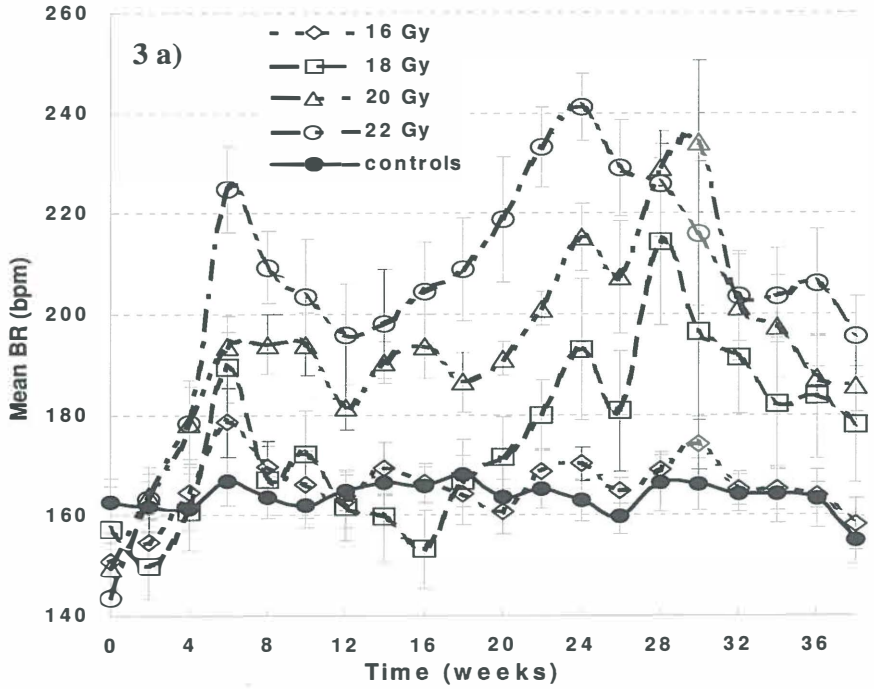
3 a)
16 Gy
18 Gy
20 Gy
22 Gy
controls
Mean BR (bpm)
260
240
220
200
180
160
140
0
4
8
12
16
20
24
28
32
36
Time (weeks)

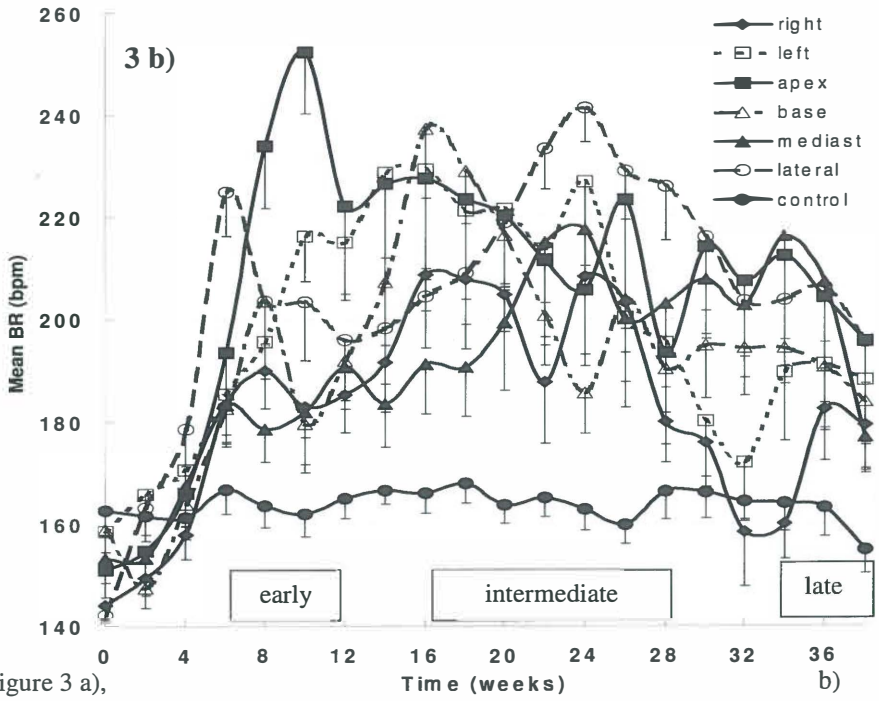
3 b)
right
left
apex
base
mediast
lateral
control
Mean BR (bpm)
260
240
220
200
180
160
140
early
intermediate
late
0
4
8
12
16
20
24
28
32
36
Time (weeks)

Figure 3 a), b)

Rather, these variations seemed to be governed by the character of organ structures contained in the irradiation field. The cohorts that contained 50% of the alveolar tissue and no heart in the irradiation portal (right and basal) behaved similarly but distinctly from the cohorts that contained either > 50% proportion of alveolar tissue (lateral) or 50% of the alveolar tissue plus heart in the irradiation field (left and apical). The mediastinal cohort containing < 50% proportion of the alveolar tissue but a major proportion of the heart stood usually apart from the other regions. As such, the data of regions containing most of the functional parenchyma (lateral), roughly half of the functional parenchyma (right and basal), the heart and the functional parenchyma (left and apical) or the heart and mostly bronchi (mediastinal), were pooled together and compared (Fig. 4). The results from this analysis indicate that for the *early* phase (Fig. 4 – Early), the left + apical (*L+A*) and lateral (*Lt*) parts of the lung were the most sensitive to radiation-induced pulmonary dysfunction and differed from the baseline significantly ($p \leq 0.021$) whereas the other regions did not. This changed in the *intermediate* phase (Fig. 4 - Intermediate) where except for the mediastinal (*M*) region, no significant differences were observed between the other regions ($p=0.7$) although all were significantly elevated above the baseline ($p \leq 0.021$). Interestingly, the differences observed in the *early* phase reappeared during the *late* phase (Fig. 4 - Late). Thus, regional differences were detected in all post-irradiation periods and the left and apical pulmonary regions showed consistently a high sensitivity in terms of functional damage.

3.3.4 Consequentiality between the phases

To examine whether a respiratory deficiency in an earlier period has a consequence in a later period, correlations between individual BR's of irradiated animals were analysed in Fig. 5. The *early* BR elevation almost always (62/65=95%) led to a dysfunction in the *intermediate* phase. However, the *intermediate* BR increase frequently developed without the antecedent *early* increase (42/100=42%; Fig. 5 a). Still, the *intermediate* dysfunction was significantly more likely in the rats that suffered the *early* dysfunction than in the rats that did not (OR = 28.5; 90%CI [10.2; 79.80]). Also the *late* dysfunction was more probable if the *early* BR increase occurred (OR = 5.9; 90%CI [3.0; 11.7]; Fig. 5 b) and even more likely if the *intermediate* BR increase occurred (OR = 7.4; 90%CI [3.3; 16.9]; Fig. 5 c). Those

Table 1: Comparison between the functional and histological damage

Phase	Region	BR 18-22 Gy (mbpm ± SEM)	Histological score 18-22 Gy (median and range)
EARLY	Apical	196.0 ± 6.1 *	2.0 (2-4)
	Left	194.3 ± 4.6 *	2.5 (0-4)
	Lateral	191.3 ± 5.2 *	2.0 (1-3)
	Right	177.8 ± 3.4	3.0 (1-4)
	Mediast.	177.5 ± 3.6	2.0 (2-3)
	Basal	175.8 ± 3.5	2.0 (1-3)
	Control	163.6 ± 3.1	0 (0-0) †
INTERMED.	Left	211.7 ± 7.1 *	4.0 (3-4)
	Apical	204.5 ± 6.5 *	3.0 (1-4)
	Lateral	200.7 ± 5.6 *	3.0 (1-4)
	Basal	200.6 ± 5.0 *	3.0 (2-3.5)
	Right	199.1 ± 3.1 *	3.5 (3-4)
	Mediast.	186.2 ± 4.6 * †	2.5 (2-4)
	Control	163.6 ± 2.7	0 (0-0) †
LATE	Apical	211.8 ± 8.6 *	3.0 (2-4)
	Left	204.9 ± 8.7	3.0 (2-4)
	Lateral	191.1 ± 5.7 *	3.0 (2-4)
	Basal	188.7 ± 3.6 *	2.0 (2-4)
	Mediast.	181.5 ± 7.9	2.0 (1-3)
	Right	172.6 ± 3.4	2.5 (2-4)
	Control	160.8 ± 5.2	0 (0-0) †

Table 1 – note:
BR 18-22 Gy = breathing rate of animals from 18 to 22 Gy dose groups pooled together;
mbpm = mean breaths per minute;
Histological score 18-22 Gy = structural damage in irradiated lungs of animals from 18 to 22 Gy dose groups evaluated on scale of 0 to 4;
Kruskal-Wallis test or Mann-Whitney *U*-test with the Bonferroni correction were used to derive the p-values:
(*) different from the control group ($p \leq 0.05$);
(†) lower than the other regions ($p \leq 0.05$);

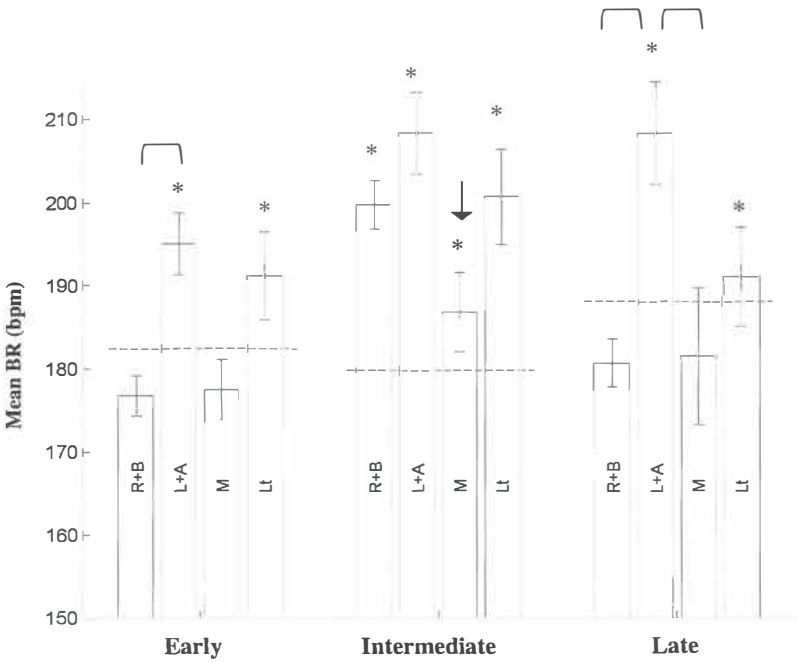

Fig. 4: Regional differences in the respiratory dysfunction. Mean BRs in 18 to 22 Gy dose groups when cohorts with similar structures encompassed in their irradiation portals were pooled together: a half of the alveolar parenchyma in the right and basal cohorts (R+B); a half of the alveolar parenchyma plus the heart in the left and apical cohorts (L+A); the heart plus minimum of the alveolar parenchyma in the mediastinal cohort (M); and a majority of the alveolar parenchyma in the lateral cohort (Lt). The BRs from the *early* (6-12 weeks), *intermediate* (16-28 weeks) and *late* (34-38 weeks) phases are shown separately. Bars indicate ± SEM. Dashed lines indicate cut-offs for elevated BR values (= baseline BR + 2SD): 182.5, 179.8 and 188.1 bpm in the *early*, *intermediate* and *late* periods, respectively. Note the regional differences in the respiratory dysfunction following fixed range of doses delivered to the identical percentage (50%) of the total lung volume. * indicates a difference from the baseline ($p \leq 0.05$), ⊓ spans over cohorts that mutually differ ($p \leq 0.05$), ↓ marks a cohort that is lower than the remaining cohorts ($p \leq 0.05$). P-values adjusted by the Bonferroni correction.

results suggest strong consequentiality between the phases. Nevertheless, still a substantial number of new cases of morbidity (not preceded by an earlier morbidity) kept appearing throughout the follow-up.

Six rats suffered a BR increase in the *late* phase without the antecedent *intermediate* increase (Fig. 5 c). Five of them also lacked the *early* increase. Interestingly, all these six rats had the heart encompassed in the irradiation field. The OR of developing the *late* BR elevation in rats *with* irradiated heart versus rats *without* irradiated heart was 2.1; 90%CI [1.1; 3.9]. The same OR limited to the subgroup of animals showing the *intermediate* BR increase was 2.4; 90%CI [1.1; 5.3], implicating heart irradiation as an independent risk factor in development of the *late* respiratory dysfunction.

A trend was observed that heart irradiation increased the likelihood of development of the *early* dysfunction (the OR for the *early* elevation in rats *with* versus *without* irradiated heart was 1.3; 90%CI [0.8; 2.3]) whereas no influence of heart irradiation could be discerned in the *intermediate* phase (OR = 0.7; 90%CI [0.4; 1.3]). Thus, atop the clear predisposing link between the consecutive phases of morbidity, heart irradiation conferred an extra risk of developing the *late*, and likely, also the *early* respiratory deficiencies.

Figure 5 (next page): Correlation between the BR increases in the *early* and *intermediate* phases **(a)**, in the *early* and *late* phases **(b)**, and in the *intermediate* and *late* phases **(c)**. Points represent individual animals, their total numbers are 165 in **(a)**, 116 in **(b)**, and 116 in **(c)**. Dashed lines indicate cut-offs for elevated BR values (= baseline BR + 2SD): 182.5, 179.8 and 188.1 bpm in the *early*, *intermediate* and *late* periods, respectively. Region labels (R+B, L+A etc.) as in Fig. 4. Rats that had elevated BR in the *early* phase mostly proceeded to show elevation also in the *intermediate* **(a)** and *late* **(b)** phases. Rats that had elevated BR in the *intermediate* phase and/or had irradiated heart (L+A and M, i.e. red and blue points) were the most likely to show elevation in the *late* phase **(c)**.

Fig. 5 a)

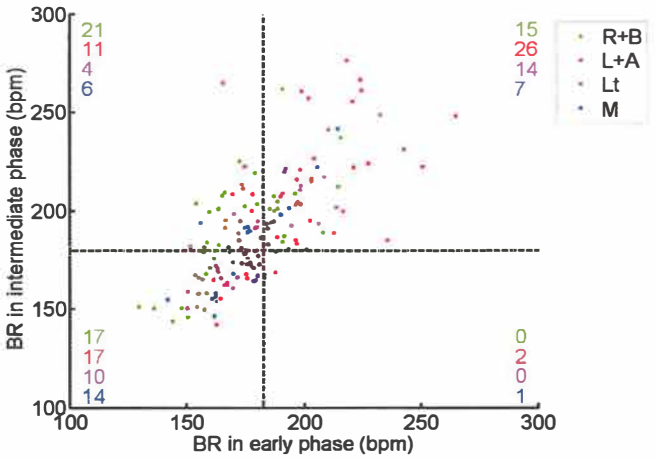

Fig. 5 b)

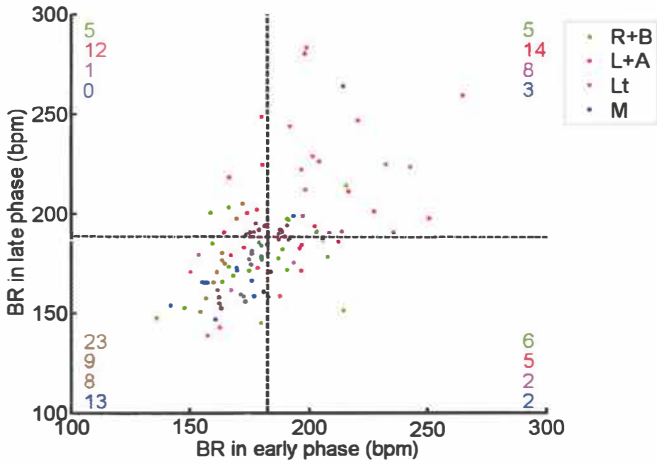

Fig. 5 c)

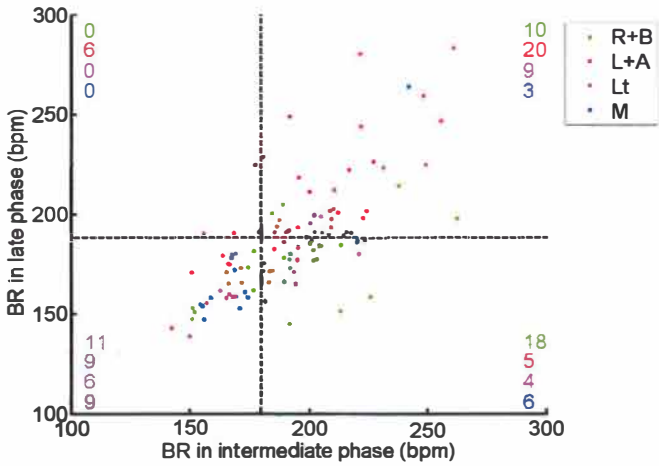

3.4 Discussion

New external irradiation techniques emerging in clinical radiotherapy allow high precision of dose delivery to a tumour. Although experimental approaches to such therapies reveal that it is not trivial how and where the dose is deposited around the tumour, knowledge on optimal dose distributions in critical normal tissues is still largely lacking. In the current study, we identify risk factors for pulmonary injury after local irradiation of six variably placed 50% sub-volumes in the rat lung. Our findings should serve as an impulse for revision of currently adopted clinical practice estimating risk of complications after a treatment based on dosimetric parameters disregarding the spatial information on dose deposition within an organ.

Our data reveal three phases of impairment in respiratory function paralleled by dose-dependent structural abnormalities in the irradiated lung parenchyma. Acute exudative inflammation indicative of pneumonitis in the *early* phase is followed by chronic productive inflammation ending in fibrosis during the *intermediate* and *late* phases. Whilst a strong consequentiality link was noted between the three consecutive phases, still a substantial number of animals that got over the *early* pneumonitis phase without obvious symptoms became symptomatic during the onset of fibrosis. This is all in agreement with broadly reported manifestation of post-irradiation pulmonary injury in both experimental (28-30) and clinical (3,4,8) settings and supports the notion that the level of damage required for the manifestation of fibrosis is lower than that required for the manifestation of pneumonitis (4,8, 10,31).

The severity of histological damage did not vary significantly among the six regions irradiated in this study. This is in agreement with previous findings in mice (19) and pigs (32). Despite the equality in the degree of histological damage, the six irradiated regions differed in the degree of their functional response. This indicates that regional hypersensitivity to radiation on the level of lung function is not due to hyperradiosensitivity of the tissue or cells in these regions in terms of inflammatory response or extracellular matrix formation. Rather, anatomical or physiological reasons may underlay these differences in regional response. In our experiments in rats (27, this study), the irradiation of the apical and left regions had the most severe impact on respiratory function, particularly in the *early* and *late* phases of the follow-up. This contradicts results of experiments carried out on mice where irradiation of sub-volumes in basal lung had more severe functional consequences than irradiation of the same sub-volumes in the apex (19,20). In the latter studies (19-21), the varying

proportion of alveoli, critical for gas exchange function, relative to air conducting bronchi, was indicated as a reason for lower sensitivity of the apex (containing large airways branching from pulmonary hila) and higher sensitivity of the base (containing mostly alveolar parenchyma). This is supported by our data as we find that the region containing the largest proportion of parenchymal tissue (the lateral region) belonged to the more sensitive during all phases. However, it can not explain why the lung apex appeared hypersensitive in rats but resistant in mice although the airway structure of both species is similar (20). A technical cause for the differences could be dose delivery precision, which likely is higher in our studies due to the larger size of rats than of mice. Biologically, the position of the heart in the irradiation field could play a role. Although it was claimed (19) that cardiac complications were not responsible for the observed differences between the apex and base in mouse lungs, it must be stated that these functional measurements were done 22 weeks after irradiation, which exactly matches the period (the *intermediate* phase) during which we also describe minimal impact of heart irradiation on the BR.

Also in rats it has been reported that the lower lung was more radiosensitive than the upper lung (33,34). The endpoint in these studies, however, was DNA-damage as measured by the micronucleus assay in fibroblasts isolated from lungs 18 hours after irradiation. These data were suggested to provide an explanation for the functional response in mice (35). However, as we now show, the lower lung in rats is not more radiosensitive than the upper lung and thus no correlation between the DNA damage (of individual cells in this region) and functional responses seems to exist.

In general, local heart irradiation is known to affect respiratory function (36) whereas lung irradiation induces changes in pulmonary vascular bed that cause pulmonary hypertension and lead to a congestive right cardiac failure in humans (4,37), dogs (38), mice (39), and rats (40). The described hypersensitivity of the apical and left regions correlates closely to the CT-verified inclusion of the heart in these fields (99.5 and 74.5 %, respectively). Thus, it is possible that differences in the anatomy, positioning and accuracy of dose delivery could explain the discrepancies between rat and mice mentioned above.

The sensitising influence of heart irradiation could well explain the differences in between the apical and left cohorts, both representing a combined damage to the heart and lung parenchyma, and the right and basal cohorts with almost an equal amount of "functional" alveolar parenchyma but no heart in the irradiation field.

However, the heart irradiation could not be the sole factor because the mediastinal exposure, encompassing 97.3% of the heart, produced the least sensitive response in terms of BR changes. It must be realized, however, that the mediastinal region contains mostly large bronchi and vessels around the pulmonary hila and only a small proportion of alveolar parenchyma. The strong impact of the proportion of the alveolar tissue irradiated on the degree of response is shown by the large effect of the lateral irradiation where no heart is in the field but more than 50% of the critical alveolar tissue is being irradiated (no large airways appear in this field). So, both the proportion of heart and proportion of alveolar tissue in the irradiation field need to be jointly taken into account when predicting the risk of functional damage after lung irradiation.

These effects of combined injuries to both organs point towards a synergy between radiation damages in lung and heart. Lung possesses substantial reserve capacity. Redistribution of perfusion to, or a compensatory expansion of previously underused alveoli may maintain an adequate gas exchange after destruction of irradiated regions (41). Also in the case of failing cardiac function, compensatory abilities have been shown either on the level of the heart itself or on the level of regulatory mechanisms of the entire cardiovascular system (42,43). Thus, it is plausible that limited damage to each of the two organs separately would remain subclinical, but its combination will exceed compensatory abilities and translate into clinically manifest symptoms.

Interestingly, the impact of heart irradiation was most dramatic during the *late* phase (OR = 2.1), whereas only a trend (OR = 1.3) was observed during the *early* phase. This is likely caused by the inclusion of the data on mediastinal region that was resistant due to minimal alveolar tissue involvement. During the *intermediate* phase, the influence of the heart irradiation disappeared (OR < 1). An explanation of this phenomenon may be derived from observations of early decline in cardiac function after heart irradiation followed by a period of recovery (likely coinciding with the *intermediate* phase) that precedes the onset of late symptoms reported for rats (43-45), dogs (38) and even humans (46,47). If true, this would change the traditional view of heart as a late reacting organ and may bear relevance for clinical practice where the combination of subclinical injuries to lung and heart may give rise to unexpected toxicity, both early and late after the radiation treatment. A separate study is under way to more specifically test this hypothesis.

In summary, we report regional differences appearing during the three phases of radiation-induced impairment of respiratory function. These differences depend on the irradiated volume of critical gas exchange pulmonary structures and on the involvement of heart in the irradiation field. This urges more attention to possible combined effects of lung and heart irradiation in clinical practice. Our data also imply that simple dosimetric parameters, like mean lung dose, that do not take into account spatial distribution of radiation dose within an organ and yet are endorsed for risk estimation in clinics (12), cannot be safely used for prediction of respiratory complications following modern radiation techniques like intensity modified radiation therapy or proton irradiations.

Acknowledgements

Presented research was supported by Interuniversitary Institute for Radiopathology and Radiation Protection (IRS grant 9.0.18) and a grant from the Dutch Cancer Society (RuG 2002-2673).

The authors thank F. Cotteleer and E.M. Wiegman for design of the collimators, P.C. van der Hulst and P.T.F. Leferink for supervision on dosimetry, H. Faber, N. de Blinde, M. Drenth, R.J. Konst, M. Wiersma and I. Platteel for excellent technical assistance and V. Fidler for guidance on statistical analysis. The authors are grateful to J. Wondergem and M. Boerma for the critical discussions on the cardiac radiation injury.

References

1. Graham MV, Purdy JA, Emami B, Harms W, Bosch W, Lockett MA, Perez CA. Clinical dose-volume histogram analysis for pneumonitis after 3D treatment for non-small cell lung cancer (NSCLC). Int J Radiat Oncol Biol Phys 1999;45:323-329.
2. Kwa SL, Lebesque JV, Theuws JC, Marks LB, Munley MT, Bentel G, Oetzel D, Spahn U, Graham MV, Drzymala RE, Purdy JA, Lichter AS, Martel MK, Ten Haken RK. Radiation pneumonitis as a function of mean lung dose: an analysis of pooled data of 540 patients. Int J Radiat Oncol Biol Phys 1998;42:1-9.
3. Marks LB, Yu X, Vujaskovic Z, Small W, Jr., Folz R, Anscher MS. Radiation-induced lung injury. Semin Radiat Oncol 2003;13:333-345.
4. McDonald S, Rubin P, Phillips TL, Marks LB. Injury to the lung from cancer therapy: clinical syndromes, measurable endpoints, and potential scoring systems. Int J Radiat Oncol Biol Phys 1995;31:1187-1203.
5. Saunders M, Dische S, Barrett A, Harvey A, Griffiths G, Palmar M. Continuous, hyperfractionated, accelerated radiotherapy (CHART) versus conventional radiotherapy in non-small cell lung cancer: mature data from the randomised multicentre trial. CHART Steering committee. Radiother Oncol 1999;52:137-148.
6. Marks LB, Fan M, Clough R, Munley M, Bentel G, Coleman RE, Jaszczak R, Hollis D, Anscher M. Radiation-induced pulmonary injury: symptomatic versus subclinical endpoints. Int J Radiat Biol 2000;76:469-475.
7. Bentzen SM, Skoczylas JZ, Bernier J. Quantitative clinical radiobiology of early and late lung reactions. Int J Radiat Biol 2000;76:453-462.
8. Maasilta P. Radiation-induced lung injury. From the chest physician's point of view. Lung Cancer 1991;7:367-384.
9. Rezvani M, Hopewell JW. The response of the pig lung to fractionated doses of X rays. Br J Radiol 1990;63:41-50.
10. Travis EL. The sequence of histological changes in mouse lungs after single doses of x-rays. Int J Radiat Oncol Biol Phys 1980;6:345-347.
11. Seppenwoolde Y, Lebesque JV. Partial irradiation of the lung. Semin Radiat Oncol 2001;11:247-258.

12. Seppenwoolde Y, Lebesque JV, De Jaeger K, Belderbos JS, Boersma LJ, Schilstra C, Henning GT, Hayman JA, Martel MK, Ten Haken RK. Comparing different NTCP models that predict the incidence of radiation pneumonitis. Normal tissue complication probability. Int J Radiat Oncol Biol Phys 2003;55:724-735.
13. Dorr W, Baumann M, Herrmann T. Radiation-induced lung damage: a challenge for radiation biology, experimental and clinical radiotherapy. Int J Radiat Biol 2000;76:443-446.
14. Vujaskovic Z, Marks LB, Anscher MS. The physical parameters and molecular events associated with radiation-induced lung toxicity. Semin Radiat Oncol 2000;10:296-307.
15. De Jaeger K, Seppenwoolde Y, Boersma LJ, Muller SH, Baas P, Belderbos JS, Lebesque JV. Pulmonary function following high-dose radiotherapy of non-small-cell lung cancer. Int J Radiat Oncol Biol Phys 2003;55:1331-1340.
16. Fan M, Marks LB, Lind P, Hollis D, Woel RT, Bentel GG, Anscher MS, Shafman TD, Coleman RE, Jaszczak RJ, Munley MT. Relating radiation-induced regional lung injury to changes in pulmonary function tests. Int J Radiat Oncol Biol Phys 2001;51:311-317.
17. Anscher MS, Marks LB, Shafman TD, Clough R, Huang H, Tisch A, Munley M, Herndon JE, Garst J, Crawford J, Jirtle RL. Risk of long-term complications after TFG-beta1-guided very-high-dose thoracic radiotherapy. Int J Radiat Oncol Biol Phys 2003;56:988-995.
18. Novakova-Jiresova A, Van Gameren MM, Coppes RP, Kampinga HH, Groen HJ. Transforming growth factor-beta plasma dynamics and post-irradiation lung injury in lung cancer patients. Radiother Oncol 2004;71:183-189.
19. Liao ZX, Travis EL, Tucker SL. Damage and morbidity from pneumonitis after irradiation of partial volumes of mouse lung. Int J Radiat Oncol Biol Phys 1995;32:1359-1370.
20. Travis EL, Liao ZX, Tucker SL. Spatial heterogeneity of the volume effect for radiation pneumonitis in mouse lung. Int J Radiat Oncol Biol Phys 1997;38:1045-1054.
21. Tucker SL, Liao ZX, Travis EL. Estimation of the spatial distribution of target cells for radiation pneumonitis in mouse lung. Int J Radiat Oncol Biol Phys 1997;38:1055-1066.

22. Wiegman EM, Meertens H, Konings AW, Kampinga HH, Coppes RP. Loco-regional differences in pulmonary function and density after partial rat lung irradiation. Radiother Oncol 2003;69:11-19.
23. Jiresova A, van Goor H, Konings AWT, Kampinga HH, Coppes RP. Dose-volume-region effects in partial irradiation of rat lung (abstract). Program & Abstracts from the 12th International Congress of Radiation Research 2003;P08/1613:371
24. Cotteleer F, Faber H, Konings AW, Van der Hulst PC, Coppes RP, Meertens H. Three-dimensional dose distribution for partial irradiation of rat parotid glands with 200kV X-rays. Int J Radiat Biol 2003;79:689-700.
25. Travis EL, Vojnovic B, Davies EE, Hirst DG. A plethysmographic method for measuring function in locally irradiated mouse lung. Br J Radiol 1979;52:67-74.
26. van Rongen E, Tan CH, Durham SK. Late functional, biochemical and histological changes in the rat lung after fractionated irradiation to the whole thorax. Radiother Oncol 1987;10:231-246.
27. Vujaskovic Z, Down JD, t' Veld AA, Mooyaart EL, Meertens H, Piers DA, Szabo BG, Konings AW. Radiological and functional assessment of radiation-induced lung injury in the rat. Exp Lung Res 1998;24:137-148.
28. Geist BJ, Trott KR. Radiographic and function changes after partial lung irradiation in the rat. Strahlenther Onkol 1992;168:168-173.
29. Travis EL, Harley RA, Fenn JO, Klobukowski CJ, Hargrove HB. Pathologic changes in the lung following single and multi-fraction irradiation. Int J Radiat Oncol Biol Phys 1977;2:475-490.
30. Ward HE, Kemsley L, Davies L, Holecek M, Berend N. The pulmonary response to sublethal thoracic irradiation in the rat. Radiat Res 1993;136:15-21.
31. Siemann DW, Hill RP, Penney DP. Early and late pulmonary toxicity in mice evaluated 180 and 420 days following localized lung irradiation. Radiat Res 1982;89:396-407.
32. Baumann M, Appold S, Geyer P, Knorr A, Voigtmann L, Herrmann T. Lack of effect of small high-dose volumes on the dose-response relationship for the development of fibrosis in distant parts of the ipsilateral lung in mini-pigs. Int J Radiat Biol 2000;76:477-485.

33. Khan MA, Hill RP, Van Dyk J. Partial volume rat lung irradiation: an evaluation of early DNA damage. Int J Radiat Oncol Biol Phys 1998;40:467-476.
34. Khan MA, Van Dyk J, Yeung IW, Hill RP. Partial volume rat lung irradiation; assessment of early DNA damage in different lung regions and effect of radical scavengers. Radiother Oncol 2003;66:95-102.
35. Moiseenko VV, Battista JJ, Hill RP, Travis EL, Van Dyk J. In-field and out-of-field effects in partial volume lung irradiation in rodents: possible correlation between early dna damage and functional endpoints. Int J Radiat Oncol Biol Phys 2000;48:1539-1548.
36. Geist BJ, Lauk S, Bornhausen M, Trott KR. Physiologic consequences of local heart irradiation in rats. Int J Radiat Oncol Biol Phys 1990;18:1107-1113.
37. Constine LS. Late effects of cancer treatment. In: Halperin,E.C.; Constine,L.S.; Tarbell,N.J., Kun,L.E.; editors. Pediatric Radiation Oncology.1999;457-537.
38. McChesney SL, Gillette EL, Orton EC. Canine cardiomyopathy after whole heart and partial lung irradiation. Int J Radiat Oncol Biol Phys 1988;14:1169-1174.
39. Travis EL, Down JD, Holmes SJ, Hobson B. Radiation pneumonitis and fibrosis in mouse lung assayed by respiratory frequency and histology. Radiat Res 1980;84:133-143.
40. Varekamp AE. Interstitial pneumonitis following bone marrow transplantation: studies in the Brown Norway rat. Thesis. Chapters 3.3-3.5.1990;
41. Marks LB. The impact of organ structure on radiation response. Int J Radiat Oncol Biol Phys 1996;34:1165-1171.
42. Franken NA, Camps JA, van Ravels FJ, van der LA, Pauwels EK, Wondergem J. Comparison of in vivo cardiac function with ex vivo cardiac performance of the rat heart after thoracic irradiation. Br J Radiol 1997;70:1004-1009.
43. Schultz-Hector S. Radiation-induced heart disease: review of experimental data on dose response and pathogenesis. Int J Radiat Biol 1992;61:149-160.

44. Cilliers GD, Harper IS, Lochner A. Radiation-induced changes in the ultrastructure and mechanical function of the rat heart. Radiother Oncol 1989;16:311-326.
45. Schultz-Hector S, Bohm M, Blochel A, Dominiak P, Erdmann E, Muller-Schauenburg W, Weber A. Radiation-induced heart disease: morphology, changes in catecholamine synthesis and content, beta-adrenoceptor density, and hemodynamic function in an experimental model. Radiat Res 1992;129:281-289.
46. Ikaheimo MJ, Niemela KO, Linnaluoto MM, Jakobsson MJ, Takkunen JT, Taskinen PJ. Early cardiac changes related to radiation therapy. Am J Cardiol 1985;56:943-946.
47. Lagrange JL, Darcourt J, Benoliel J, Bensadoun RJ, Migneco O. Acute cardiac effects of mediastinal irradiation: assessment by radionuclide angiography. Int J Radiat Oncol Biol Phys 1992;22:897-903.

CHAPTER 4: Radiation damage to the heart enhances early radiation – induced lung function loss

Peter van Luijk[1], Alena Novakova-Jiresova[2], Hette Faber[2], Jacobus M. Schippers[3], Harm H. Kampinga[2], Harm Meertens[1] and Rob P. Coppes[1,2]

[1] Department of Radiation Oncology, University Medical Center Groningen, The Netherlands

[2] Department of Cell Biology, section Radiation and Stress Cell Biology, University Medical Center Groningen, The Netherlands

[3] Accelerator Department, Paul Scherrer Institut, Villigen, Switzerland

Cancer Research 2005; 65 (15): 6509 – 6511.

Abstract

In many thoracic cancers, the radiation dose that can safely be delivered to the target volume is limited by the tolerance dose of the surrounding lung tissue. It has been hypothesised that irradiation of the heart may be an additional risk factor for the development of early radiation-induced lung morbidity. In the current study the dependence of lung tolerance dose on heart irradiation is determined. Fifty percent of the rat lungs were irradiated either including or excluding the heart. Proton beams were used to allow very accurate and conformal dose delivery. Lung function toxicity was scored using a breathing rate assay. We confirmed that the tolerance dose for early lung function damage depends not only on the lung region that is irradiated, but also that concomitant irradiation of the heart severely reduces the tolerance of the lung. This study for the first time shows that the response of an organ to irradiation does not necessarily depend on the dose distribution in that organ alone.

4.1 Introduction

Many frequently occurring malignant tumours in the thoracic region are routinely treated by radiotherapy, often in combination with chemotherapy. The tolerance dose of normal tissues surrounding the target volume, such as the lung in the case of lung cancer, poses a limit on the dose that can be given safely to the tumour. This in turn determines the maximum probability of cure[1-3].

Technological improvements to the radiotherapy treatment such as intensity-modulated radiotherapy and the use of particles such as protons[4] or carbon ions[5] have resulted in a decrease in the amount of normal tissue that is irradiated to the same dose as the tumour. With protons and carbon ions, an additional advantage is that dose is only deposited to the tumour and proximal to the tumour. This means that by choosing a beam angle one can choose to spare specific (distally located) parts of the normal tissue surrounding the target volume. High-precision information on the effect of irradiation on different regions of the thorax is needed to be able to fully exploit these advances for the treatment of thoracic tumours.

Using rats[6] or mice[7], it has been shown that there are large variations in radiation-induced lung morbidity depending on the location irradiated. Our recent data on rats[6] not only revealed that more sensitive regions encompassed the largest amount of alveolar tissue, but also suggested that including the heart in the radiation field enhanced loss of lung function. Classically, clinically and experimentally, radiation-induced heart damage is considered to be a late effect[8,9]. Surprisingly however, irradiating the heart not only resulted in late (>34 weeks) radiation-induced lung function loss but also a trend for increased early (<12 weeks) lung function loss was found. The finding that dose to the heart adds to early function loss of the lung would suggest that radiation-induced heart damage also has a highly relevant early component, which may manifest itself in combination with early (sub-clinical) lung damage. As such it would be necessary to consider functional damage to the lung in terms of multi-organ damage.

However, in our previous study[6], the early effect of the heart just did not reach statistical significance. This was most likely due to the field design, which was not tailored to include or exclude the entire heart, thereby diluting the possible influence of the heart. For the present study, we therefore developed a high-precision proton irradiation to further optimize uniformity in the irradiated regions and to minimize the dose to shielded regions. Next, irradiation fields were designed to specifically include

or exclude the entire heart and/or most alveolar tissue. We now conclusively show that the early radiation-induced function loss of the lung is greatly enhanced when the heart lies within the radiation field. This result implicates that the function loss of an organ does not necessarily depend on the dose distribution in that organ alone and has significant implications for treatment planning with high-precision radiotherapy modalities.

4.2 Materials and Methods

Wistar rats were irradiated with 150 MeV protons from the cyclotron at the Kernfysisch Versneller Instituut, Groningen, The Netherlands, using the shoot-through technique as previously published[10]. In short, the shoot-through technique only employs high-energy protons and no lower-energy (Bragg peak) protons. This results in a very uniform dose distribution in the longitudinal direction (±1%) and sharp lateral field edges (20-80% isodose distance: 1 mm.) Four different irradiation fields were used. The shape of each field is shown in Fig. 1A. The irradiation ports were designed using CT scans of animals of the same age and weight, by a previously described procedure[6]. For both the heart and the lung, separate contours were designed based on multiple individually positioned animals. In the resulting heart contour, the heart of each individual animal was contained. This ensures that for animals irradiated on the heart, the heart is always entirely included in the irradiated volume. For the lung, the variation in position resulted on average in 3% spread in the irradiated lung volume. Each dose group (16-21 Gy, single dose) consisted of five to seven animals.

The first field (Fig. 1A, red) contained the heart with the smallest possible amount of lung tissue (25 ± 4% of the lung). The second field (Fig. 1A, black) contained the heart with a portion of the mediastinally located lung tissue. The total lung volume in this field was 50 ± 2%. The third field (Fig. 1A, blue) also contained the heart but now combined with laterally located lung tissue, again adding up to 51 ± 3% of the total lung volume. In the last field (Fig. 1A, purple), the heart was fully spared. To obtain 50 ± 2% irradiated lung volume, part of the mediastinally located lung tissue was spared as well.

After the irradiations, breathing rate measurements were performed biweekly as described before[6]. In our previous study, it was found that the early (weeks 6 to 12

after irradiation) increase in breathing rate is mainly characterised by inflammation. Therefore, the increase of the mean breathing rate in this period, relative to the mean breathing frequency in weeks 0 to 4 after irradiation, was used as an indicator of the functional status of the lung. To distinguish between animals showing radiation-induced function loss and healthy animals, a threshold on this increase was defined based on measurements of non-irradiated controls. From these control measurements, the mean increase and its standard deviation (SD) was calculated. The mean value plus two SDs was used. An increase of breathing rate above this threshold was defined as functional impairment.

For each dose group, the fraction of symptomatic animals was determined. This fraction equals the normal tissue complication probability (NTCP). To these NTCP data, probit curves were fitted[11]. Lastly, the *effective dose* for which 50% of the animals responded (ED_{50}) was predicted, as well as its 95% confidence limits.

4.3 Results and Discussion

To assess the effect of the heart on regional differences in lung function damage after irradiation, four different dose distributions, either including or excluding the heart (Fig. 1A), were delivered to the thorax of the rat. The time course of the change in breathing rate as a measure of lung function after a dose of 20 Gy is shown in Fig. 1B. The radiation-induced lung function loss, starting at week 6, is clearly visible and the data show large heterogeneity in response depending on the dose distribution used. This was confirmed for all doses as depicted in Fig. 1C where the mean increase in breathing rate during weeks 6 to 12 is plotted as a function of dose. Increases larger than the threshold (+19 bpm) calculated from the controls (i.e., higher than the range marked in green in Fig. 1C) indicate symptomatic radiation-induced function loss. Irradiation of the heart alone results in a low response similar to whole mediastinal region irradiation including the heart (Fig. 1C). Irradiation of a similar volume of lateral lung tissue alone, excluding the heart, resulted in a larger breathing rate increase and a lowering of the ED_{50} dose from 23.5 Gy [20.6-700 Gy, 95% confidence interval (95% CI), mediastinal] to 19.0 Gy (18.2-20.1 Gy, 95% CI, lateral; Fig. 1D). This confirms our previous findings that the severity and the ED_{50} for radiation-induced lung function loss are determined by the amount of alveolar tissue that is irradiated. If, however, the heart is irradiated together with lateral parts of the lung (same lung volume with even slightly less alveolar tissue), a much more

pronounced response is seen compared with the lateral field in which the heart was spared (Fig. 1C). Including the heart in the irradiation field resulted in a pronounced reduction of the ED_{50} from 19.0 (lateral without heart) to 17.3 Gy (16.8-17.8 Gy, 95% CI; lateral with heart; Fig. 1D).

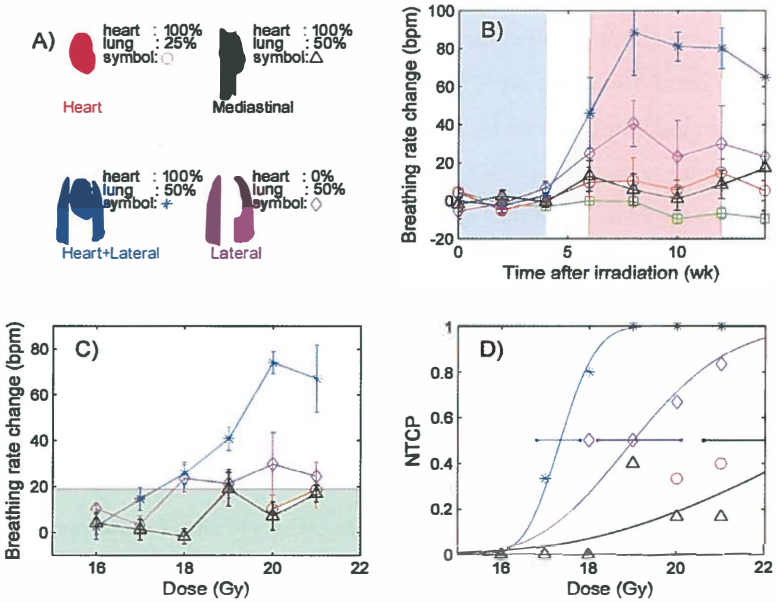

Figure 1: Panel B shows the breathing rate as a function of time after irradiation using 20 Gy with different radiation fields shown in panel A. The time span of the early radiation-induced function loss phase (weeks 6 to 12) is indicated in red. Note the increase in the mean breathing rate in this phase with respect to the latent phase (marked in blue). An increase above the green region in panel C indicates pneumonitis. The error bars represent the standard error of the mean (panels B, C). Panel D shows the fraction of animals manifesting symptomatic lung function loss. The horizontal lines indicate 95% confidence limits of ED_{50}.

These data are the first to conclusively demonstrate that co-irradiation of the heart has a strong effect on the clinical manifestation of radiation-induced lung function loss early after radiation. Local heart irradiation is known to affect respiratory function[12], whereas lung irradiation induces changes in pulmonary vascular bed that cause pulmonary hypertension and lead to a congestive right cardiac failure in humans[13] and several animal models[14,15]. Also in our previous study, it was clearly shown that irradiation of the heart results in late radiation-induced pulmonary toxicity[6]. The late time point (38 weeks after irradiation) coincides with occurrence of late cardiac post-irradiation toxicity, similar to the situation in humans. Yet, early effects of heart irradiations on lung function have not been reported before.

In animal studies, however, morphological changes to the heart were already observed around 10 weeks after irradiation[16]. An early decline in cardiac function after heart irradiation followed by a period of recovery that precedes the onset of late symptoms was reported for rats, dogs and even humans[16-18]. Early heart damage, however, has never received that much attention, as it was not recognised as a clinical problem. In our current study, however, we show that early damage to the heart can have severe consequences on the radiation induced function loss of the lung. This may be due to loss of functional reserve capacity of the cardio-pulmonary system, leading to enhanced manifestation of respiratory function loss. Therefore, when looking at early morbidity of the lung, also radiation dose received by the heart should be regarded.

It has been suggested that a dose up to 102.9 Gy (in 2.1 Gy fractions) can be safely delivered to limited lung volumes with minimal toxicity[19]. In this study, 70% freedom from local progression (Stage I, non-small cell lung cancer [NSCLC]) was obtained when more than 92.4 Gy was given. For larger irradiated lung volumes, the maximum tolerated dose was established at 65 Gy with very poor freedom from local progression[20]. New techniques that are currently being introduced in radiotherapy aim at reducing the dose to and volumes of normal tissues irradiated to subsequently allow dose escalation. Exploiting regional differences in radiation response and avoidance of function loss enhancement due to heart irradiation may allow for dose escalation even to somewhat larger volumes. Extrapolation of data from this study suggest that when the heart would be completely avoided, a gain of ~10% lung tolerance dose might be expected, thus allowing a significant dose escalation. This may have important implications for radiotherapy of NSCLC, where the early lung morbidity

(radiation pneumonitis) is the main dose-limiting complication. Moreover, as previously shown[6], excluding the heart from the radiation field will also reduce late effects after thoracic irradiation because the occurrence of radiation pneumonitis predisposes to late radiation fibrosis.

In summary, using high-precision proton irradiations of the rat lung, we established that radiation damage to the heart combined with damage to the lung may result in a symptomatic lung function loss early after radiation. Therefore, when irradiating the thorax, it is important to prevent irradiating the heart. This finding stresses the importance of newly developed high-precision radiation techniques that allow the clinician to keep specific regions dose-free.

Acknowledgements

This study was financially supported by grant RuG 2002-2673 from the Dutch Cancer Society and grant IRS 9.0.18 from the Interuniversitary Institute for Radiopathology and Radiation Protection.

The authors want to thank Harry Kiewiet and the cyclotron crew of the Kernfysisch Versneller Instituut, Groningen, The Netherlands, for their excellent assistance with the rat irradiation procedure.

Reference List

1. Lee CH, Tait D, Nahum AE, Webb S. Comparison of proton therapy and conformal X-ray therapy in non-small cell lung cancer (NSCLC). Br J Radiol 1999;72:1078-84.

2. Engelsman M, Remeijer P , van Herk M, Lebesque JV, Mijnheer BJ, Damen EM. Field size reduction enables iso-NTCP escalation of tumor control probability for irradiation of lung tumors. Int J Radiat Oncol Biol Phys 2001;51:1290-8.

3. Ishikura S, Nihei K, Ohtsu A, et al. Long-term toxicity after definitive chemoradiotherapy for squamous cell carcinoma of the thoracic esophagus. J Clin Oncol 2003;21:2697-702.

4. Koyama S, Tsujii H. Proton beam therapy with high-dose irradiation for superficial and advanced esophageal carcinomas. Clin Cancer Res 2003;9:3571-7.

5. Kamada T, Tsujii H, Tsuji H, et al. Efficacy and safety of carbon ion radiotherapy in bone and soft tissue sarcomas. J Clin Oncol 2002;20:4466-71.

6. Novakova-Jiresova A, van Luijk P, van Goor H., Kampinga HH, Coppes RP. Pulmonary radiation injury: identification of risk factors associated with regional hypersensitivity. Cancer Res 2005;65:

7. Travis EL, Liao ZX, Tucker SL. Spatial heterogeneity of the volume effect for radiation pneumonitis in mouse lung. Int J Radiat Oncol Biol Phys 1997;38:1045-54.

8. Gyenes G, Rutqvist LE, Liedberg A, Fornander T. Long-term cardiac morbidity and mortality in a randomized trial of pre- and postoperative radiation therapy versus surgery alone in primary breast cancer. Radiother Oncol 1998;48:185-90.

9. Gagliardi G, Lax I, Soderstrom S, Gyenes G, Rutqvist LE. Prediction of excess risk of long-term cardiac mortality after radiotherapy of stage I breast cancer. Radiother Oncol 1998;46:63-71.

10. van Luijk P, Bijl HP, Coppes RP, et al. Techniques for precision irradiation of the lateral half of the rat cervical spinal cord using 150 MeV protons. Phys Med Biol 2001;46:2857-71.

11. van Luijk P, Delvigne TC, Schilstra C, Schippers JM. Estimation of parameters of dose-volume models and their confidence limits. Phys Med Biol 2003;48:1863-84.

12. Geist BJ, Lauk S, Bornhausen M, Trott KR. Physiologic consequences of local heart irradiation in rats. Int J Radiat Oncol Biol Phys 1990;18:1107-13.

13. McDonald S, Rubin P, Phillips TL, Marks LB. Injury to the lung from cancer therapy: clinical syndromes, measurable endpoints, and potential scoring systems. Int J Radiat Oncol Biol Phys 1995;31:1187-203.

14. McChesney SL, Gillette EL, Orton EC. Canine cardiomyopathy after whole heart and partial lung irradiation. Int J Radiat Oncol Biol Phys 1988;14:1169-74.

15. Travis EL, Down JD, Holmes SJ, Hobson B. Radiation pneumonitis and fibrosis in mouse lung assayed by respiratory frequency and histology. Radiat Res 1980;84:133-43.

16. Schultz-Hector S. Radiation-induced heart disease: review of experimental data on dose response and pathogenesis. Int J Radiat Biol 1992;61:149-60.

17. Ikaheimo MJ, Niemela KO, Linnaluoto MM, Jakobsson MJ , Takkunen JT, Taskinen PJ. Early cardiac changes related to radiation therapy. Am J Cardiol 1985;56:943-6.

18. Lagrange JL, Darcourt J, Benoliel J, Bensadoun RJ, Migneco O. Acute cardiac effects of mediastinal irradiation: assessment by radionuclide angiography. Int J Radiat Oncol Biol Phys 1992;22:897-903.

19. Narayan S, Henning GT, Ten Haken RK, Sullivan MA, Martel MK, Hayman JA. Results following treatment to doses of 92.4 or 102.9 Gy on a phase I dose escalation study for non-small cell lung cancer. Lung Cancer 2004;44:79-88.

20. Hayman JA, Martel MK, Ten Haken RK, et al. Dose escalation in non-small-cell lung cancer using three-dimensional conformal radiation therapy: update of a phase I trial. J Clin Oncol 2001;19:127-36.

CHAPTER 5: Relation between radiation-induced whole lung function loss and regional structural changes in partially irradiated rat lung

Peter van Luijk[1*], Alena Novakova-Jiresova[2*], Hette Faber[2], Marloes N.J. Steneker[1], Harm H. Kampinga, PhD[2], Haarm Meertens[1], Rob P. Coppes[1,2]

[1]Department of Radiation Oncology

[2]Department of Cell Biology, section Radiation and Stress Cell Biology

University Medical Center Groningen, University of Groningen, The Netherlands

* equally contributed to this study

International Journal of Radiation Oncology, Biology and Physics 2006; 64 (5): 1495 – 1502.

Abstract

Purpose: Radiation-induced pulmonary toxicity is characterized by dose, region and time-dependent severe changes in lung morphology and function. This study sought to determine the relation between structural and functional changes in the irradiated rat lung at three different phases after irradiation.

Materials and methods: Six groups of animals were irradiated to 16-22 Gy to six different lung regions, each containing 50% of the total lung volume. Before and every 2 weeks after irradiation, the breathing rate (BR) was measured, and at weeks 8, 26 and 38, computed tomography (CT) was performed. From the CT scans, the irradiated lung tissue was delineated using a computerized algorithm. A single quantitative measure for structural change was derived from changes of the mean and standard deviation of the density within the delineated lung. Subsequently, this was correlated with the BR in the corresponding phase.

Results: In the mediastinal and apex region, the BR and CT density changes did not correlate in any phase. After lateral irradiation, the density changes always correlated with the BR; however, in all other regions, the density changes only correlated significantly (r^2=0.46-0.85, $p<0.05$) with the BR in week 26.

Conclusions: Changes in pulmonary function correlated with the structural changes in the absence of confounding heart irradiation.

5.1 Introduction

In non-small cell lung cancer (NSCLC), escalation of the radiation dose to the tumor is expected to result in increased local control[1,2]. However, the dose that can be administered without inducing life-threatening complications is limited by the tolerance of the lung to radiation.

Several groups have used different strategies to achieve dose escalation. These strategies have in common that they try to identify sub-groups in the NSCLC patient population who show certain properties indicating that they have an increased tolerance to radiation-induced lung complications. The approaches used have been based on tumor size[3], individual differences in radiosensitivity determined by pro-fibrotic cytokine levels[4], and identification of lung regions less vital to the function of the lung[5-11].

Our recent studies have revealed that co-irradiation of the heart enhanced early and late radiation-induced lung function loss[10,11], which is in part responsible for regional hypersensitivity. In addition, it was suggested that radiation-induced structural changes in areas containing the greatest percentage of alveoli contributed most to loss of lung function. Answering the question to what extent regional structural changes in the lung contribute to radiation-induced lung dysfunction requires an accurate quantification of such changes.

Many studies have been published in which computed tomography (CT) scanning was used to quantify radiation-induced pulmonary injury in humans[12-15] and animal models[8,16-19]. Only in a few studies were these changes subsequently compared with the functional changes. Lehnert and El-Khatib[20] observed similar time trends for functional and structural changes. Quantitatively, however, their data did not show a correlation between both parameters. Similarly, in patients treated for breast cancer, Wennberg et al[15] concluded that the mean density changes in a central slice of the lung are more important for the development of clinical radiation pneumonitis than changes in an apical slice.

In many studies, only the mean density of the entire lung or portions thereof have been used as a quantitative measure for structural changes in the lung[8,12,14,15,18,19]. The mean lung density alone, however, is insufficient to relate the changes to function due to hyperinflation occurring around the local increases in density[19,20]. In our laboratory, a study on rat lung[8] revealed only minor changes in mean lung density. In both this study and the study by El-Khatib et al[19], however,

using the mean lung density in small regions of interest situated within the irradiated volume resulted in significant density increases. But also the analysis of these small regions of interest has several drawbacks, such as the use of only part of the available data and the risk of a bias in the placement of the region of interest within the irradiated volume.

In the present study, the aim was to develop a method by which structural changes in the rat lung, detected by CT imaging, could be quantified objectively and in an automated fashion. This method should further be used for an investigation of the extent to which structural changes in the lung could explain the observed regional differences in functional response. We hypothesized that the extent to which structural changes in the lung explain the functional changes will depend on the region irradiated and on the time after irradiation. For the lateral region, consisting mostly of alveolar tissue, function is expected to correlate strongly with structure. In other regions, the contribution of pulmonary structural changes to functional loss will be less pronounced either because the heart has been irradiated, which co-determines functional loss, or because the anatomical structures present in that region (i.e., large bronchi and vessels) do not contribute to lung function directly. As early and late functional loss are more strongly influenced by the heart dose[10] than is functional loss in the intermediate phase, it is expected that the impact of altered pulmonary structure on respiratory function during the early and late spans would be weaker than in the intermediate phase.

5.2 Methods and Materials

Animals: Adult male albino Wistar rats (n=232) of the Hsd/Cpb:WU strain bread in a specific pathogen-free colony (Harlan-CPB, Rijswijk, The Netherlands) were used in the experiments. They were housed five to a cage under a 12-h light/12-h dark cycle and fed rodent chow (RMH-B, Hope Farms, Woerden, The Netherlands) and water *ad libitum*. The Groningen University Animal Welfare Committee approved all animal procedures and the experiments were performed in agreement with the Netherlands Experiments on Animals Act (1977) and the European Convention for the Protection of Vertebrate Animals Used for Experimental Purposes (Strasbourg, 18.III.1986).

Lung irradiation protocol and follow-up: The details on the study design can be found in our previous report[10]. In brief, different 50% subvolumes of the lungs of

adult male albino Wistar rats were irradiated using 16, 18, 20 or 22 Gy, because published data[8] and pilot experiments have revealed that the tolerance dose for pneumonitis for 50% irradiated volume lies within this dose range. The subvolumes used were the left, right, apex, base, mediastinal and lateral. Radiation ports (Fig. 1) were designed using the CT scans of five animals[10]. The resulting uncertainty in irradiated lung volume was ± 5%.

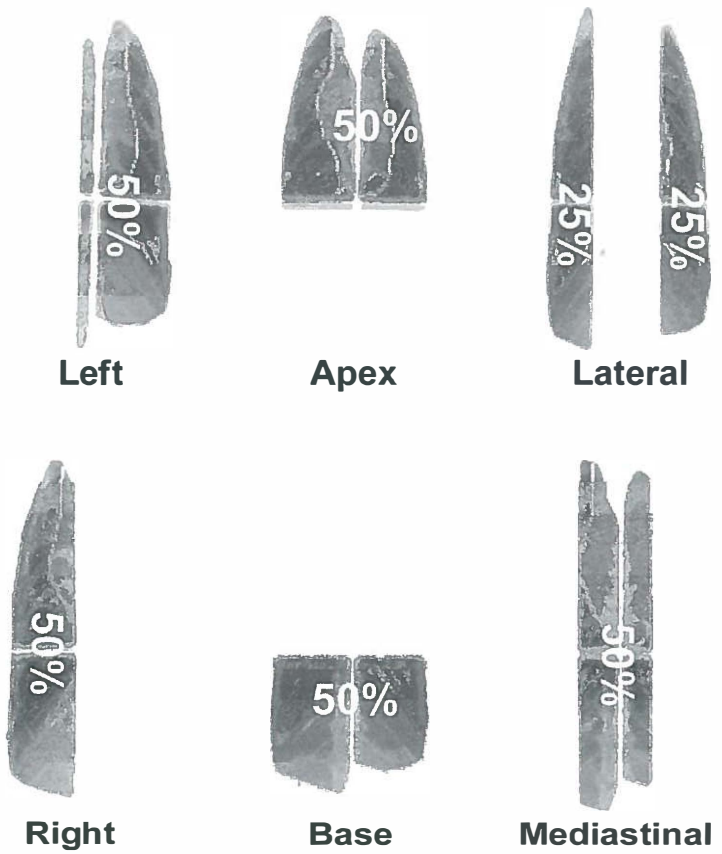

Figure 1: Portal images of the beams used for all regions. Redrawn from Novakova-Jiresova *et* al. [10]

To assess the effect of irradiation on function, the breathing rate (BR) was measured. After two training sessions, a BR at rest was recorded for each rat less than one week before the irradiation and then every two weeks till 38 weeks post-irradiation. In the present study, functional loss was expressed as the increase in the mean BR in the intervals of weeks 6 to 12, weeks 16 to 28 and weeks 34-38, relative to the mean BR in weeks 0 to 4 after irradiation, for the pneumonitic, fibrotic and late phases, respectively. The time intervals were chosen based on the three phases of functional loss observed[10].

Structural changes were registered using CT scanning in weeks 8, 26 and 38 after irradiation. At each point, the same three randomly chosen rats from each subvolume and dose group were anaesthetized using ketamine/xylazine and scanned in a specially designed CT holder and a Siemens Sensation 16 CT scanner (Siemens AG, Munich, Germany). We could scan three rats at once in the holder using the upper incisors as a fixed point. This resulted in a vertical positioning of the animals and longitudinal CT slices. The holder also contained two different plastic rods for verification of the CT density scale. The parameters used were: tube voltage 120 kV, exposure 75 mA, pixel size 0.37x0.37 mm^2, slice thickness 1 mm. The dose received from the CT scanning was < 1 cGy per session and was neglected.

Identification of regions of interest: Within the CT scan of each rat, the irradiated parts of the lung had to be first identified. This was achieved by delineating the whole lung contour and subsequently using the 50% lung volume information of age-matched, non-irradiated control animals. At the end of the follow-up period, a set of 374 scanned lungs was available. A computerized procedure was developed to delineate the lungs in an objective and reproducible manner. Initially, in each slice, all regions with grey values less than –200 HU were contoured. Similar to the finding of Nicholas and Down[18], this level produced the most consistent results. On the basis of the position within the slice, all contours not linked to the lung and trachea could be discarded. The contours of the trachea were discarded cranially of the slice at which the trachea contour joined the contour of the right lung to minimize the contribution of the trachea to the analysis, because our primary interest was to analyze the changes within the lung. Using this computerized lung segmentation procedure, the contours of the lung for all animals could be automatically determined, except for three of the 374 scans. In these three scans, the separation of air-inflated bowel with lung was so

thin that part of the bowel was erroneously included in the lung contour. For these three animals, the bowel contour was removed manually.

Second, within the selected lung volume, a differentiation between the irradiated and non-irradiated tissue was needed. A simple division of the lung volume into two equal sub-volumes would produce inaccurate results owing to shrinkage of the irradiated parts of the lung. To avoid this, the positions of the edge of the radiation fields were estimated based on the volume measured in age-matched non-irradiated controls. Thus, for the irradiated animals, 50% of the control volume was selected on the non-irradiated side of the lung. The residual lung volume was analyzed as being the irradiated tissue. Expansion of the non-irradiated lung into the irradiated region might result in a slight underestimate of the radiation effect.

Statistical analysis: To determine strength of the relation between the structural and functional changes, Pearson's product-moment correlation coefficients were determined. A correlation was considered significant if the hypothesis of no correlation was rejected at $p<0.05$.

5.3 Results

5.3.1 Quantifying structural changes from CT imaging

Our first aim was to summarize the information contained in all pixels in the selected lung region into a limited number of parameters to allow a more comprehensive insight into the nature of the density changes in the lung. Therefore, the CT data of the contoured irradiated lung tissue were first summarized in a density histogram. Figure 2 A) shows examples obtained from an animal irradiated to the lateral parts of the lung and a non-irradiated control at 8 weeks after irradiation. From these histograms, the mean density and its standard deviation were calculated as characteristics of the density distribution (Fig. 2 B). This analysis was performed on animals that were irradiated to the same region to doses of 16 to 22 Gy. Figure 2 B) shows examples obtained from the group irradiated to the lateral parts of the lung. This analysis was also performed in the same lung region of non-irradiated controls. For the comparison of the groups, using a summary of the clouds of data points was more illustrative than using the individual points. Therefore, we choose to characterize the clouds of points using the bivariate normal distribution, which in turn can be characterized by its bivariate standard deviation. The resulting ellipses are

shown in Fig. 2 B). These ellipses illustrate the early density changes in the lung resulting from lateral irradiation. They are characterized by a minor increase in mean density and an increase in the standard deviation of the density, consistent with the focal pattern of radiation pneumonitis.

Analysis of different regions in control animals showed that even in control animals differences in density exist between regions as can be seen by comparing the ellipses for the lateral and base region of the control animals (Fig. 2 B). Therefore, to calculate and compare the radiation-induced structural changes of different regions, the results obtained from the irradiated animals had to be expressed relative to the results obtained in the same region in the non-irradiated controls. As an example, Fig. 2 C) shows the radiation effect after lateral irradiation and its shift from the corresponding control ellipse. This ellipse describes the density changes in absolute numbers.

Information on the functional significance of variations in structure, as measured by CT density changes, can be obtained from the ellipse of healthy controls. This ellipse describes the spread in the density parameters that corresponds to normal function for a specific region. In regions where this spread is larger (i.e., base vs. lateral, Fig. 2 B), corresponding post-irradiation changes will not relate to reduced function. This spread must be taken into account when structural parameters are translated into functional parameters. Thus, we divide the distance r [distance of the effect of a treated individual to the origin, which is the mean of the control population; Fig. 2 D)] with the spread c of the control population in the same direction. This allowed comparison of function (BR measurements) on an individual basis with the severity of structural changes as represented by the scalar quantity S.

5.3.2 Region dependence of radiation response

To compare the radiation response of the various lung regions, we calculated the ellipses depicted in Fig. 2 C) for weeks 8, 26 and 38 after irradiation for all regions. Figure 3 A) - C) shows this analysis for all regions and times. Although minor differences between the ellipses were observed, they were largely non-significant. For each region individually, however, significant variations occurred in time. To illustrate this, the data of all regions were combined for each time point and plotted in Fig. 3 D). This plot shows that early damage (week 8) was largely characterized by changes in the standard deviations, but at later points, an overall

increase in density was observed. The early increases in standard deviation were due to focal density increases combined with density decreases resulting from hyperinflation. This pathological finding is consistent with pneumonitis as described previously[10]. The observed overall increase in density at later time points (weeks 26 and 38) is consistent with the development of more confluent fibrosis[10].

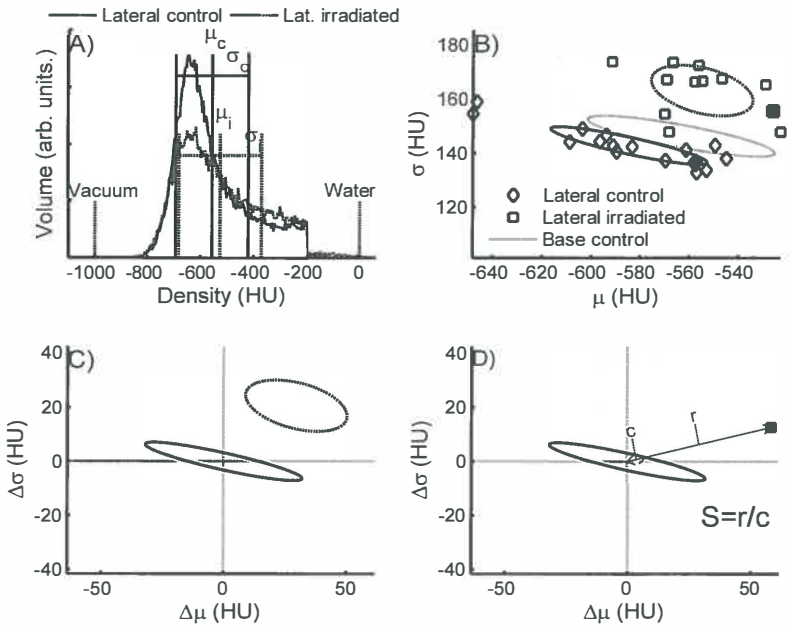

Figure 2: In computed tomography scans, irradiated lung tissue was selected using computerized contouring procedure. **A**) Hounsfield unit (HU) histogram of reconstructed irradiated lung volume of animal irradiated to the lateral parts of the lung (dashed lines) and the same region of control animal (solid lines). These histograms were characterized by their means (μ) and standard deviations (σ). This procedure was repeated for all control and laterally irradiated animals. **B**) Obtained standard deviations plotted against corresponding mean values. Solid points were derived from histograms shown in A. The covariance ellipse can be used to characterize the clouds of points. **C**) These ellipses, corrected for values obtained in control population (whose ellipse is consequently centered at the origin). **D**) Our method for quantifying structural changes for individual animals. This was achieved by dividing the distance between *r* of an individual animal and the origin by the population spread *c* in the same direction.

5.3.3 Dose, structure and function

Next, we determined the quantitative dose-response relationships of the structural changes in the lung, using the method described in Fig. 2 D). Figures 4 A) and B) show the curves for lateral and mediastinal irradiation, respectively, demonstrating that the parameter *S* shows an increase with an increasing dose at all time points, indicative of a dose-related structural change. The steepness of the dose-response curves was different between the lateral and mediastinal region, with the latter showing a very shallow response. This would imply that in this region, hardly any functionally relevant structural changes occur after irradiation.

To investigate the relation between overall lung function and structural changes, the increases in the average BR in weeks 6 to 12, 16 to 28, and 34 to 38, as defined in our previous study[10], were plotted against the parameter *S* in the CT scans of weeks 8, 26 and 38, respectively, for the animals that received lateral irradiation (Fig. 4 C). For the lateral irradiation, a significant correlation between the two endpoints was observed that was similar for all three time points. This suggests a relation between the functional and structural changes that was consistent over time, regardless of the pathological features involved. In contrast, for the data obtained after mediastinal irradiation, no correlation was found at any point (Fig. 4 D).

Figure 3 (next page): **A) – C)** Ellipses representing measured response (see Fig. 2 C) in mean and standard deviations of density in Hounsfield units (HU) shown for all regions and time points. No clear differences were detected among responses of different regions. **D)** Data for all regions at each time point were pooled, revealing a pronounced shift towards increased density as a function of time in all regions.

Figure 4 (next page): **A)** Structural change *S* (see Fig. 2 D) as a function of dose for animals irradiated on lateral parts of lung 8, 26 and 38 weeks post-irradiation. Clear dose-response relationship was observed. **C)** Change in breathing rate vs. structural change *S* at the same time points. Strong and significant ($p<0.001$) correlation was observed. **B), D)** The same analysis for animals with irradiated mediastinum. No dose dependency was observed and functional changes did not correlate with structural ones in this region cohort.

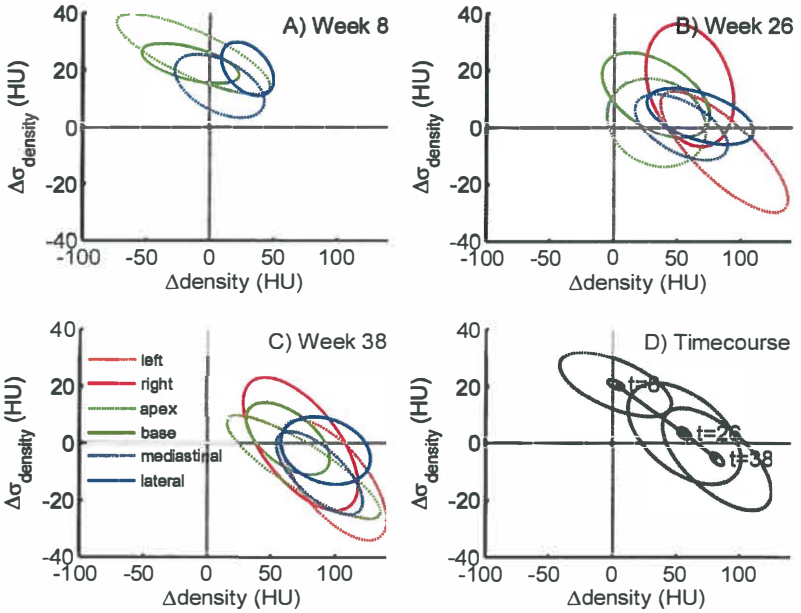

Figure 3 A)- D)

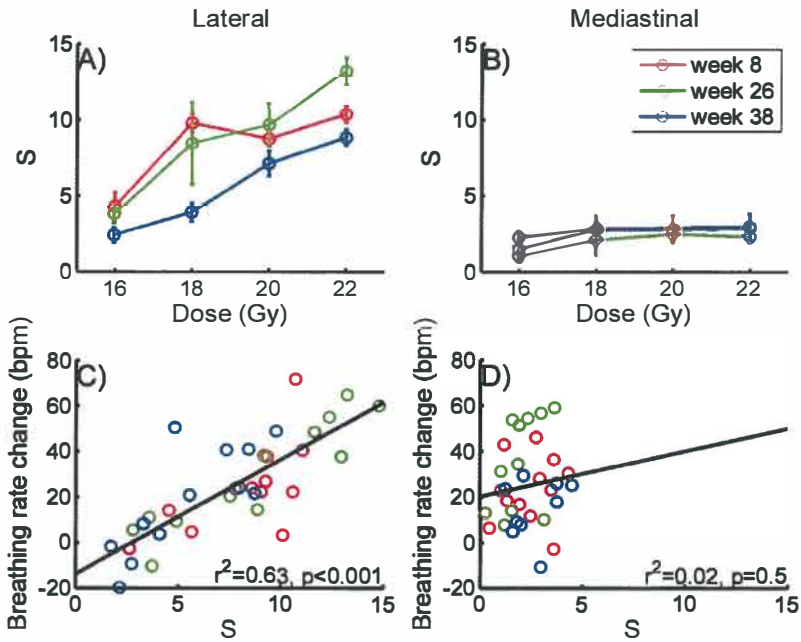

Figure 4 A)- D)

Table 1 summarizes the correlation analysis for all time points and different regions that were irradiated. For none of the three time points were correlations between these parameters found after irradiating the apex or mediastinum. For all other regions, parameter *S* correlated significantly with the functional changes during the intermediate phase after irradiation. At that interval, the parameter *S* could explain 46% (right lung irradiation) to 85% (lateral irradiation) of the changes in the BR. The lateral and base regions are the only ones not containing the heart and major bronchi[10]. In agreement with this, the functional and density changes in these regions showed the highest correlation coefficients. As hypothesized, the magnitude of functional changes explained by structural changes in the lung (as measured by the parameter *S*) was greatest for these regions, but diminished if the irradiated heart volume increases and/or if the amount of alveolar tissue involved decreased (owing to a larger proportion of major bronchi).

5.4 Discussion

5.4.1 Phases of damage

Radiation-induced pulmonary damage is known to manifest itself in two distinct pathological phases: early inflammatory pneumonitis and late pulmonary fibrosis. Radiation pneumonitis is marked by inflammatory foci with interstitial, and at higher doses, also intra-alveolar edema. Radiation fibrosis presents itself as an excessive deposition of connective tissue replacing normal lung parenchyma[10]. These different pathological findings manifest differently on CT imaging. Radiation pneumonitis is usually characterized by ground-glass opacities and patchy consolidation within the irradiated tissue[21,22]. Fibrosis is characterized by discrete or solid consolidation conforming to the shape of radiation portals[21]. In our study, we used a quantitative approach to evaluate the radiation-induced changes using the mean and standard deviation of the density distribution of the lung as obtained from CT processing. This method revealed that, similar to the conventional qualitative classification[21], the radiological appearance of structural changes differed between the different phases. It was dominated by changes in the standard deviation during the pneumonitic phase, with the mean density change becoming more important in the fibrotic phase.

Table 1. Correlation coefficients between lung function and structural changes

Field	Pearson's correlation coefficient					
	Week 8		Week 26		Week 38	
	r^2	p	r^2	p	r^2	p
Left	ND		0.62*	0.0009	0.04	0.51
Right	ND		0.46*	0.02	0.01	0.72
Apex	0.01	0.78	0.15	0.21	0.13	0.25
Base	0.39*	0.03	0.71*	0.0005	0.17	0.19
Lateral	0.41*	0.02	0.85*	0.00002	0.62*	0.003
Mediastinal	0.02	0.70	0.24	0.13	0.05	0.58

Abbreviation: ND = not determined.
* Significant correlations; significant correlations predominantly occured in week 26, at which point, the only region in which structural and functional changes did not correlate was the mediastinal region. This can be explained by the absence of a radiation effect in both parameters. A correlation was observed only after lateral irradiation in week 38. Data in week 8 on the left and right fields were not determined because a different type of scanner was used with these animals.

Furthermore, we found that when the post-irradiation lung density changes were corrected for the pre-irradiation variations, no significant regional differences in radiation response were observed. In a previous study from our laboratory[8], regional differences in post-irradiation lung density changes were reported. This discrepancy could have been the result of the different dose levels used in the present analysis, which might have diluted regional differences. Second, in the previous study, only the mean density of a limited region of interest was used to characterize the structural changes. In contrast, in the present study, information on the whole irradiated lung sub-volume was used and characterized by the mean density and its standard deviation. Therefore, the present study was not sensitive to operator bias and used more information to quantify the density changes.

5.4.2 Regional differences in S

When evaluating the absolute change in the mean and standard deviation of the density corrected for control values, regional differences appeared to be minor or absent. However, regional differences could be found when analyzing the normalized density changes using parameter *S*. This indicates that the outcome of the analysis was influenced by the initial variation in the control situation (*c* vs. *r*, Fig. 2 D) used for normalization and was not due to differences in absolute changes. The rationale of this normalization is that all appearances in the control population resulted in acceptable function. As such, the functional consequences of density changes were related to this spread. This implies that it is necessary to characterize a healthy control population before regional lung density changes resulting from treatment can be properly translated into functional changes. This is a novel finding outlining a new perspective for CT-based analysis of lung damage.

5.4.3 Relation between functional and structural changes

The major goal of the present study was to develop tools and methods to quantitatively analyze CT images of the irradiated lung. The dose-response curves, derived from CT scans obtained after lateral irradiation, showed a clear dose dependency. This result is indicative of the consistency of the method. Despite the differences in the nature of the structural changes at the different time points (pneumonitis vs. fibrosis), the CT analysis was highly consistent with functional loss after lateral irradiations for all time points. No correlation between the functional damage and CT-density changes was observed after mediastinal irradiation. In contrast to the lateral radiation port, which only includes alveolar tissue, the mediastinal lung contains large bronchi and blood vessels. These structures will not contribute much to lung function loss, even when damaged. In addition, our previous studies[10,11] showed that heart irradiation has a profound impact on lung function. However, even with irradiation of the heart, only a limited functional loss was found after mediastinal irradiation. Our present findings suggest that this may be a result of the absence of functionally relevant changes in lung structure in this region. As hypothesized, the role of heart irradiation as a second factor influencing respiratory function loss is further emphasized by the lack of correlation between lung structure and function observed 8 weeks (early) and 38 weeks (late) after the apex and left irradiations which encompass the heart (Fig. 1). This correlation improved in the

intermediate phase in which the role of the heart appears reduced due to compensatory mechanisms[10]. This is best visualized by the correlation found between function and lung structure after the 50% left irradiation at this time point. The correlation was lost again with the ensuing late cardiac damage and its expected influence on lung function in the late period[10]. On the contrary, the effect of the lateral lung irradiation, that is not influenced by the heart[10] or by pulmonary compensatory mechanisms[10], showed good correlation with structural damage throughout all follow-up periods.

5.4.4 Generalization of structural change parameter S

In the present study, the mean and standard deviation of the density were used as characteristics of a CT scan and subsequently translated into a functionally relevant scalar quantity *S*. In our previous studies, however, we identified the importance of other characteristics, such as the percentage of alveolar tissue involved or the presence of confounding heart damage[11]. In principle, the method of constructing a structural change parameter from a number of characteristics can be easily generalized to include additional characteristics (see Appendix for details). An examples is the volume fraction containing air or regional contrast[23]. In the present study, however, we showed that for the characterization of radiation damage in alveolar tissue (e.g., the lateral and base irradiations), the mean and standard deviation of the density sufficed.

The method used in the present study could also be used to construct a structural change parameter for characteristics obtained from other spatially matched imaging modalities, such as local perfusion, ventilation and gas exchange measured by single-photon emission CT[24] and hyperpolarized Xenon MRI[25]. This may be of interest, because it directly adds information on local function, thus taking into account regional differences in function.

5.4.5 Clinical application

To be able to decide which irradiation treatment plan is effective and yet safe for an individual patient, all factors determining the probability and severity of RT-induced lung injury need to be identified. The method described in the present study shows how relative density changes in the lung can be used to translate local effects of radiation into global lung function, which improves insight into factors determining

the risk and severity of RT-induced lung injury. We demonstrated that relevance of CT-detected density changes for global functional outcome depends on the lung region they occur in and on the interval from irradiation. This may offer an explanation for the conflicting results obtained by other investigators, who observed correlations between radiographic density changes[26] and global function, correlations for specific regions only[15], or even no correlation at all[13]. Therefore, also in a clinical setting, the localization and timing of radiographic density changes under investigation should be taken into account when radiological methods are used for assessment of post-irradiation lung damage in patients[13,15]. Our method could find direct application in extracranial radiosurgery in the lung, in which high-dose, single-fraction treatments are used. However, it may also be of use in more commonly used fractionated irradiation, in which the same pathological changes, as found after single-dose irradiation (used in this study), are induced, albeit within a different time frame.

It must be realized that clinical application of the method developed in the present study requires the characterization of a healthy control population in humans before it can be applied. This characterization is challenging for two reasons. First, the lungs of many patients have been exposed to toxic agents or may not be considered normal because of lung disease. Therefore, careful selection of a healthy control population would be required in which the thorax was scanned for indications other than lung disease (e.g. breast cancer, etc…). A second challenge concerns the larger variation in lung anatomy among humans compared with rats. Additional study is needed on how to deal with this.

Conclusion

Lung function loss after partial lung irradiation is known to show regional variations. In the present study, we investigated to what extent these differences can be explained by local structural changes occurring after irradiation. We developed a method to quantify radiation damage in the rat lung, observed by CT, and demonstrated that, in the absence of confounding heart irradiation, the presented analysis to measure structural changes corresponds well to lung functional changes.

Acknowledgements

This study was supported by a grant from the Interuniversitary Institute for Radiopathology and Radiation Protection (IRS grant 9.0.18) and a grant from the Dutch Cancer Society (RuG 2002-2673).

The authors thank the Department of Radiology, University Medical Center Groningen, especially W.G.J. Tukker, for performing the scanning of the rats.

Appendix:

From multiple parameters to a scalar structural change parameter S

In the present study, the mean and standard deviation of the density were used as characteristics of a CT scan and subsequently translated into a functionally relevant scalar quantity *S*. The specific analysis based on these two characteristics, however, was a special case of a more general formalism in which an arbitrary number of characteristics is used to describe some image (such as a specified lung region in CT). Although in the present study, the mean and standard deviation of the density distribution proved sufficient, it is possible that for other studies more characteristics would be needed or even that imaging modalities would have to be combined. Therefore, in this appendix, a generalized formalism has been outlined.

First, we defined a vector consisting of n components representing different characteristics derived from the images. The method outlined in the present study was based on the assumption that all values of this vector occurring in the control population ($p_{1...k}$) correspond to functionally normal situations. As such, the deviation of a sample *r*, normalized on the spread in the control population provides the functional consequence of a structural change.

For each animal in the control population, consisting of k animals, the structure vector r is determined and given by vectors $p_{1...k}$. From these control data, an n-dimensional ellipsoid representing the n-dimensional standard deviation can be calculated. This ellipsoid is uniquely defined by the inverse of the covariance of all characteristics:

$$C = \mathrm{cov}\,(p_{1...k})^{-1} \qquad [1]$$

The parameter S can now be calculated from r and C using:

$$S^2 = r^T \cdot C \cdot r \qquad [2]$$

Reference List

1. Vijayakumar S, Myrianthopoulos LC, Rosenberg I, et al. Optimization of radical radiotherapy with beam's eye view techniques for non-small cell lung cancer. *Int J Radiat Oncol Biol Phys* 1991;21:779-88.

2. Choi N, Baumann M, Flentjie M, et al. Predictive factors in radiotherapy for non-small cell lung cancer: present status. *Lung Cancer* 2001;31:43-56.

3. Hayman JA, Martel MK, Ten Haken RK, et al. Dose escalation in non-small-cell lung cancer using three-dimensional conformal radiation therapy: update of a phase I trial. *J Clin Oncol* 2001;19:127-36.

4. Anscher MS, Marks LB, Shafman TD, et al. Risk of long-term complications after TFG-beta1-guided very-high-dose thoracic radiotherapy. *Int J Radiat Oncol Biol Phys* 2003;56:988-95.

5. Liao ZX, Travis EL, Tucker SL. Damage and morbidity from pneumonitis after irradiation of partial volumes of mouse lung. *Int J Radiat Oncol Biol Phys* 1995;32:1359-70.

6. Travis EL, Liao ZX, Tucker SL. Spatial heterogeneity of the volume effect for radiation pneumonitis in mouse lung. *Int J Radiat Oncol Biol Phys* 1997;38:1045-54.

7. Khan MA, Hill RP, Van Dyk J. Partial volume rat lung irradiation: an evaluation of early DNA damage. *Int J Radiat Oncol Biol Phys* 1998;40:467-76.

8. Wiegman EM, Meertens H, Konings AW, et al. Loco-regional differences in pulmonary function and density after partial rat lung irradiation. *Radiother Oncol* 2003;69:11-9.

9. Seppenwoolde Y, De Jaeger K, Boersma LJ, et al. Regional differences in lung radiosensitivity after radiotherapy for non-small-cell lung cancer. *Int J Radiat Oncol Biol Phys* 2004;60:748-58.

10. Novakova-Jiresova A, van Luijk P, van Goor H, et al. Pulmonary radiation injury: identification of risk factors associated with regional hypersensitivity. *Cancer Res* 2005;65:3568-76.

11. van Luijk P, Novakova-Jiresova A, Faber H, et al. Radiation damage to the heart enhances early radiation-induced lung function loss. *Cancer Res* 2005;65:

12. Mah K, Van Dyk J. Quantitative measurement of changes in human lung density following irradiation. *Radiother Oncol* 1988;11:169-79.

13. Marks LB, Fan M, Clough R, et al. Radiation-induced pulmonary injury: symptomatic versus subclinical endpoints. *Int J Radiat Biol* 2000;76:469-75.

14. Theuws JC, Kwa SL, Wagenaar AC, et al. Dose-effect relations for early local pulmonary injury after irradiation for malignant lymphoma and breast cancer. *Radiother Oncol* 1998;48:33-43.

15. Wennberg B, Gagliardi G, Sundbom L, et al. Early response of lung in breast cancer irradiation: radiologic density changes measured by CT and symptomatic radiation pneumonitis. *Int J Radiat Oncol Biol Phys* 2002;52:1196-206.

16. El Khatib E, Sharplin J, Battista J. The density of mouse lung in vivo following X irradiation. *Int J Radiat Oncol Biol Phys* 1983;9:853-8.

17. Van Dyk J, Hill RP. Post-irradiation lung density changes measured by computerized tomography. *Int J Radiat Oncol Biol Phys* 1983;9:847-52.

18. Nicholas D, Down JD. The assessment of early and late radiation injury to the mouse lung using X-ray computerised tomography. *Radiother Oncol* 1985;4:253-63.

19. El Khatib E, Lehnert S. Lung density changes observed in vivo in rat lungs after irradiation: variations among and within individual lungs. *Int J Radiat Oncol Biol Phys* 1989;16:745-54.

20. Lehnert S, El Khatib E. The use of CT densitometry in the assessment of radiation-induced damage to the rat lung: a comparison with other endpoints. *Int J Radiat Oncol Biol Phys* 1989;16:117-24.

21. Libshitz HI, Shuman LS. Radiation-induced pulmonary change: CT findings. *J Comput Assist Tomogr* 1984;8:15-9.

22. Koenig TR, Munden RF , Erasmus JJ, et al. Radiation injury of the lung after three-dimensional conformal radiation therapy. *AJR Am J Roentgenol* 2002;178:1383-8.

23. Uchiyama Y, Katsuragawa S, Abe H, et al. Quantitative computerized analysis of diffuse lung disease in high-resolution computed tomography. *Med Phys* 2003;30:2440-54.

24. Theuws JC, Seppenwoolde Y, Kwa SL, et al. Changes in local pulmonary injury up to 48 months after irradiation for lymphoma and breast cancer. *Int J Radiat Oncol Biol Phys* 2000;47:1201-8.

25. Ward ER, Hedlund LW, Kurylo WC, et al. Proton and hyperpolarized helium magnetic resonance imaging of radiation-induced lung injury in rats. *Int J Radiat Oncol Biol Phys* 2004;58:1562-9.

26. Theuws JC, Kwa SL, Wagenaar AC, et al. Prediction of overall pulmonary function loss in relation to the 3-D dose distribution for patients with breast cancer and malignant lymphoma. *Radiother Oncol* 1998;49:233-43.

CHAPTER 6: Changes in expression of injury after irradiation of increasing volumes in rat lung

Alena Novakova-Jiresova[1], Peter van Luijk[2], Harry van Goor[3], Harm H. Kampinga[1], Rob P. Coppes[1,2]

[1] Department of Cell Biology, section Radiation and Stress Cell Biology

[2] Department of Radiation Oncology

[3] Department of Pathology

University Medical Centre Groningen, University of Groningen, The Netherlands

International Journal of Radiation Oncology, Biology and Physics 2007; 67 (5): 1510 – 1518.

Abstract

Purpose: To improve cure rates of thoracic malignancies by radiation-dose escalation, very accurate insight is required in the dose-delivery parameters that maximally spare normal lung function. Radiation-induced lung complications are classically divided into an early pneumonitic and a late fibrotic phase. This study investigated the relative dose-volume sensitivity, the underlying pathologic findings, and consequentiality of early to late pathophysiologic phases.

Materials and Methods: We used high-precision, graded dose-volume lung irradiations and followed the time dependency of the morphological sequelae in relation to overall respiratory function.

Results: Two distinct pathologic lesions were identified in the *early* post-irradiation period (6-12 weeks): vascular inflammation and parenchymal inflammation. Vascular inflammation occurred at single doses as low as 9 Gy. This translated into early respiratory dysfunction only when a large lung volume had been irradiated and was reversible in time. Parenchymal inflammation was seen after

higher doses only (onset at 16 Gy), progressed into later fibrotic remodelling but did not translate into dysfunction at a 25% lung volume even after single doses up to 36 Gy.

Conclusion: Our data imply that a low dose scattered over a large lung volume causes more early toxicity than an extreme dose confined to a small volume. Such findings are crucial for clinical treatment planning of dose escalations and choices for modern radiotherapy techniques.

6.1 Introduction

The inclusion of healthy lung tissue into the radiation field is inevitable during the radiotherapy (RT) of thoracic tumours. Since the resulting pulmonary toxicity may be life threatening, efforts have been aimed at finding reliable measures that would predict whether a treatment plan is safe for an individual patient. Modern three-dimensional (3D) treatment planning techniques yield accurate dosimetric data throughout a patient's lung, enabling investigations of the relation between toxicity and various dose-volume parameters. Several simple parameters (e.g., mean lung dose, volume irradiated to ≥ 20 or ≥ 30 Gy) have been related to the development of symptomatic radiation - induced lung injury and models have been created that relate the dose-volume histogram to the normal tissue complication probability (NTCP) (1,2). Nevertheless, if used alone, none of these parameters offers a predictive power sufficient for clinical decision-making (3). It is generally agreed that multiparameter predictive models are necessary for clinical use. Information on the pre-RT overall lung function (3,4), on the inhomogeneous lung perfusion (3,5), upper or lower lung tumour location (6,7), and cytokine expression (8) have all been shown to improve the prediction if used in conjunction with the dose-volume parameters. However, even those models cannot separate patients who develop or stay free of respiratory symptoms with sufficient accuracy. Thus, the optimal combination of predictive parameters remains unknown. This has seriously hampered efforts to improve cancer cure rates by escalating the radiation dose to a tumour.

Experimental studies have allowed testing of a better defined set of different treatment conditions than is achievable in clinical practice. Such studies have lead to the concepts of dose-volume interactions and regional differences in pulmonary radiosensitivity (9-12). Also, experimental studies have allowed detailed investigations on pathophysiologic mechanisms that can help to improve the formulation of predictive models and offer explanations for the enduring contradictory observations found in published reports. Radiation - induced lung injury has been traditionally divided into an early inflammatory phase, termed *radiation pneumonitis*, and a late fibroproductive phase, termed *fibrosis*, in humans (13-15) and animals (16,17). Dispute exists as to whether the two entities are a cascade of consequential and sequential processes, albeit involving multiple cell types (18,19) or whether they are independent events (2,16,20).

In the present study, we addressed these latter questions and investigated the morphologic abnormalities emerging at different times after irradiation at three different volume levels (100%, 50% and 25%) in rat lung and how they translated into impairment of overall lung function. Phases with distinct morphologic and functional characteristics were defined within the experimental follow-up. It was found that the character of morphologic lesions in the *early* phase differed qualitatively according to the dose administered and that this was critical for the development (or non-development) of the consequential *late* damage. Furthermore, the volume irradiated had a marked influence on the probability of each type of morphologic damage to translate into respiratory dysfunction. Clearly, the responses to irradiation of a small volume to a high dose or of a large volume to a low dose followed different rules with regard to their impact on overall lung function at increasing time lengths after the exposure.

6.2 Materials and methods

Animals: Adult male albino Wistar rats of the Hsd/Cpb:WU strain bread in a specific pathogen free colony (Harlan-CPB, Rijswijk, The Netherlands) were used in the experiments. They were housed five to a cage under a 12 h light - 12 h dark cycle and fed rodent chow (RMH-B, Hope Farms, Woerden, The Netherlands) and water ad libitum. The experiments were performed in agreement with the Netherlands Experiments on Animals Act (1977) and the European Convention for the Protection of Vertebrate Animals Used for Experimental Purposes (Strasbourg, 18.III.1986).

Collimator design and irradiation procedure: Based on thoracic computed tomography (CT) scans of five healthy rats weighing 300-340g, the borders of the collimators were calculated to expose either 100% (whole lung plus margin), 50% (± 5%) or 25% (± 5%) of the total lung volume, including both the alveolar parenchyma and bronchial structures encompassed within. Three-millimeter lead collimators were then constructed. Details of the procedure have been published earlier (21,22). Simulator images of the five resulting irradiation portals are shown in Fig. 1 a)-e). The alveoli essential for the gas exchange were not homogeneously distributed over the whole lung volume as perihilar regions contained more large bronchi than did the peripheral regions (Fig. 1 f). A similar finding was earlier shown in mice (11). The two 50% volume irradiation cohorts represented two distinct cases: Almost the entire

right lung was irradiated in the 50% right cohort (Fig. 1 b). The irradiation field thus encompassed not only the alveolar parenchyma but also the large bronchi and vessels branching from the right hilum, reducing the affected volume of alveolar tissue (decisive for the functional response) to slightly < 50%. This cohort was therefore labelled "50%min". The 50% lateral cohort was irradiated to the lateral parts of both lungs that consisted exclusively of alveolar tissue (Fig. 1 c). Therefore, the volume of affected alveolar tissue in this case was truly 50% of total lung volume and was even slightly > 50% of total alveolar tissue volume. For this reason, the cohort was labelled "50%plus".

The volume of the heart in the irradiation fields was 99 % ± 1% for the whole lung irradiation, 25 % ± 5% for the 50% right and the 25% apex irradiations, 3 % ± 3% for the 50% lateral irradiation and 1 % ± 1% for the 25% base irradiation. However, the radiation doses used in the whole lung irradiation were below the threshold, estimated to be 18-19 Gy, for *early* sub-clinical cardiac injury (23). Irradiation of 25% of the heart volume has previously been shown not to influence global respiratory function as measured by breathing rate assay (9). Thus, the extent of heart irradiation in the present set-up was considered insignificant.

Details of the irradiation procedure and dosimetry were published earlier (9). In brief, the total doses were delivered using 200 kV X-ray source from two opposing anterior-posterior and posterior-anterior (AP/PA) fields. The nominal dose rate was 2.68 to 2.90 Gy/min. The rats (from all dose-groups) had to be turned around in the irradiation holder for the AP/PA irradiation. Including this "time lag", the total irradiation time did not exceed 25 minutes for each animal. Using dose – profile films, the 15% and 10% iso-doses were found to extend 1.0 - 4.5 mm and ≤ 10 mm beyond the edge of the shield, respectively. The total irradiation doses were 9, 10, 11 or 12 Gy delivered to the 100% lung volume, 16, 18, 20 or 22 Gy delivered to the 50% lung volume, and 27, 30, 33 or 36 Gy delivered to the 25% lung volume. The dose ranges were chosen based on literature data (22,24-26) and on small pilot feasibility experiments. Care was taken to avoid lethal pulmonary toxicity, as well as complications from radiation injury to other thoracic structures while, at the same time, cover the range of dose-response in breathing rate assay. The control animals were anaesthetized and sham irradiated.

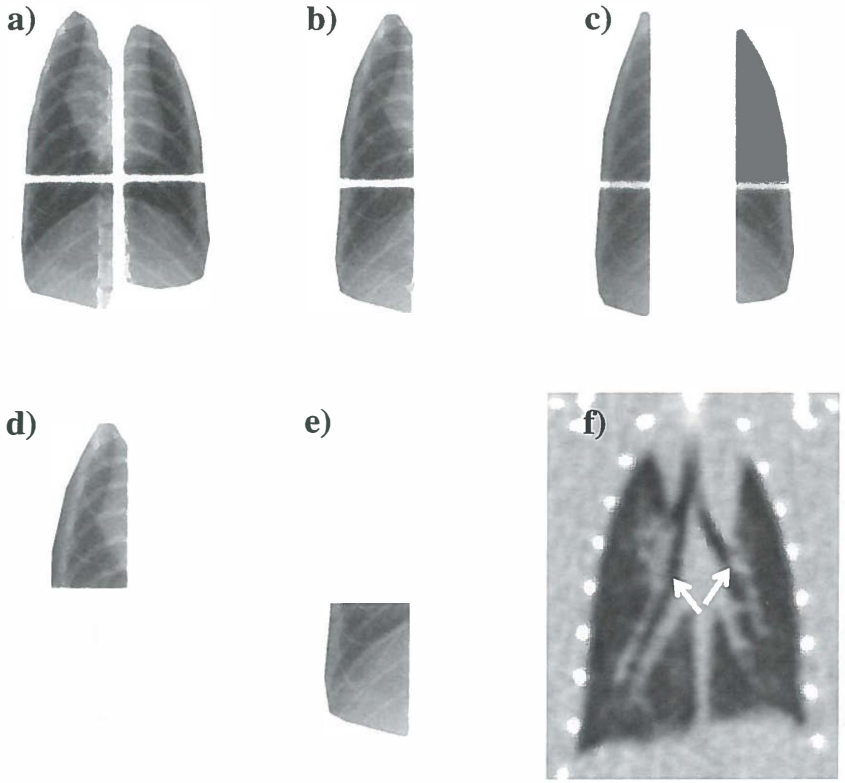

Figure 1: Simulator films of anteroposterior irradiation portals for: **(a)** whole lung irradiation (100% volume), **(b)** 50% right irradiation (50%min), **(c)** 50% lateral irradiation (50%plus), **(d)** 25% right apex and **(e)** 25% right base irradiations. Note the offset of the partial volumes from the midline to avoid irradiation of spinal cord and oesophagus. **(f)** CT image of control rat thorax at week 0 showing longitudinal slice through lung hila with branching of lobar bronchi (white arrows). Air-filled alveolar tissue appears black.

Follow-up and morbidity: A total of 194 animals (including 14 controls) involved in the study were inspected a minimum of twice a week for general health and weighed biweekly. The rats continued to grow but the 11-12 Gy dose groups of the 100% volume cohort and 18-22 Gy dose groups of the 50% volume cohort lagged behind the controls by ≤ 12 % in their weight gain. The only extrapulmonary toxicity encountered was a moist skin desquamation in the irradiation fields of animals irradiated to doses of ≥ 20 Gy. It was successfully managed by topical application of

gentian violet. The number of animals per dose group decreased over the follow-up period due to regular sacrifices for histology examination. The numbers of rats per dose group were 9, 7 and 5 at 0-8, 10-26 and 28-38 weeks, respectively. The control group consisted of 14, 10 and 7 animals in these periods. The different volume cohorts were irradiated 2-3 months apart. Because of the 9-month follow-up period, they overlapped in time and were housed in the same room of the animal laboratory. Several control animals were sham irradiated and followed up with each cohort. We also performed an inter-experiment comparison between the first and last cohort that confirmed the reproducibility of the data.

Breathing rate assay: The breathing rate (BR) at rest was recorded for each rat at less than one week before irradiation and then every two weeks till 38 weeks post-irradiation using a whole-body plethysmograph. Details of the procedure have been published earlier (9). The mean BR of each dose group in breaths per minute (bpm) was calculated at each time point, as well as for periods of weeks 6 - 12, 16 - 28 and 34 - 38. Those three intervals encompassed three distinct periods of BR dynamics: the *early*, the *intermediate* and the *late*, respectively, on the basis of differences in lung function as described previously (9). Also, an individual mean BR was calculated for each animal in those three periods. The ordinal BR data were converted into quantal BR data by applying a rule: If the individual mean BR in a given period exceeded a cut-off value defined as the mean BR of the age-matched control group in that period + 2SD, the rat was considered a responder (meeting the nominal level of statistical significance of 0.05). The cut-off value was 183, 180 and 188 bpm in the *early*, *intermediate* and *late* periods, respectively.

Histology: Two rats per dose group and three controls were sacrificed at random for morphologic examination of their lung tissue at 8, 26 and 38 weeks post-irradiation. Details of the procedure have been published earlier (9). Three-micrometer serial sections containing standardized samples of every irradiated lobe were stained with haematoxylin - eosin (H-E) or Masson's trichrome (MT) stain for collagen fibres (bluish-green) and examined by light microscopy. In the entire tissue cross-section on each slide, blinded scoring of vascular changes and parenchymal changes (as described in the "Results" section) was done separately using two semiquantitative scoring scales. The vascular changes were scored using a 0-3 point

scale, with 0 indicating 0-5, 1 indicating 6-12, 2 indicating 13-20, and 3 indicating >20 affected vessels with a diameter of > 300 μm, or double the number of vessels with a smaller diameter (≤ 300 μm). The scoring scale for parenchymal injury was based on the size of inflammatory or fibrotic focal lesions on each slide: no foci present = score 0; small foci present (focus < half of the 100 x magnification field) = score 1; medium foci present (focus > half of, but not exceeding the 100 x field) = score 2; large foci present (focus ≤ 40 x field) and total affected area not exceeding 50% of the total tissue cross-section = score 3; and confluent foci present (focus exceeds 40 x field) and total affected area exceeds 50% of the total tissue cross-section = score 4. One H-E and one MT slide per rat were examined and assigned a joint score for vascular damage (VD) and a joint score for parenchymal damage. See Table 2 for a simplified version of the scores.

Statistical analysis: The dose-dependency of the BR response was evaluated by calculating the significance of Pearson's correlation coefficient from scatter plots of the data. The levels of morphologic and functional responses after the irradiation of 25% volume in the lung apex or in the lung base were compared using the nonparametric Mann-Whitney *U*-test. The nominal level of statistical significance was 5%. The quantal BR data were analyzed using a probit model. This yielded sigmoid dose - response curves representing estimates of normal tissue complication probability (NTCP) and estimates of the dose inducing the response in 50% of the irradiated animals (ED_{50}) during each of the three follow-up periods. The ED_{50} values with their 95% confidence intervals (CI) allowed the comparison of the functional response of the irradiated volumes.

6.3 Results

Whole lung irradiation (100% volume, dose range 9-12 Gy) resulted in alterations in both pulmonary morphology and function within the first 3 months after irradiation. Morphologically at 8 weeks, the prominent finding was edema of vascular walls and perivascular mononuclear infiltrates affecting both large and small vessels (Fig. 2 d, g). This inflammatory vascular damage (VD) had disappeared at week 26 (Fig. 2 e, h) and week 38 (Fig. 2 f, i), although a variable degree of vascular sclerosis persisted (Fig. 2 e, f, h). In contrast to the prominent VD, the changes within the alveolar parenchyma, either inflammatory or fibrotic, were rare and, if found, minimal

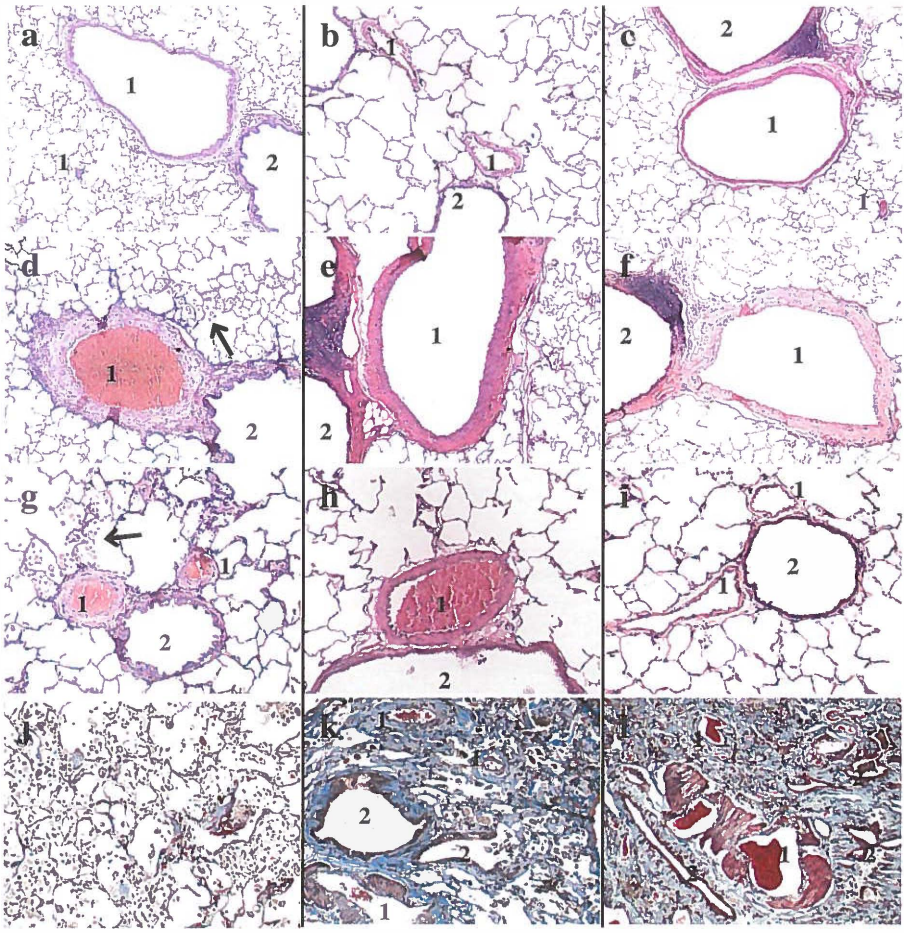

Figure 2: Lung morphology. The left panel **(a,d,g,j)** 8 week time point; the middle panel **(b,e,h,k)** 26 week time point; the right panel **(c,f,i,l)** 38 week time point. Upper **(a-c)** Normal lung parenchyma and vessels in controls. **d)-i)** Vascular damage after whole lung irradiation to 12 Gy. Vascular wall edema and perivascular inflammatory infiltrate (marked by arrows) of large vessel **(d)** and of arteriols **(g)** in the same section. Wall hypertrophy of large vessel **(e)** and arteriole **(h)**. Wall hypertrophy of large vessel **(f)** but no obvious pathologic features in arterioles **(i)**. Hematoxylin - eosin staining, original magnification 100x **(a,c,d-f)** or 200x **(b, g-i)**. Lower **(j-l)** Parenchymal damage after 25% volume irradiation by 36 Gy to lung apex **(k)** or lung base **(j,l)**. Acute inflammation with initial collagen deposition **(j)**. Fibrotic obliteration of alveoli, hypertrophy and sclerosis of vascular walls **(k,l)**. Masson's trichrome staining - collagen dyed blue-green, 200x magnification **(j-l)**. 1 denotes vessel, 2 denotes bronchus.

at all time points. Respiratory function, as represented by BR, showed dose-dependent ($p<0.01$) impairment between 4 and 14 weeks but had returned to normal at 16 weeks and continued so for the rest of the follow-up (Fig. 3 a). Thus, this low-dose / large-volume irradiation resulted in marked functional deficit during the *early* phase but induced almost no alterations in the later periods (Fig. 4 a, c, e). This suggested that the threshold for the early injury was lower than the threshold for the chronic injury after this type of irradiation, as evidenced by the NTCP curves (Fig. 4 b, d, f) and the dose required to obtain 50% effect (ED_{50} values, Table 1).

The effects of the 50% volume irradiation (dose range 16-22 Gy) have been previously described (9). Only the two 50% volume cohorts that did not entail significant cardiac irradiation were included in the present study to exclude an indirect effects on pulmonary function (9,12). Those cohorts also represented irradiation of slightly different volumes of alveolar tissue due to the varying proportion of bronchi (see Fig. 1 and the "Materials and Methods" section). Three phases of response were distinguished: an *early* phase (weeks 6-12) of focal exudative inflammation in the lung parenchyma paralleled by the first BR peak (Fig. 4 a); an *intermediate* phase (weeks 16-28), and a *late* phase (weeks 34-38), both characterized by fibro-productive inflammation with either an increase in BR (*intermediate* phase, Fig. 4 c) or a variable BR recovery (*late* phase, Fig. 4 e). Although the intraparenchymal inflammatory foci dominated the morphology findings at 8 weeks, the VD was also present, both inside the foci and around them. The NTCP curves for each period are shown in Fig. 4 b, d, f) and the ED_{50} estimates are listed in Table 1. The expression of symptoms in the *early* and *late* periods was stronger in the 50%plus cohort (50% lateral) while the 50%min irradiation (50% right) was tolerated better (Fig. 4 a-b, e-f). This subtle

Figure 3 (next page): Mean breathing rate (BR) in the four dose groups (9-12 Gy) of 100% volume irradiation plotted as function of time **(a)**. Mean BR in the four dose groups (27-36 Gy) of 25% volume irradiation to the right lung apex **(b)** or right lung base **(c)** plotted as function of time. Error bars represent standard error of mean, arrows on time axes mark points of morphologic examinations (week 8, 26 and 38), as shown in Fig. 2.

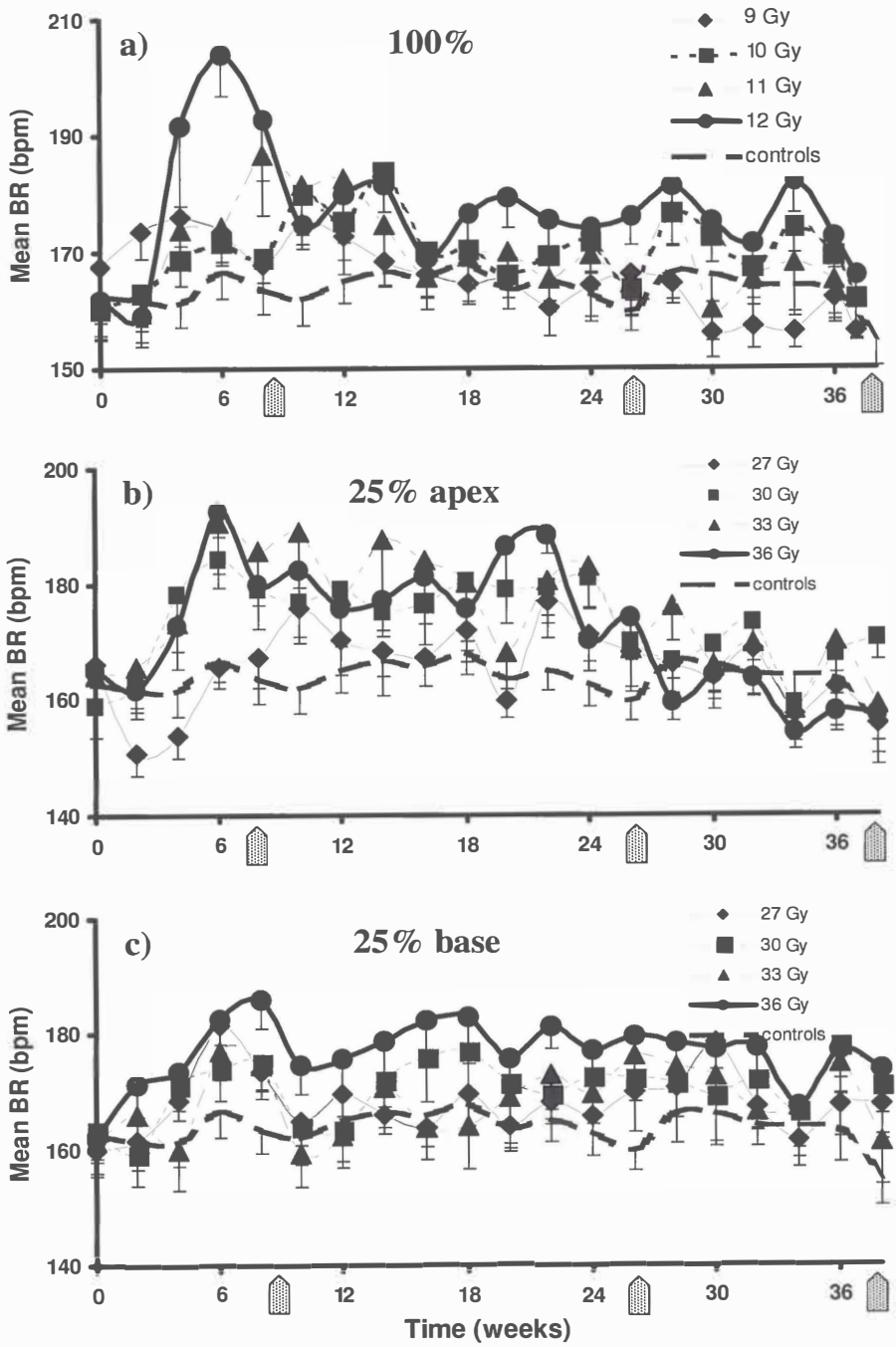
a)
100%
9 Gy
10 Gy
11 Gy
12 Gy
controls
Mean BR (bpm)
210
190
170
150
0
6
12
18
24
30
36
b)
25% apex
27 Gy
30 Gy
33 Gy
36 Gy
controls
Mean BR (bpm)
200
180
160
140
c)
25% base
Time (weeks)

Figure 3

change in volume did not matter in the *intermediate* period when both 50% irradiation groups experienced severe functional detriment (Fig. 4 c-d). Further, almost all of the *early* symptoms (100% and 93% in the 50%min and 50%plus cohorts, respectively) lead to morbidity in the later phases. In addition, some symptoms (58% and 22% in the 50%min and 50%plus cohorts, respectively) arose *de novo* in the *intermediate* phase, hallmarked by the onset of fibrosis. Thus, the threshold for symptoms of late fibrosis appeared lower than that for symptoms of early pneumonitis after this intermediate-dose / intermediate-volume irradiation.

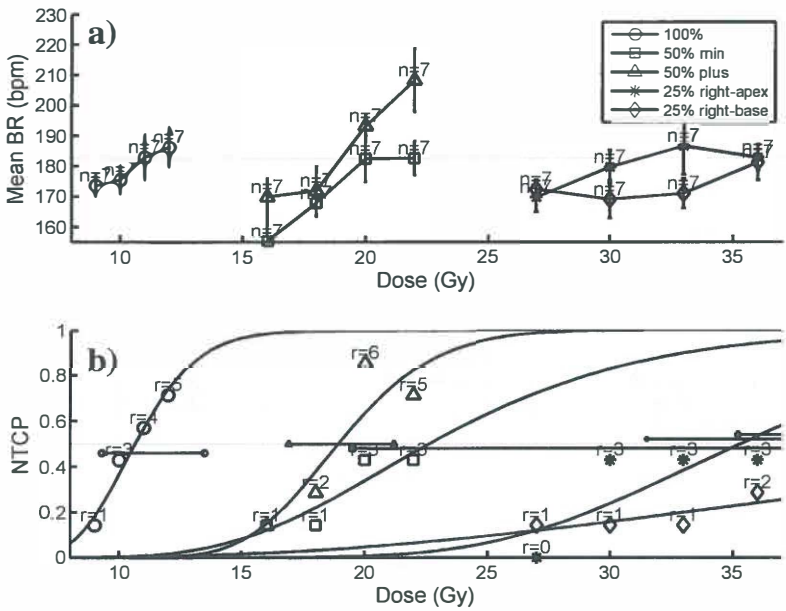

Figure 4: Overview of functional effects in the *early* **(a,b -** above), *intermediate* **(c,d** – next page) and *late* **(e,f** – next page) periods after irradiation of lung volumes: 100% (circles), 50%min (squares), 50%plus (triangles), 25% apex (asterisks) and 25% base (diamonds). Upper panels **(a,c,e)** show relation between mean breathing rate (BR) and radiation dose. Lower panels **(b,d,f)** show the quantal BR data as percentage of responders (≥ cut-off value) in each dose group. Data points were fitted by probit model to yield sigmoid curves representing NTCP estimates. Cut-off value (= mean BR of the age-matched control group + 2SD), represented by horizontal dotted lines, was 183, 180 and 188 bpm in the *early*, *intermediate* and *late* periods, respectively.

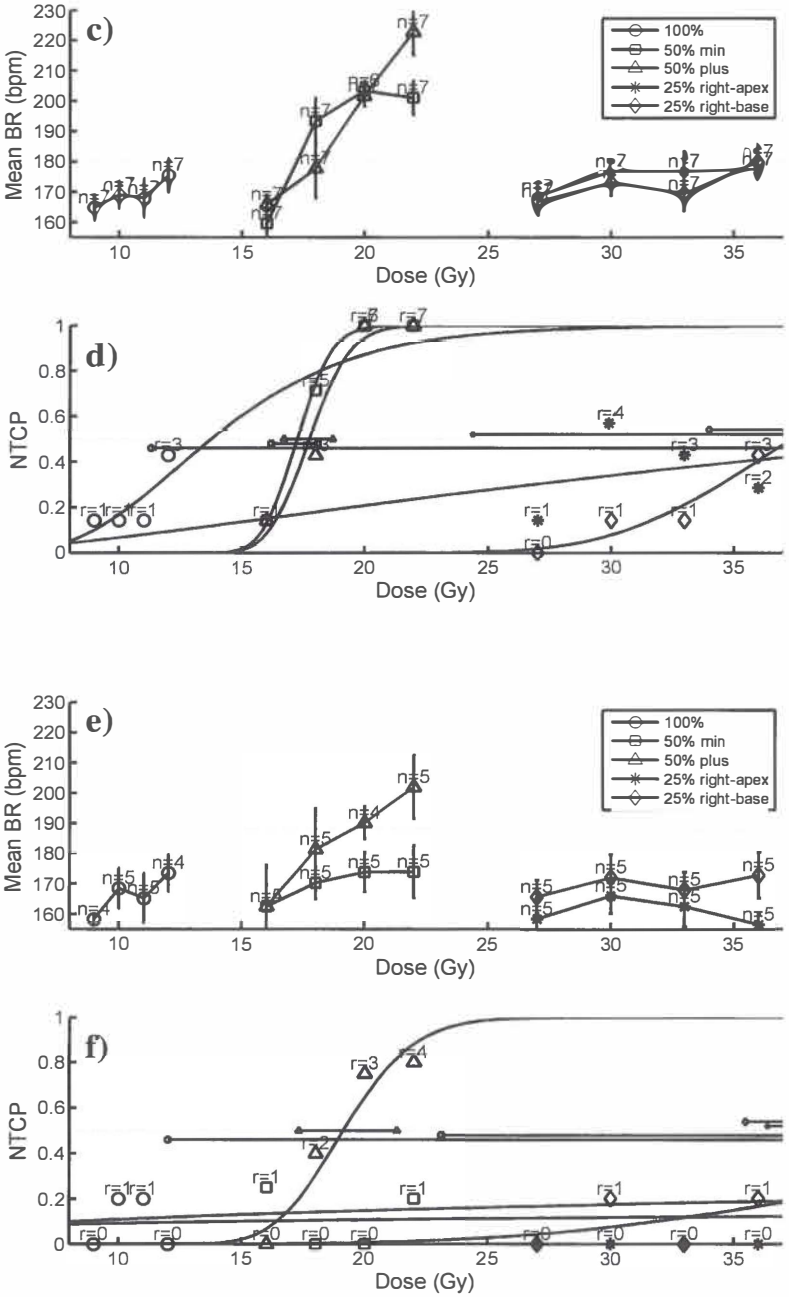

Figure 4 – cont.

Table 1: ED_{50} estimates calculated from probit analyses of BR data in the *early*, *intermediate* and *late* periods after irradiation of varying volumes in rat lung

Period	Volume cohort	ED_{50} (Gy)	95% CI
EARLY	100%	10.7	9.3 - 13.5
	50%min	[22.6]	[19.5 – ND]
	50%plus	18.9	16.9 - 21.2
	25% apex	[35.3]	[31.5 – ND]
	25% base	[55.1]	[35.2 – ND]
INTERMEDIATE	100%	[13.7]	[11.3 – ND]
	50%min	17.2	16.2 – 18.1
	50%plus	17.7	16.7 – 18.7
	25% apex	[45.4]	[24.4 – ND]
	25% base	[37.4]	[34.0 – ND]
LATE	100%	[971.6]	[12.0 – ND]
	50%min	[457842.9]	[23.1 – ND]
	50%plus	19.1	17.3 – 21.3
	25% apex	[244.5]	[36.4 – ND]
	25% base	[52.2]	[35.5 – ND]

Abbreviations: ED_{50} = estimate of dose inducing response in 50% of irradiated animals; 50%min = 50% right cohort; 50%plus = 50% lateral cohort; ND = upper confidence limit can not be determined.
Brackets indicate extrapolated value.

The 25% volume irradiation (dose range 27-36 Gy), aimed at either the right lung apex or right lung base, led to a formation of inflammatory foci in the irradiated parenchyma 8 weeks after irradiation. Just as after the 50% irradiation, the foci were marked by mononuclear infiltration of alveolar spaces and interstitial edema, but collagen deposition was already more pronounced at this early time point (Fig. 2 j). This progressed into confluent fibrosis at weeks 26 and 38 when the interstitium, expanded by collagen, and mononuclear infiltration obliterated the alveolar spaces (Fig. 2 k, l). Also here, signs of VD were present as vascular wall edema in the *early* period (not shown) and vascular hypertrophy and sclerosis at the *intermediate* and *late*

time points (Fig. 2 k, l). Functionally, the 25% volume irradiation induced moderate BR increases in the *early* and *intermediate* periods with generalized recovery beyond 28 weeks (Fig. 3 b, c and Fig. 4 a, c, e). Dose-dependency was neither expressed in morphology nor function, indicating that a maximum effect had already been achieved at (or below) the lowest dose of 27 Gy. Differences in the level of response between the apex and base were not observed in morphology and were non-significant in function (p_{early}=0.09, p_{interm}= 0.3, p_{late}= 0.06). The NTCP curves are shown in Fig. 4 b, d, f) and the ED_{50} estimates are listed in Table 1. As after the 50% volume irradiation, most of the *early* symptoms (71%) were followed by *intermediate* symptoms, but 33% of the latter arose *de novo*. However, the level of respiratory dysfunction after this high-dose / small-volume irradiation was never as severe as after the 50% volume irradiation. This confirms that the effect on global function is very volume-dependent.

The patterns of responses for all volumes irradiated are summarized in Table 2. In the 100% volume cohort, VD was the only morphologic lesion observed across the applied dose-range and thus had to be responsible for the functional response noted in the *early* phase (Fig. 4 a, b). In the case of the two 50% volume cohorts (50%min and 50%plus), the vascular changes were widespread following 16 Gy while the inflammatory (later fibrotic) parenchymal foci were sparse and small. Because little functional deficit was detected in the 16 Gy dose groups (Fig. 4 b, d, f), it can be deduced that neither the VD spread over the ±50% lung volume, nor the mild parenchymal injury were sufficient to influence function. Larger doses (≥18 Gy) given to the 50% volume, however, lead to substantial parenchymal injury with functional consequences in all phases of follow-up for the 50%plus cohort and, to a lesser extent, for the 50%min cohort (Fig. 4 b, d, f). Although the VD was also present, the morphologic and functional outcomes were clearly dominated by the parenchymal injury. The same applied to the morphologic picture in the 25% volume cohorts, and yet, the functional outcome was completely different, marked by good tolerance throughout the follow up.

In summary, the respiratory symptoms in the *early* phase were linked to the VD resulting from low-dose / large-volume irradiation and to acute parenchymal inflammation resulting from intermediate-dose / intermediate-volume irradiation. During the *intermediate* phase, functional loss occurred after intermediate-dose / intermediate-volume irradiation that lead to a blending of acute inflammation with

Table 2: Relation between morphologic and functional findings after irradiation of varying volumes in rat lung.

Period	Endpoint	Volume cohort and dose group					
		100%	50%min	50%min	50%plus	50%plus	25%
		9-12 Gy	16 Gy	18-22 Gy	16 Gy	18-22 Gy	27-36 Gy
EARLY	VD inflammatory	++	+	++	NSc	NSc	+
	Parench. inflam.	+/-	+/-	++	+	++	++
	Parench. fibrosis	0	0	+/-	0	+/-	+
	Function	++	+/-	+	+/-	++	+
INTERMEDIATE	VD – H/S	+	+/-	+	NSc	NSc	+/-
	Parench. inflam.	+/-	+	+	+	+	+
	Parench. fibrosis	0	+	++	+	++	++
	Function	+	+/-	++	+/-	++	+
LATE	VD – H/S	+/-	0	+	NSc	NSc	+/-
	Parench. inflam.	+/-	+/-	+	+/-	+	+
	Parench. fibrosis	+/-	+/-	++	+/-	++	++
	Function	+/-	+/-	+/-	0	++	+/-

Abbreviations: 50% min = 50% right cohort; 50% plus = 50% lateral cohort; VD = vascular damage; Parench. inflam. = parenchymal inflammation; Parench. fibrosis = parenchymal fibrosis; H/S = hypertrophy and sclerosis of vascular walls; NSc = not scored. Semiquantitative scale for morphologic and functional findings: 0 lesion absent or no responders, +/- lesion mostly absent or few individual responders, + lesion present or less than 50% of responders, ++ lesion widespread or more than 50% of responders.

progressive fibrosis. *Late* phase functional injury was caused by confluent fibrosis propagated over the 50%plus volume. Fibrotic remodelling limited to less then 50% of alveolar volume, regardless of the radiation dose used, was without any consequences for function at those late time points.

6.4 Discussion

In order to develop clinically reliable NTCP models for pulmonary radiation treatments, a thorough knowledge on how the dose-volume parameters interact with the responding tissue and its biology is necessary. In this study, we investigated the dose-volume-time dependency of the morphologic sequelae of lung irradiation and its relation to overall lung function. We identified two distinct pathogenetic processes appearing in the *early* time window of radiation pneumonitis and having an unequal impact on later pathology. The VD induced by lower doses showed a large capacity for recovery with minimal structural or functional consequences beyond 4 months post-irradiation, while the parenchymal inflammation, produced by higher doses, almost invariably ended in morphologically and clinically expressed fibrosis. Furthermore, the irradiated volume determined whether or not a specific type of morphologic damage resulted in function loss. Large - volume irradiation produced the VD with early functional loss already at low doses, whereas small - volume irradiation did not lead to substantial function loss at any post-irradiation interval despite the very high doses and severe parenchymal injury. Our findings may facilitate risk prediction of dose-escalation treatments and intensity modulated radiation therapy (IMRT) in lung cancer patients where both the high-dose and low-dose exposures are involved.

To this date, risk-predictive models have considered pneumonitis as one pathogenetic unit with uniform dose-volume-response parameters (27). We have shown that although the "classic" parenchymal inflammation required a large dose and an intermediate irradiated volume to become expressed as an *early* functional deficit, the damage to the pulmonary vascular bed was elicited by doses far less than the threshold for parenchymal injury but needed to involve larger volumes to influence lung function. Moreover, the VD, unlike the parenchymal inflammation, had largely receded by four months after the exposure. Several observations published in the past support our findings. Two types of damage, endothelial and epithelial, have been previously described to occur in the early phase of pulmonary radiation injury

(28-30). Rubin and Casarett (15) suggested that injury to the pulmonary vasculature played a primary role in the early radiation response and that mild damage could subside with no chronic reaction. Furthermore, early changes in lung perfusion showed a tendency for recovery with time in patients receiving fractionated lung doses ≤ 50 Gy (31) as opposed to a continuous progression in patients irradiated to > 50 Gy (32). Similarly, early radiographic pulmonary changes in breast cancer patients, in whom the lung dose is typically < 50 Gy, have shown complete resolution (19,33) in contrast to reports of chronic fibrotic scarring seen in majority of patients after thoracic RT (13,14,30). Even in rats, an early reduction in pulmonary blood flow returned to normal after single doses ≤ 13.5 Gy, but higher doses (≥ 18 Gy) led to a second reduction at 16 weeks (34). All these findings suggest that milder VD is reparable but more severe parenchymal injury progresses into fibrosis. If, hypothetically, our single dose regimens were translated into fractionated treatment using the linear quadratic model (α/β = 3.3 Gy), the VD would have already occurred after 25 fractions of 1 Gy - a dose commonly delivered to the lung during photon beam therapy for breast cancer. The disappearance of sequelae with the passing of the acute phase after such treatment (19,33) would match the occurrence of VD. On the other hand, the potential of the early VD to cause serious hemodynamic problems, if spread over a large volume, should not be underestimated. In particular, during dose-intensified IMRT, low to intermediate doses can be delivered to significant portions of healthy lung and yield an unexpected toxicity (35,36). This underscores the need for investigations on the dose-volume thresholds for clinically relevant VD in humans.

When a higher dose producing the parenchymal injury was given, a smaller irradiated volume sufficed to cause functional response. In our experiments, the cut-off was about 50% of the total lung volume, because the 50%plus volume cohort showed functional deficits consistently throughout the follow-up, but in the 50%min cohort, the impairment was seen only in the *intermediate* phase. It seemed that the pulmonary reserve capacity during the early and late periods was just sufficient when slightly less than 50% of alveolar tissue had been affected (the 50%min volume as opposed to the 50%plus volume) suggesting a very steep volume effect for tolerance at this volume interval. At lower volumes (25% volume irradiation), even extreme doses (the highest single dose used in this study was a biological equivalent of 267 Gy in 2-Gy fractions, α/β = 3.3 Gy) that induced severe parenchymal inflammation and

fibrosis, had only a minor impact on respiratory function. This argues against the propriety of risk prediction based on dose-averaging approaches such as the mean lung dose (5,37). Inversely, it supports clinical findings that a safe volume to irradiate with high doses is probably <25 % (38,39). In patient population, where the pre-RT respiratory function is often compromised by pre-existing pulmonary morbidity, limits for caution would definitely be more stringent than in our experiment. Nevertheless, the results may be summarized in a dictum: "A lot to a little" is tolerated better than "A little to a lot". It would be of interest to assess in further studies how the development of the VD versus the parenchymal inflammation / fibrosis may be influenced by a prophylactic or therapeutic application of anti-inflammatory agents (40).

Conclusion

We have reported for the first time how two distinct forms of post-irradiation morphologic damage have different implications for tolerance after irradiation of small or large volumes in the rat lung. The inflammatory vascular damage occurring at low doses affected lung function when a large volume was irradiated. This could have implications for treatment techniques in which the dose is spread over a large volume, such as with IMRT. The parenchymal injury occurred at higher doses but was already able to compromise function already at intermediate irradiated volumes. Nevertheless, the functional consequences following irradiation of small volumes were minimal owing to the reserve capacity of the lung. This indicates that dose-escalation to very high doses, but involving small lung volumes, is a feasible therapeutic strategy, provided the larger lung volumes are protected from low to intermediate dose exposures. Such findings may be utilized in designing clinical trials that study NTCP prediction following novel radiation treatments for lung cancer such as IMRT or proton RT.

Acknowledgements

The study was financially supported by the Interuniversitary Institute for Radiopathology and Radiation Protection (IRS grant # 9.0.18) and a grant from the Dutch Cancer Society (RuG 2002-2673).

The authors thank H. Faber, R.J. Konst and I. Platteel for technical assistance, F. Cotteleer and E.M. Wiegman for design of the collimators and P.C. van der Hulst and P.T.F. Leferink for supervision on dosimetry. The authors are grateful to R. Lohynska for discussions on clinical applicability.

Reference List

1. Marks LB. Dosimetric predictors of radiation-induced lung injury. *Int J Radiat Oncol Biol Phys* 2002;54:313-6.

2. Seppenwoolde Y, Lebesque JV. Partial irradiation of the lung. *Semin Radiat Oncol* 2001;11:247-58.

3. Lind PA, Marks LB, Hollis D, et al. Receiver operating characteristic curves to assess predictors of radiation-induced symptomatic lung injury. *Int J Radiat Oncol Biol Phys* 2002;54:340-7.

4. Marks LB, Munley MT, Bentel GC, et al. Physical and biological predictors of changes in whole-lung function following thoracic irradiation. *Int J Radiat Oncol Biol Phys* 1997;39:563-70.

5. De Jaeger K, Seppenwoolde Y, Boersma LJ, et al. Pulmonary function following high-dose radiotherapy of non-small-cell lung cancer. *Int J Radiat Oncol Biol Phys* 2003;55:1331-40.

6. Seppenwoolde Y, De Jaeger K, Boersma LJ, et al. Regional differences in lung radiosensitivity after radiotherapy for non-small-cell lung cancer. *Int J Radiat Oncol Biol Phys* 2004;60:748-58.

7. Yorke ED, Jackson A, Rosenzweig KE, et al. Dose-volume factors contributing to the incidence of radiation pneumonitis in non-small-cell lung cancer patients treated with three-dimensional conformal radiation therapy. *Int J Radiat Oncol Biol Phys* 2002;54:329-39.

8. Fu XL, Huang H, Bentel G, et al. Predicting the risk of symptomatic radiation-induced lung injury using both the physical and biologic parameters V(30) and transforming growth factor beta. *Int J Radiat Oncol Biol Phys* 2001;50:899-908.

9. Novakova-Jiresova A, van Luijk P, van Goor H, et al. Pulmonary radiation injury: identification of risk factors associated with regional hypersensitivity. *Cancer Res* 2005;65:3568-76.

10. Travis EL, Liao ZX, Tucker SL. Spatial heterogeneity of the volume effect for radiation pneumonitis in mouse lung. *Int J Radiat Oncol Biol Phys* 1997;38:1045-54.

11. Tucker SL, Liao ZX, Travis EL. Estimation of the spatial distribution of target cells for radiation pneumonitis in mouse lung. *Int J Radiat Oncol Biol Phys* 1997;38:1055-66.

12. van Luijk P, Novakova-Jiresova A, Faber H, et al. Radiation damage to the heart enhances early radiation-induced lung function loss. *Cancer Res* 2005;65:6509-11.

13. Marks LB, Yu X, Vujaskovic Z, et al. Radiation-induced lung injury. *Semin Radiat Oncol* 2003;13:333-45.

14. McDonald S, Rubin P, Phillips TL, et al. Injury to the lung from cancer therapy: clinical syndromes, measurable endpoints, and potential scoring systems. *Int J Radiat Oncol Biol Phys* 1995;31:1187-203.

15. Rubin, P. and Casarett, G. W. Respiratory System - Radiopathologic basis of the clinical course. Clinical Radiation Pathology, Volume I ed, pp. 446-459. Philadelphia: W.B. Saunders Company, 1968.

16. Coggle JE, Lambert BE, Moores SR. Radiation effects in the lung. *Environ Health Perspect* 1986;70:261-91.

17. Travis EL. The sequence of histological changes in mouse lungs after single doses of x-rays. *Int J Radiat Oncol Biol Phys* 1980;6:345-7.

18. Rezvani M, Hopewell JW. The response of the pig lung to fractionated doses of X rays. *Br J Radiol* 1990;63:41-50.

19. Trott KR, Herrmann T, Kasper M. Target cells in radiation pneumopathy. *Int J Radiat Oncol Biol Phys* 2004;58:463-9.

20. Travis EL, Down JD. Repair in mouse lung after split doses of X rays. *Radiat Res* 1981;87:166-74.

21. Cotteleer F, Faber H, Konings AW, et al. Three-dimensional dose distribution for partial irradiation of rat parotid glands with 200kV X-rays. *Int J Radiat Biol* 2003;79:689-700.

22. Wiegman EM, Meertens H, Konings AW, et al. Loco-regional differences in pulmonary function and density after partial rat lung irradiation. *Radiother Oncol* 2003;69:11-9.

23. van Luijk P, H Faber, H Meertens et al. Subclinical heart damage enhances radiation-induced lung function loss. Int J Radiat Oncol Biol Phys 2005;63.

24. Newcomb CH, Van Dyk J, Hill RP. Evaluation of isoeffect formulae for predicting radiation-induced lung damage. *Radiother Oncol* 1993;26:51-63.

25. Vujaskovic Z, Down JD, t' Veld AA, et al. Radiological and functional assessment of radiation-induced lung injury in the rat. *Exp Lung Res* 1998;24:137-48.

26. Ward HE, Kemsley L, Davies L, et al. The pulmonary response to sublethal thoracic irradiation in the rat. *Radiat Res* 1993;136:15-21.

27. Bentzen SM, Skoczylas JZ, Bernier J. Quantitative clinical radiobiology of early and late lung reactions. *Int J Radiat Biol* 2000;76:453-62.

28. B. Roswit and D. C. White. Severe radiation injuries of the lung. *Am J Roentgenol* 1977;129 (1):127-136.

29. M. P. Law and R. G. Ahier. Vascular and epithelial damage in the lung of the mouse after X rays or neutrons. *Radiat Res* 1989;117 (1):128-144.

30. Gross NJ. The pathogenesis of radiation-induced lung damage. *Lung* 1981;159:115-25.

31. Theuws JC, Seppenwoolde Y, Kwa SL, et al. Changes in local pulmonary injury up to 48 months after irradiation for lymphoma and breast cancer. *Int J Radiat Oncol Biol Phys* 2000;47:1201-8.

32. Woel RT, Munley MT, Hollis D, et al. The time course of radiation therapy-induced reductions in regional perfusion: a prospective study with >5 years of follow-up. *Int J Radiat Oncol Biol Phys* 2002;52:58-67.

33. Lingos TI, Recht A, Vicini F, et al. Radiation pneumonitis in breast cancer patients treated with conservative surgery and radiation therapy. *Int J Radiat Oncol Biol Phys* 1991;21:355-60.

34. Peterson LM, Evans ML, Graham MM, et al. Vascular response to radiation injury in the rat lung. *Radiat Res* 1992;129:139-48.

35. De Neve W, De Wagter C. Lethal pneumonitis in a phase I study of chemotherapy and IMRT for NSCLC: the need to investigate the accuracy of dose computation. *Radiother Oncol* 2005;75:246-7.

36. Holloway CL, Robinson D, Murray B, et al. Results of a phase I study to dose escalate using intensity modulated radiotherapy guided by combined PET/CT imaging with induction chemotherapy for patients with non-small cell lung cancer. *Radiother Oncol* 2004;73:285-7.

37. Kwa SL, Lebesque JV, Theuws JC, et al. Radiation pneumonitis as a function of mean lung dose: an analysis of pooled data of 540 patients. *Int J Radiat Oncol Biol Phys* 1998;42:1-9.

38. Graham MV, Purdy JA, Emami B, et al. Clinical dose-volume histogram analysis for pneumonitis after 3D treatment for non-small cell lung cancer (NSCLC). *Int J Radiat Oncol Biol Phys* 1999;45:323-9.

39. Hernando ML, Marks LB, Bentel GC, et al. Radiation-induced pulmonary toxicity: a dose-volume histogram analysis in 201 patients with lung cancer. *Int J Radiat Oncol Biol Phys* 2001;51:650-9.

40. Moulder JE. Pharmacological intervention to prevent or ameliorate chronic radiation injuries. *Semin Radiat Oncol* 2003;13:73-84.

CHAPTER 7: General discussion, conclusions

This thesis addressed the development of radiation-induced lung injury following thoracic irradiation. In experimental and clinical setting, we evaluated relevance of known and new parameters that could potentially be used as predictive factors for probability of pulmonary complications occurring as a side-effect of thoracic radiotherapy. This is especially urgent in treatment of non-small cell lung cancer (NSCLC) where about 45% of the patients present with locally advanced disease that is not amenable to surgical resection (72). Despite recent technological advances in radiotherapy techniques and combined modality approach of chemoradiation, treatment outcomes in these patients are not satisfactory (5-y overall survival rates < 30%) and treatment toxicity relatively high (72). Identification of patients whose susceptibility to complications is low (due to location and size of their tumours and/or their physiologic background) and who may thus benefit from more aggressive treatment schedules involving escalation of radiation dose, is essential. No one single of the known parameters is able to predict with sufficient reliability which patient is going to experience complications following radiation treatment and which is not. The selection of candidate parameters and their incorporation into clinically reliable multi-parameter predictive models is still a subject of research. Reports in this thesis were a part of this effort.

7.1 Evaluation of endocrine effects of cytokine TGF-β

Initially, we concentrated on profibrogenic cytokine transforming growth factor β1 (TGF-β1) and its alleged *endocrine effects*, i.e. an ability to transfer from the circulation into the irradiated lung tissue and enhance there the local pathophysiologic processes set in motion by the initial radiation insult. The association between rising TGF-β1 levels in plasma during radiotherapy treatment for NSCLC and increased risk for later development of symptomatic radiation induced lung injury has been observed in a number of studies originating from the Duke University Medical Center, Durham, USA (2,3,25) as well as from our institution (80). Namely the decrease of TGF-β1 plasma concentration at the end of radiotherapy seemed to be predictive of freedom

from radiation induced lung injury (predictive value of 90%) (2) and this criterion was used with a relative success to select patients for radiation dose escalation (4,5). We evaluated the effects of circulating TGF-β on a group of 46 NSCLC patients from the outpatient clinic of the Department of Pulmonary Diseases at the University Medical Center Groningen (**Chapter 2**). This group represented an expanded set of patients compared to the earlier reported study (80). We found no significant link between either absolute levels of TGF-β in plasma or their increases/decreases during the radiotherapy course (relative to the pre-treatment level) and the incidence of symptomatic radiation pneumonitis. What we did find was a trend ($p=0.055$) towards higher mid-treatment TGF-β plasma value as compared to the pre-treatment plasma value, i.e. the TGF-β ratio of $w3/w0 > 1$, among patients who later developed radiation pneumonitis. This lead to a high negative predictive value of the w3/w0 ratio, i.e. this ratio being < 1 identified patients in low risk for toxicity, yet with large uncertainty (negative predictive value = 91% with wide 95%CI [59-100%]). This confirmed the tendency of patients at low risk of radiation-induced lung injury to experience decreases rather than increases of plasma TGF-β levels during their treatment consistent with the reports cited above. However, disappearance of this trend at the end of the radiotherapy course (weeks 4-6) together with the fact that some of the patients with pneumonitis and high TGF-β ratios had relatively low absolute plasma levels exposed the low reliability of this parameter in terms of risk prediction as well as the complexity of the biologic mechanisms behind the putative endocrine effects of this cytokine. Several research groups, including the team from the Duke University Medical Center, have since come up with similarly unequivocal results where circulating TGF-β fell short of its promise as an independent risk predictor of symptomatic pulmonary toxicity (11,14,17,18,53). As was shown by De Jaeger et al (14), rising plasma TGF-β concentrations at the end of radiotherapy were closely related to the mean lung dose (MLD) and the extent of morphologic sequelae assessed by CT but not to the symptomatic toxicity. We conclude that even though a clear-cut endocrine activity of circulating TGF-β remains unproven, rising TGF-β levels in plasma seem to be an indicator of the extent of the inflicted injury by the radiation treatment and thus they should be expected to show some relation to the symptomatic pulmonary toxicity. However, this relation does not appear straightforward and strong enough to grant a sufficient predictive power for clinical decision-making based on this parameter alone.

7.2 Regional variations in lung radiosensitivity

In following research, we turned to variations in regional sensitivity of the lung as a possible determinant of risk of symptomatic radiation induced lung injury. Pioneering work done in mice indicated that lung base was significantly more sensitive to radiation effects in terms of impaired function (assayed by breathing rate) and mortality than lung apex or mid-portion (45,76). This was attributed to a denser distribution of target cells, i.e. larger proportion of alveolar parenchyma vs. conducting airways in the lung base compared to the apical regions (76,77). We designed an experimental study using a rat model with larger thorax allowing more accurate dose delivery to an identical 50% lung volume in six clinically relevant pulmonary regions: right, left, apical, basal, mediastinal (central) and lateral (**Chapter 3**). Using the breathing rate (BR) as a functional endpoint, we detected varying degree of respiratory function impairment between 6 and 38 weeks following single dose X-ray exposure of 16 – 22 Gy. Two periods of recovery judged from a decrease in BR between 12 and 16 weeks and beyond 30 weeks divided the course of a functional response into three phases: *early* (6-12 weeks), *intermediate* (16-28 weeks) and *late* (34-38 weeks). Histopathologic evaluation showed focal acute exudative inflammation to be the morphological correlate of functional changes at 8 weeks and chronic fibroproductive inflammation with progressive accumulation of interstitial collagen at 26 and 38 weeks. While the character of morphological findings did not differ among the regions, the functional response was significantly more severe in the left, apical and lateral cohorts than in the right, basal and mediastinal cohorts, most notably during the *early* and *late* follow-up periods. Contrary to the findings in mice (45,76), the lung base belonged to the less sensitive regions that showed largely non-significant increases in BR during the *early* and *late* periods. These differences in regional sensitivity almost leveled out during the *intermediate* period when all region cohorts showed significant BR increases above the baseline. On one hand, these results confirmed the conclusion of the mice study (45,76,77) about the importance of the proportion of gas-exchange structures (alveoli) encompassed in the irradiation field. The lateral region, virtually devoid of large airways and thus harboring maximal portion of alveolar parenchyma, ranked consistently among the most radiosensitive regions in terms of function. On the other hand, this factor could not explain the marked hypersensitivity of the apical and left regions as the proportion of alveolar

parenchyma versus airways was roughly comparable in the left, right, apical and basal portals. Also, cellular hypersensitivity could not be the issue because the extent of morphological damage assayed by histopathology was comparable between all regions. What set the apical and left region cohorts apart, however, was the fact that their irradiation portals almost entirely encompassed the heart (74.5 % and 99.5% heart volume in the left and apex portal, respectively). This was in contrast to the right and basal regions that included heart volume of 25% or less. The heart was also covered in the mediastinal irradiation (97.3%) but the proportion of alveolar parenchyma was the far lowest in this cohort due to the inclusion of hilar parts of the lungs abundant in large vessels and airways. Functionally, the mediastinal cohort came out as the least sensitive in all three periods. When pooled data from all cohorts were analyzed, combination of heart and lung irradiation was significantly linked to higher likelihood of symptomatic respiratory dysfunction during the *late* phase and a trend (odds ratio = 1.3, 90% CI 0.8-2.3) was observed during the *early* phase. Such effect was absent during the *intermediate* phase. These observations led us to a novel hypothesis that an interaction between the radiation-induced pulmonary parenchymal injury and the cardiac injury could constitute an additional factor that contributed to regional variations in lung sensitivity during the *early* and *late* follow-up periods.

7.3 Influence of heart co-irradiation on respiratory function

Anatomically, the position of the heart in the upper / central thoracic cavity (6,13) is similar in the rat and the mouse. Therefore, our hypothesis of respiratory dysfunction being enhanced by heart irradiation seemed to contradict the hypersensitivity of lung base (not containing the heart) reported for the mouse model (45,76). It should be noted, however, that in the mice experiments, the evaluation of BR changes was based on a single time point of 22 weeks that conspicuously falls into the *intermediate* window (16-28 weeks) between the *early* and *late* responses as shown in our study. Neither we could detect an influence of heart irradiation in this period and the lung base and lung apex appeared equally radiosensitive. Thus, other factors like precision of dose delivery (facilitated by the larger size of rat thorax) could come into play and account for the different outcomes regarding rats and mice.

The unresolved case for the interaction between the *early* pulmonary and *early* cardiac radiation injuries that fell just short of statistical significance in the previous study became a focus of our follow-up work (**Chapter 4**). We employed high-energy

proton beam to further increase the precision of dose delivery and designed collimators to specifically include or exclude the entire heart in combination with purely parenchymal or mixed hilar portions of the lung in the same rat model. Four fields were irradiated by a single dose of 16-21 Gy: a cardiac field (100% heart volume + 25% lung volume), a mediastinal field (100% heart volume + 50% central lung volume including hili), cardio-lateral field (100% heart volume + 50% lung volume including lateral parenchymal regions) and lateral only field (0% heart volume + 50% lateral lung volume). Again, BR assay was used as a measure of respiratory function. For the *early* post-irradiation period (6-12 weeks), the fraction of animals with dysfunction (i.e. responders) was determined in each dose group and the dose causing effect in 50% of the animals (ED_{50}) was estimated. In agreement with the former study, cardiac exposure and mediastinal exposure did not result in a significant *early* impairment. Following lateral only irradiation, the fraction of responding animals increased progressively with dose resulting in a significant reduction in ED_{50}. The steepest dose-response and the significantly lowest ED_{50} were, however, produced by the combined cardiac and lateral lung irradiation.

Firstly, these findings reconfirmed the importance of proportion of alveolar parenchyma within the irradiated lung volume, with or without cardiac irradiation, for the probability of symptomatic lung injury. Secondly, the data validated our hypothesis that already in the first three months following radiation treatment, co-irradiation of the heart could enhance the respiratory dysfunction associated with pulmonary irradiation. To our knowledge, this is the first time a conclusive evidence has been presented showing that acute radiation-induced cardiac toxicity can have a clinically relevant manifestation.

It has long been recognized that elevated BR can be an indicator of not only pulmonary, but also cardiac or joint cardiopulmonary decompensation (27,65). BR reflects the efficacy of gas exchange in the lungs as well as the efficacy of transport of these gases by the cardiovascular system. Thus, altered pulmonary gas exchange together with suboptimal heart performance should translate into more severe BR increases than lung injury alone. We did not directly evaluate morphological or functional status of hearts during our experiments. But we can judge the probable pathophysiological mechanism behind the assumed reduction in cardiac function in our experimental animals (albino Wistar rats) from a summary of literature data.

7.4 Radiation pathology of the heart and functional consequences – literature review and implications

Historically, the heart was considered a radioresistant organ due to postmitotic character of cardiac myocytes (1,26). During the 1960s, awareness grew about the late cardiac complications of mediastinal irradiation in Hodgkin's lymphoma patients treated by radiation techniques suboptimal by today's standards (1,22,70,71). Since 1970's, radiation effects in the heart became a subject of experimental studies on rabbits (19,20,21), rats (39,42,66,84,86,87) and dogs (56,57). But it wasn't until 1990's when the extent of excess cardiovascular mortality in Hodgkin's lymphoma and breast cancer survivors – and consequently the clinical relevance of late cardiac radiation toxicity - became widely recognized (1,8,26,30,64,71). In contrast, early cardiac radiation effects have never received that much attention as their clinical consequences (i.e. transient reversible depression in myocardial function) have generally been considered insignificant (1,65).

In animal studies, several aspects of an early radiation damage to the heart have been studied. A course of morphological changes following 20 Gy single dose was investigated in the rabbit heart (19,20,21). Three stages of injury were postulated: acute inflammatory stage with neutrophilic infiltrate involving all layers of the heart (6-48 hours), latent stage with alterations in capillary endothelial cells detectable only by electron microscopy (2-70 days) that led to the reduction in number of patent capillaries in the late stage (11-21 weeks), also distinct by myocardial and pericardial fibrosis. A hypothesis was formulated, that is still widely accepted today, stating that the myocyte death and diffuse fibrosis were consequences of destruction of microvascular network and ensuing ischemia. And since the late lesions were identical to those observed in humans, also the mechanism of pathogenesis was presumed the same (1,19,21,22,71). Signs of an early microvascular damage have also been reported in the dog heart in terms of edema linked to increased capillary permeability 1 month after fractionated exposure, accompanied by a transient decrease in ventricular function assayed by echocardiography and reversible by 6 months (56,57). Pericardial effusions appeared at 3 months and regressed spontaneously. In contrast to rabbits and humans, fibrosis in later stages (12 months) was mostly limited to epicardium and pericardium (57). The main late pathology within canine myocardium was myocyte degeneration and muscle atrophy that, at 12 months, still appeared functionally compensated (56,57).

Strain differences in the radiation response of the heart exist in rats. Early pericardial and pleural effusions have been reported 12-16 weeks after single doses of ≥ 20 Gy to the heart (and roughly 16% of the lung) in Wistar rats (42), the strain also used in our study. Those early effusions were reversible after doses ≤ 20 Gy and were not associated with signs of congestion, neither from the left-sided heart failure (no pulmonary edema) nor right-sided heart failure (no liver congestion) (39,42,65). Thus, it was concluded that those were not a consequence of failing heart but rather an exudative reaction of the irradiated mesothelial (pleural and pericardial) surfaces. By themselves, they were believed to accelerate the consequent development of cardiac failure. In contrast, Sprague-Dawley rats have been known for a delayed response with signs of congestive cardiac failure and pleural effusions that, however, were not evident before 6 months following single dose (≥ 20 Gy) whole heart exposure (39,66,84,86). Here, the delayed pleural effusions were believed to be a consequence of cardiac failure (39,65,84). Also fibrosis, mainly subendocardial, was a late feature apparent from about six months onwards (7). As in rabbits and dogs, capillary damage has been a prominent microscopic finding in both rat strains. Within the myocardium of the ventricles, focal reduction in capillary density and loss of alkaline phosphatase activity in the capillary endothelial cells have been reported after single doses of 10-20 Gy at 28 days in Wistars and at 70 days in Sprague-Dawley rats (40,42,87). They seemed to precede degeneration of myocardium fibers developing in these focal areas from about 10 weeks on with a maximum at 14 or 41 weeks in Wistar and Sprague-Dawley rats, respectively (40,42,66,86,87). Endothelial damage and capillary destruction, when evaluated by electron microscopy in Wistar rats following 20 Gy to the heart, were visible already within first 24 hours post-irradiation, peaked at 8 weeks and then partially receded at 14 - 26 weeks (12). Myocytes displayed early alterations in intercalated discs (providing mechanical and electrical connection between neighbouring cells) ranging from vesiculation at six hours to dissociation of discs during peak damage at four weeks. Also those changes were restored by 14 - 26 weeks. Using an *ex vivo* working rat heart preparation, authors further showed an early transient depression in cardiac mechanical function at four and eight weeks with suboptimal recovery by 17 – 26 weeks (12). The functional recovery correlated conspicuously with the ultrastructural repair suggesting causal relationship between them. Using the same method (*ex vivo* isolated working rat heart preparation) but Sprague-Dawley rat strain, similar timing of onset was detected for a decline in

myocardial function, i.e. two to four months after 20-30 Gy (23,84). However, this decline was progressive and no indication of recovery could be seen until a decompensation and death between 6 to 16 months. More stable parameters of cardiac contractile function following 20 Gy single dose heart irradiation were revealed by "*in vivo*" (*in situ*) radionuclide ventriculography. For cardiac output in Sprague-Dawley rats, a significant decline was reported only after 10 months (86), 16 months (23) or 6 months, however, with a relatively sufficient performance (about 70% of the control level) lasting till the end of follow-up at 12 months (66). In the Wistar strain, *in vivo* cardiac output dropped significantly already at 11 weeks but then remained also relatively constant at around 60% of the control value until a decompensation marking heart failure between 8 and 9 months (66). Such disparity between *in vivo* and *ex vivo* functional measurements, as well as the clear delay between the full expression of structural damage (myocardial degeneration) and hemodynamic failure, has been viewed as an evidence for compensatory mechanisms being operative *in vivo* that maintain sufficient cardiac output despite the compromised contractile status (23,56,57,65,66). Those mechanisms likely involve an increased sympathetic stimulation as well as an enhanced positive inotropic response of remaining myocytes through an up-regulation of myocardial β-adrenergic receptor density (24,41,66).

The animal experimental studies mentioned so far involved only small irradiated lung volumes and focused on cardiac damage alone. Apart from symptoms of terminal cardiac failure, they did not evaluate early, subtle effects of declined cardiac performance on global respiratory function that would have direct relevance for observations made in our studies. However, such reports provide us with evidence that the heart is an organ that responds acutely to irradiation with a range of morphological and functional consequences that likely reduce tolerance to any additional cardiovascular stress. The notion of acute radiation-induced heart disease being aggravated by additional pulmonary damage has become a focus of an investigation using a canine model (28). The authors suggested for the first time that irradiation of one organ (the lung) may adversely impact radiation response of another organ (the heart) within first six months after the exposure. Following single dose (12 Gy) irradiation of three different thoracic volumes, they detected increased mean pulmonary artery pressure, an indicator of pulmonary hypertension, severity of which correlated to the volume of lung irradiated. It was most severe in the whole thorax group, less pronounced in the 80% lung volume / shielded heart group and only

moderate in the heart irradiation group (including just 36% of lung volume). Cardiac function (stroke volume) was most significantly impaired following the whole thorax irradiation compared to just a moderate decrease after the local heart exposure and no change in the group with shielded heart. The authors concluded that conditions that reduce pulmonary capillary volume (like radiation lung injury) lead to pulmonary hypertension and pumping against this increased pulmonary vascular resistance may precipitate the failure of the irradiated heart. Although this study approached the issue of interaction between cardiac and pulmonary radiation damage from an opposite standpoint showing that pulmonary process was able to intensify cardiac dysfunction, the proof of a principle is very well applicable to, and in support of, conclusions of our investigations.

Pulmonary hypertension could be the factor explaining why manifest cardiac failure following thorax irradiation is usually right-sided in rats and dogs (28,39,42,56,66,84) and even humans (58). The signs of chronic congestive right heart failure in terms of inactivity, subcutaneous edema, congested liver, ascites and pleural effusions dominate the picture. However, symptoms of failing left heart (i.e. dyspnea) are frequently present, too, and they are concretized in assays of cardiac function (*ex vivo* working rat heart preparation, radionuclide ventriculography and echocardiography) that, in fact, mostly measure parameters belonging to the left ventricle (e.g. left ventricle cardiac output, stroke volume or ejection fraction).

In summary, the radiation-induced morphological and functional alterations in the animal heart could be divided into early and late with a potential period of compensation in between them. The early symptoms and/or measurements of failing cardiac function within the first 16 weeks following irradiation have been linked to pleural and pericardial effusions in Wistar rats (27,39,42), decrease in myocardial capillary density in Wistar rats (42), ultrastructural damage in capillary endothelia and myocytes in Wistar rats (12), myocardial edema due to increased capillary permeability in dogs (56), pulmonary hypertension in dogs (28) and to incipient myocardial degeneration in Wistar rats (42,66). The early pleural and pericardial effusions were viewed as a factor contributing to heart failure by some (27,39,42) while their correlation to declines in cardiac output or to BR increases has been disputed by others (28,65). Instead, myocardial degeneration apparent from 10 weeks onwards was suggested as the dominant cause for the early compromised

haemodynamic function and a term "*radiation-induced cardiomyopathy*" was used for this syndrome (in an analogy to a clinically recognized condition) (65).

The late symptoms and/or measurements of failing cardiac function appearing beyond six months have also been considered a consequence of cardiomyopathy, i.e. myocardial degeneration, together with an exhaustion of compensatory mechanisms in Wistar rats (42,66) and Sprague-Dawley rats (23,39,66,86). In studies on other models (rabbits and dogs), the follow-up was not long enough for late cardiomyopathy to fully develop (65). Nevertheless, reduction in cardiac performance 6 months post-irradiation in dogs has been linked to concomitant pulmonary hypertension (28).

In some studies, the early effects and late cardiac failure were separated by a period of recovery or functional compensation. Examples include restoration of capillary density and endothelial enzymatic activity in hearts of Wistar and Sprague-Dawley rats following < 20 Gy (40), an ultrastructural repair and improved cardiac performance between 14 and 26 weeks in Wistar rats (12) and compensation of cardiac function (after an initial drop) despite advancing myocardial degeneration observed in rats (23,65,66) and dogs (56,57).

As follows from this overview, multiple pathophysiological mechanisms are known that could produce the assumed reduction in cardiac function in our experimental animals and, thus, corroborate the hypothesis of interaction between pulmonary and cardiac radiation injuries, as presented in **Chapters 3** and **4** of this thesis. In the *early* period (6-12 weeks post-irradiation), morphological signs of an acute exudative inflammation were evident in the irradiated lung tissue and their adverse effects on respiratory function were significantly enhanced by heart irradiation. We reason that the cardiac contractile function probably declined due to radiation-induced microvascular and myocyte injury and incipient myocardial degeneration at this period. The observation that functional response of regions with or without irradiated heart leveled out in the *intermediate* period (16-28 weeks) could suggest involvement of compensatory mechanisms (described above) that stabilized the cardiac performance. Thus, only the extent of chronic inflammation and progressive fibrotic remodeling within the irradiated lung parenchyma itself were to determine the severity of respiratory dysfunction at that interval. Also the lung is known for substantial reserve capacity in terms of redistribution of perfusion to, or a compensatory expansion of previously underused alveoli when other parts of lung

were destroyed by radiation (49). Engaging this pulmonary reserve capacity likely improved respiratory function of regions without irradiated heart during the *late* period (34-38 weeks post-irradiation), when the parenchymal inflammation had largely receded and irradiated fibrotic areas of the lung shrunk into mere rudiments. In contrast, this late compensation was insufficient when both the heart and substantial proportion of pulmonary parenchyma were included in the irradiation field. Respiratory function of animals in these cohorts remained impaired until the end of follow-up at 38 weeks.

It is unlikely that pulmonary hypertension played a role in the regional variations observed in our studies as the irradiated lung volume was almost identical between more and less sensitive regions. Also the influence of pleural effusions was difficult to ascertain as those were seen rather indiscriminately across all the regional cohorts and at all time points in about one third of animals irradiated to ≥ 20 Gy.

7.5 Interaction between radiation injury to the lung and heart – application in NTCP modeling using preclinical data

When cancer patients have to undergo thoracic radiotherapy, several radiation plans are being drafted to select the most effective and, simultaneously, the least harmful treatment variant. The proportion of irradiated healthy lung volume and delivered radiation dose are being calculated in advance and used to estimate the probability of severe pulmonary complications arising from any given plan. This may be done in a form of mathematical functions that factor in the dose and the volume and relate them, based on an experience, to a certain level of *normal tissue complication probability* (NTCP). It has been repeatedly shown, however, that the accuracy of these NTCP predictive models based solely on dosimetric parameters is not sufficient for clinical use (37,47). Identification of additional parameters that would help predict the risk of symptomatic radiation-induced lung injury, especially the acute radiation pneumonitis, is viewed essential.

We showed that subclinical radiation damage to lung and heart might interact, exceed compensatory capacity and lead to clinically manifest cardiopulmonary dysfunction not only during the late, but also during the early period following hemithoracic irradiation in albino Wistar rats. Such finding warrants testing whether addition of the factor of heart co-irradiation into the NTCP models could improve their predictive strength with regard to the risk of early pulmonary complications.

Recent work from our laboratory tested such model modification on a set of preclinical data acquired during an early post-irradiation period (78). Thoracic single dose proton irradiation was carried out in rats that targeted 25% – 100% of lung volume with or without co-irradiation of the heart. To separate the influence of heart and lung exposure, the doses to these two organs were varied independently. BR elevation between 6 – 12 weeks post-irradiation served as the endpoint for symptomatic loss of function. *The critical volume model* was fitted to the data and was able to describe the loss of function following lung irradiation excluding the heart. However, to adequately fit all the data including combined lung-heart irradiations, the model had to be modified by addition of a single parameter denoting the reduction of pulmonary reserve capacity in consequence of heart co-irradiation. This modified *critical volume model* was consistent to all the experimental data. Its accuracy far exceeded the predictive abilities of clinically applied models that have been based on pulmonary dosimetric (dose and volume) and functional (pre-RT pulmonary function and perfusion) parameters only (47). This result provides further support for the notion that heart co-irradiation could be one of the long pursued additional biological risk determinants for development of symptomatic radiation pneumonitis following radiation treatment.

7.6 Interaction between radiation injury to the lung and heart – clinical relevance

There is more evidence that our experimental findings are relevant for clinical radiotherapy setting. Even though cardiac radiation toxicity is still viewed as a predominantly late event in cancer survivors (1,62,71), clinical evidence in support of early radiation induced cardiac injury and its possible interaction with early radiation damage to the lungs is available. Four main forms of post-irradiation cardiac morbidity have been documented in Hodgkin's disease and breast cancer patients: acute or chronic *pericarditis* with pericardial effusion and fibrosis, *cardiomyopathy* with myocardial fibrosis and long-term ventricular dysfunction, *coronary artery disease* with fibrointimal thickening and accelerated atherosclerosis and late *conduction disturbances* (arrhythmias) linked to the fibrosis of atrio-ventricular conduction system (1,71). Those are typically late effects separated by months to years from the completion of radiation treatment. Their clinical significance in lung cancer patients will likely grow with improvements in treatment outcomes (62).

However, before these late effects become manifest, subclinical cardiac injury is likely occurring and has been identified in several reports. Myocardial perfusion defects suggestive of microvascular damage have been detected 6 months following radiotherapy for left-sided breast cancer in 27 – 60 % of subjects and, in some cases, they were associated with cardiac wall motion abnormalities (1,31,54,62). In breast cancer patients treated by a technique obsolete by today's standards, even earlier changes in terms of transient, reversible depression in left ventricular function were found already during the first week and lasting until three months post-treatment (34). They were not related to pericardial effusions as those appeared after their resolution. Similarly, in a diverse group of patients with thoracic tumours treated by radiotherapy, Lagrange et al measured significant decreases in ejection fraction of both ventricles at 15 + days after the treatment (38). In both reports, the decreases in cardiac contractile function were asymptomatic in patients with no pre-existing cardiovascular morbidity and resolved spontaneously within two to six months. In analogy to animal studies, those acute changes might be a consequence of an acute reaction of vasculo-connective tissue as opposed to the long-term effects linked more firmly to myocardial fibrosis (38). Although their prognostic significance is unknown (1,65,71), it seems plausible to expect that those subclinical alterations would reduce the tolerance to any additional cardiovascular stress.

Heart in humans is positioned in the central to lower thoracic cavity what means that it receives higher doses during irradiation of lower lung tumours (52). Thus, a dose to the caudal parts of the lung may be a surrogate for incidental cardiac irradiation (50,55). Therefore it is of interest, that although majority of NSCLC tumours is typically located in the upper lung region, multitude of clinical studies found the incidence of symptomatic radiation injury to be significantly higher among patients with lower lung tumours than with upper lung tumours (29,33,67,85,88,89). Most of them used the endpoint of early radiation pneumonitis diagnosed within 6 months post-irradiation (67,85,89). In those studies, the incidence of early pneumonitis could be predicted based on dosimetric indices (mean regional dose and Lyman model NTCP) derived from dose distributions in the lower lung but not from dose distributions in the upper lung (67,88,89). Hope et al (33) showed that respiratory symptoms occurring up to 14 months post-irradiation were more frequent following lower lung exposure and that addition of a tumour location parameter (superior-inferior) into a multi-parameter predictive model significantly improved its

correlation to the incidence data compared to the previously tested dosimetric parameters and models (V_{20}, V_{13}, MLD, Lyman NTCP model). These reports suggested that radiation injury to the lower lung was more causative in terms of early and late respiratory dysfunction than injury to the upper lung. Such finding could be attributed to a number of mechanisms including the non-uniform distribution of target cells (77), better perfusion/ventilation and thus bigger physiological importance of lower lung in upright position in humans (33,89) and a greater extent of respiratory motion in the lower lung that likely increases the exposed volume of functional lung tissue when tumours in the lung base are treated (33,67,89). In our and others opinion, the "tip-over" effect of heart co-irradiation represents yet another very credible explanation for the relative hypersensitivity of lower lung in humans (50,55). To our knowledge, three clinical investigations attempted to correlate the dose to the heart with the probability of symptomatic radiation pneumonitis. The first two used univariate correlation as the mean of the analysis. Marks et al evaluated rates of dyspnea consistent with grade $\geq$ 2 pneumonitis, rates of heart toxicity (largely pericarditis) and their relation to mean lung and mean heart radiation doses in 215 lung cancer patients treated by conventional radiotherapy (52). While the mean heart dose and the incidence of heart injury were highly correlated, no association between the mean heart dose and dyspnea was detected. Similarly, Yorke et al found no significant correlation between the maximum heart dose, the mean heart dose or the dose in the "hottest" 5% irradiated heart volume and grade $\geq$ 3 pneumonitis among 78 NSCLC patients included in a dose-escalation trial (88). Based on our animal data and the considerations given above, it can be argued that the focus on univariate correlation between the cardiac dose and the respiratory symptoms, out of the context of other factors, could be to blame for these disappointing results. Cardiac irradiation alone or even in connection with irradiation of the mediastinal lung region had no to minimal impact on respiratory dysfunction in all three experimental studies done at our laboratory [**Chapters 3** and **4**, van Luijk et al, 2007 (78)]. What we propose is a joint consideration of damage to vulnerable lung alveolar tissue (parenchyma) and subclinical heart injury when predicting the risk of developing respiratory complications after a thoracic radiation treatment. Such approach (multivariate logistic regression) was adopted in the third study that evaluated incidence of radiation pneumonitis requiring steroid use in 209 NSCLC radiotherapy patients and searched for its association with multiple clinical, dosimetric and location parameters

pertaining to both the lung and the heart (15). The strongest correlation was found between the pneumonitis and heart D5, heart D30 (minimum doses in the hottest 5% or 30% irradiated heart volume, respectively), mean lung dose and tumour location parameter (superior vs. inferior lung). Those results are in clear support of our conclusions and warrant further testing of heart related parameters, alongside the common lung parameters, against new clinical datasets.

7.7 Radiological assessment of regional variations in lung radiosensitivity

We also investigated how the earlier described regional variations in lung radiosensitivity (section 7.2) could be accurately assessed by non-invasive, radiological means and whether such monitoring could be instrumental in predicting the risk of developing respiratory symptoms associated with the radiation-induced lung injury. For that purpose we explored ways how to quantitatively measure changes in radiological lung density by means of computerized tomography (CT) and examined how this structural endpoint could relate to global respiratory function (**Chapter 5**). In addition to the biweekly BR measurements, three animals (albino Wistar rats) from each dose group (16-22 Gy) underwent sequential thoracic CT scans before and at 8, 26 and 38 weeks after the single dose irradiation of 50% lung volume in six different lung regions (right, left, apical, basal, mediastinal and lateral). CT is a clinically important imaging modality allowing non-invasive evaluation of local pulmonary structural changes secondary to thoracic radiotherapy (46,48,51,73,75,82). However, objective quantitative assessment of this endpoint have been hampered by focal nature of radiation-induced lung lesions where, typically, areas of consolidation (increased density) are surrounded by areas of hyperinflation (decreased density) in both man (49) and rat (16,44,83). Attempts have been made in our laboratory (83) and by others (16) to circumvent this obstacle by computing the density changes in small regions of interest what yielded significant density increases. However, such method discarded large part of the data and could be a subject to bias in the placement of the region of interest. In the present study, a novel method was developed that enabled summing the complete information from the irradiated lung region into a single *structural change parameter S* based on the mean and standard deviation of the CT density distribution in an individual animal. According to this quantitative analysis, the character of the density changes did not vary between the regions but it did vary in time. The main finding within the irradiated field in the *early* phase (8 weeks post-

irradiation) was an increase in standard deviation with non-significant fluctuations in density itself. However, significant, progressive increase in density of irradiated lung regions was observed at the later time points (*intermediate* and *late* phases at 26 and 38 weeks, respectively). This was consistent with the histological description of the predominantly focal pneumonitic inflammatory lesions in the *early* phase and increasingly confluent fibrotic remodeling during the *intermediate* and *late* phases (**Chapter 3**). Also, this agreed well with the reported qualitative radiological patterns of patchy, non-homogeneous consolidation seen in the pneumonitic phase and solid, homogeneous consolidation prevailing in the fibrotic phase in humans (46). But most importantly, the structural change parameter allowed an evaluation of the relevance of radiologically assayed structural changes for the development of symptomatic pulmonary dysfunction. Here, regional differences reappeared again, and remarkably, they were consistent with the previously formulated hypothesis of interaction between pulmonary and extrapulmonary factors in determining the probability of respiratory dysfunction (**Chapters 3** and **4**). The severity of local structural change in the lung correlated strongest and at all time points with the probability of dysfunction after irradiation of 50% lateral lung volume. This lung region has been shown to contain majority of lung alveolar parenchyma decisive for gas exchange while it was almost devoid of large bronchial and vascular structures, as it did not include the heart (**Chapter 3**). Thus, the strong and lasting correlation between CT lung density measurements and functional impairment testified for a solid, straightforward causal relationship between parenchymal damage and respiratory symptoms in this cohort. Inversely, no correlation existed at any times between the CT lung density changes and respiratory symptoms following the 50% apical and 50% mediastinal lung volume exposures. Those two regions encompassed both the pulmonary hili (abundant in large air-ways and vascular structures) and the extrapulmonary factor of heart co-irradiation, but less of the alveolar parenchyma in their irradiation portals. Not surprisingly, the influence of altered pulmonary structure on the functional outcome was the weakest in these cohorts. The lung density changes of the third cohort with co-irradiated heart, the 50% left lung volume, could not be evaluated in the *early* phase due to logistic reasons, showed significant correlation with functional impairment in the *intermediate* phase and lost the correlation in the *late* phase. In agreement with our previous observation (**Chapter 3**), this could suggest temporary cardiovascular compensation that buffered the influence of heart injury during the

intermediate phase, allowing the global function to be determined predominantly by the local pulmonary damage even in a region containing the heart. In general, the correlations between lung structure and global function were strongest during the *intermediate* period in a majority of cohorts (i.e. left, right, basal and lateral). In all but the lateral cohort however, this correlation disappeared in the *late* period, suggesting diminished impact of the radiologically identifiable lung injury, either due to the strengthening influence of late cardiac failure or, inversely, due to the engagement of pulmonary reserve capacity. Thus, we demonstrated that the location and the time of onset of radiologically detected post-irradiation pulmonary changes had impact on their clinical manifestation. Similar regional and temporal dependency could exist in humans and could explain the so far conflicting findings with regard to the relation between pulmonary CT density changes and symptomatic / measurable function loss diagnosed in patients after thoracic radiotherapy (51,74,82). It appears that in patients, the most reliable connection between clinical manifestation and increases in CT density was found for the peripheral lung on the transition between acute and chronic radiation effects, i.e. between 3 and 12 months post-radiotherapy. Our method allows differential assessment of radiological changes in individual pulmonary regions and their easy comparison to the functional endpoints. Its clinical applicability should be assessed in future studies.

7.8 Dose – volume effects in the lung: time dependency and implications for high precision radiotherapy modalities

The dependency of incidence and severity of radiation induced lung injury on the irradiated lung volume has been firmly established (see **Chapter 1**, section 1.7.). However, uncertainties linger as to which volume parameter is the best predictor of respiratory complications, as well as to how risky are the extreme dose distributions, i.e. low doses spread over large volumes or high doses concentrated into small volumes (so called "A lot to a little or a little to a lot"). Those questions gained more and more urgency with introduction of novel radiation techniques, three-dimensional conformal radiotherapy (3D-CRT), intensity modulated radiation therapy (IMRT) and proton radiation therapy that tend to expand low dose volumes or deliver escalated doses to limited portions of the lung (9,10,43,59,60). Also, a great deal of controversy has been associated with the exact interrelation between the syndromes of early radiation pneumonitis and late radiation fibrosis in terms of the pathophysiological

mechanisms and target cell populations involved, and their reciprocal consequentiality (see **Chapter 1**, section 1.5.). We decided to investigate the possibility of these two entities being independent processes triggered by different dose and volume thresholds. This research has been presented in **Chapter 6**. Five cohorts of male Wistar rats were irradiated to three different volume and dose levels: total lung volume (9-12 Gy single dose level), 50% lung volume – right region or lateral region (16-22 Gy single dose level) and 25% lung volume at right apex or right base (27-36 Gy single dose level). The 50% right lung volume cohort encompassed large airways and vessels branching from the right hilum and thus the volume of truly alveolar tissue was slightly less than 50% of total. This cohort was labeled "50%min". The 50% lateral cohort consisted exclusively of alveolar tissue and thus the volume of affected alveolar parenchyma was slightly more than 50% of total. This cohort was labeled "50%plus". None of the cohorts entailed significant heart irradiation. Either the dose was below the threshold for induction of cardiac damage relevant for respiratory effects (78) or the included heart volume was $\leq$ 25%. The respiratory function (BR assay) was followed biweekly for 38 weeks and lung histology was performed at 8, 26 and 38 weeks. The fraction of animals with dysfunction (i.e. responders) in the three previously described phases of radiation induced lung injury (**Chapter 3**) was determined in each dose group.

A notable observation was that the character of morphologic lesions in the *early* phase (8 weeks) differed qualitatively depending on the dose. Up to 16 Gy single dose, the main histological finding in the irradiated parts of the lung was *vascular damage* in terms of pronounced wall edema and perivascular mononuclear infiltrates concerning small and large vessels. Capillaries could not be evaluated with optical microscopy. When this vascular damage involved more than 50% lung volume (i.e. following total lung irradiation but not the 50%min or 50%plus irradiation), it became manifest as an *early* respiratory dysfunction between four and 14 weeks. Then it would recede with little residual vascular changes (hypertrophy of tunica media) and minimal effect on global lung function during the rest of the 38-week follow-up. After higher doses however ($\geq$ 18 Gy single dose), the histological picture in the irradiated lung tissue at 8 weeks was dominated by an *acute parenchymal inflammation* with focal areas of interstitial and even intra-alveolar edema and dense inflammatory infiltration. This parenchymal process proceeded into *interstitial fibrosis* at 26 and 38 week time points and, depending on irradiated volume,

influenced the respiratory function in all phases of follow-up. In the *early* period (6-12 weeks), parenchymal inflammation in the 50%plus volume produced functional detriment in majority of animals irradiated to 20-22 Gy while the 50%min and 25% lung volume irradiations were well tolerated (i.e. less than 50% of animals were responders even in the highest dose groups). Parenchymal inflammation blending in with fibrosis in the *intermediate* period (16-28 weeks) caused severe dysfunction in nearly all animals that obtained dose of $\geq$ 18 Gy to 50% lung volume (in both 50%plus or 50%min cohorts). Irradiation of 25% lung volume, however, remained mostly without consequences despite complete destruction of the irradiated regions. Compact fibrosis in the *late* period (34-38 weeks) had adverse effects on function only in the case of 50%plus irradiation. Obliteration of slightly less than 50% of alveolar volume (i.e. the 50%min irradiation), even more so of the 25% volume, was very successfully compensated.

Based on this we hypothesized that the syndrome of *early radiation pneumonitis* occurring in the first weeks and months following lung irradiation likely encompassed two distinct pathogenetic processes, the *vascular damage* and the *parenchymal inflammation*, that were elicited by different dose levels and had inverse outcomes in terms of late morphologic and functional sequelae. The former resolved in recovery, the latter led to the *late interstitial fibrosis* and, in a volume dependent manner, to persistent functional impairment. Although often ignored, this idea is supported by numerous literature accounts as mentioned in **Chapter 6**. Furthermore, it could reconcile the many controversial observations with regard to the consequentiality between the early and late phases of radiation induced lung injury (**Chapter 1**, section 1.5). In our studies (**Chapters 3** and **6**), we observed strong *consequentiality* between the acute parenchymal inflammation manifest as a respiratory dysfunction between 6-12 weeks after the exposure (in the *early* post-irradiation period) and the chronic parenchymal inflammation and interstitial fibrosis manifest as respiratory dysfunction between the 16-28 weeks and 34-38 weeks after the exposure (i.e. in the *intermediate* and *late* post-irradiation periods, respectively). When analyzing the BR response in the individual animals from all the six 50% lung volume cohorts, the *early* respiratory symptoms were succeeded by symptoms in the *intermediate* and *late* periods in more than 90% of cases. Among the animals from the 25% lung volume cohorts, where, generally, the relationship between the structural damage and global dysfunction was weaker due to the small size of affected volume,

the *early* BR elevation led to the *intermediate* and *late* BR elevations in 71% of cases. In contrast, only 38% of the symptoms from the *early* period lasted until the *intermediate* period in the animals from the total lung irradiation cohort, where, as we have showed, the early morphological lesions did not have a character of parenchymal inflammation and, subsequently, fibrosis did not develop. Such findings corroborated the hypothesis of two different pathogenetic processes existing in the *early* post-irradiation period of which only one, the acute parenchymal inflammation induced by higher doses, had the potential and tendency to progress into late fibrosis with late respiratory insufficiency.

The biologically equivalent fractionated dose given in standard 2 Gy per fraction could be calculated for the single doses used in our studies with the help of linear-quadratic model and α/β ratio for the endpoint of pneumonitis = 3.3 Gy (35). We are aware that comparing radiation effect between rats and humans at an exact dose level may be misleading. The tolerance is not identical among species as can be judged, for example, from the dose inducing lethal effects in 50% of subjects following single dose whole lung irradiation that is much lower in humans (LD_{50} = 9.3 Gy) (36,63) than in rats (LD_{50} between 14 – 16 Gy) (61,79,81). Thus, if we observed vascular damage in rat lung following single doses of 9-16 Gy with the fractionated equivalent being 21-58 Gy, such lesion should be expected at lower doses in radiotherapy patients. Recent clinical reports found some of the strongest correlations between severe ($\geq$ grade 3) early radiation pneumonitis and lung volumes V_{5-13} irradiated to low total doses of only 5-13 Gy (68,88). It would be plausible to speculate that vascular damage with its hemodynamic consequences could have contributed to such marked early respiratory deficits linked to very low lung doses. Similarly, the parenchymal inflammation and subsequent fibrosis became prominent in rat lung following single doses of 18 Gy and more (the fractionated equivalent would be $\geq$ 72 Gy), but they have been reported to occur in a form of persisting radiographic abnormalities in a substantial proportion of patients at total doses starting already from 30 - 40 Gy (46,48,51,55,69).

Despite this strong consequentiality between the early and late parenchymal injury (resulting from doses $\geq$ 18 Gy), where most of the symptoms occurring in the *intermediate* and *late* periods were initially seen during the *early* period, still large number of the responders in the *intermediate* period (42% among the 50% lung volume cohorts and 33% among the 25% lung volume cohorts) developed the

dysfunction *de novo* without an antecedent *early* BR increase. This would suggest a lower dose threshold for the clinical manifestation of interstitial fibrosis than that of interstitial pneumonitis, possibly due to larger pulmonary reserve available in the course of focally expressed inflammation than during the more confluent fibrotic remodeling. However, in terms of morphology, both conditions were likely present in those cases even though they might not have resulted in detectable symptoms. Amidst the long-term controversy regarding the sequence between the post-irradiation syndromes of pneumonitis and fibrosis, others have reached such reconciliatory conclusion before us (58).

In summary, we offer a modified paradigm (compared to the one presented in **Chapter 1**, section 1.5) of pathogenesis of radiation-induced lung injury and its two main clinical manifestations, the *early radiation pneumonitis* and *late radiation fibrosis* (Fig. 1). We propose that the character of the initial tissue injury is determined by the magnitude of the delivered dose, as is the progression of this initial injury into the late, chronic damage. In the acute period following low single doses ≤ 16 Gy, we observed congestive vascular changes that appeared in the absence of parenchymal inflammation and did not progress into chronic fibrosis. Their clinical manifestation in terms of an early onset respiratory dysfunction depended on the affected lung volume. With time, both the morphological changes and symptoms associated with this type of injury showed clear tendency towards resolution. In contrast, higher single doses of 18 Gy and more produced not only vascular changes, but also an acute exudative parenchymal inflammation that dominated the morphological picture in the early post-irradiation period and gradually blended in with progressive interstitial fibrosis over the time span of 38 weeks. This type of damage manifested itself as respiratory dysfunction in all three post-irradiation periods (*early*, *intermediate* and *late*) depending mostly on the volume of affected

Figure 1 (next page): Modified pathogenesis summary of the pulmonary syndromes of radiation pneumonitis and radiation fibrosis based on literature data and our findings. See text for details. Abbreviations: AM alveolar macrophages, VD vascular damage, ECM extracellular matrix, RP radiation pneumonitis, RF radiation fibrosis.

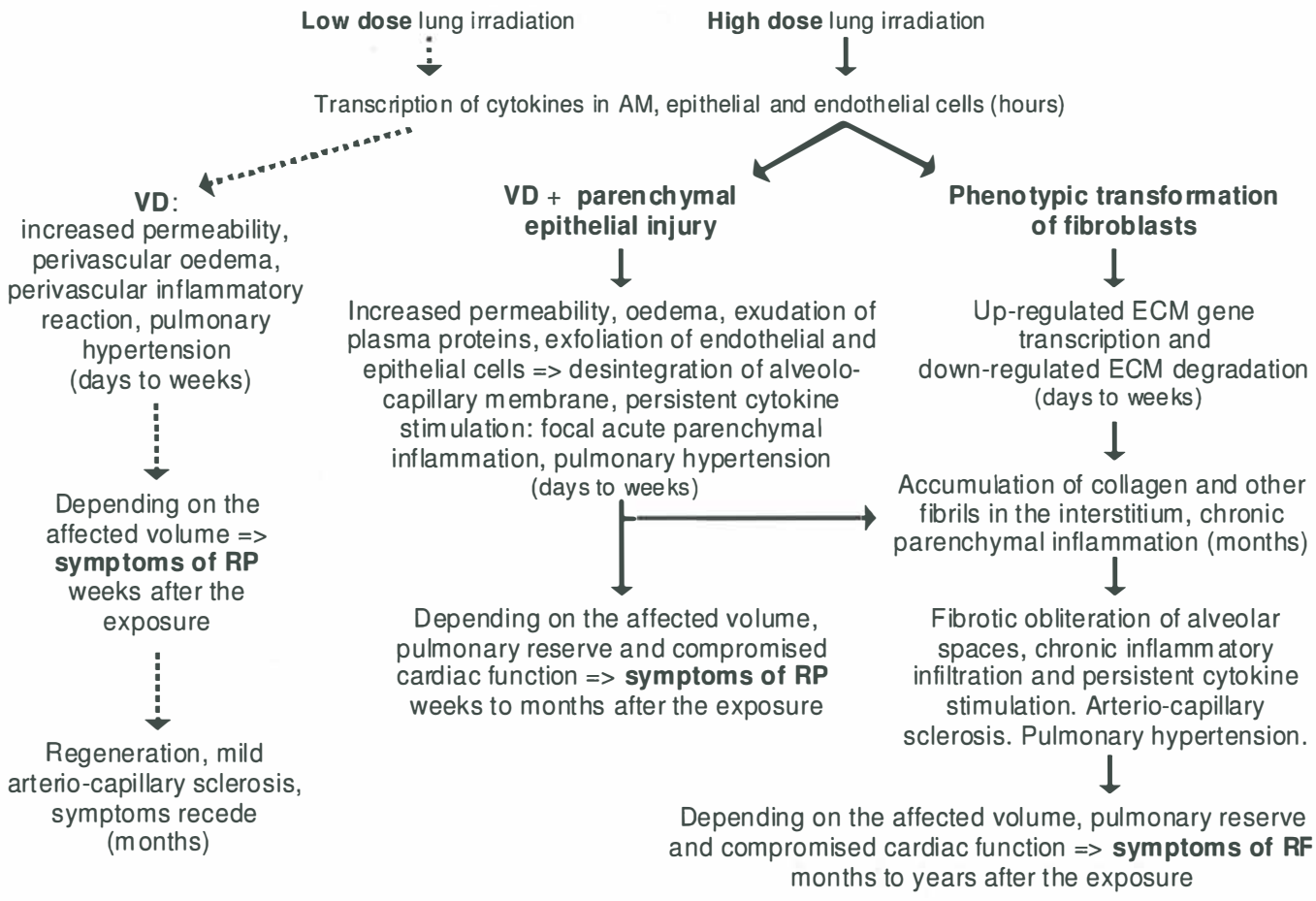
Low dose lung irradiation
High dose lung irradiation
Transcription of cytokines in AM, epithelial and endothelial cells (hours)
VD:
increased permeability, perivascular oedema, perivascular inflammatory reaction, pulmonary hypertension
(days to weeks)
Depending on the affected volume => **symptoms of RP** weeks after the exposure
Regeneration, mild arterio-capillary sclerosis, symptoms recede
(months)
VD + parenchymal epithelial injury
Increased permeability, oedema, exudation of plasma proteins, exfoliation of endothelial and epithelial cells => desintegration of alveolo-capillary membrane, persistent cytokine stimulation: focal acute parenchymal inflammation, pulmonary hypertension
(days to weeks)
Depending on the affected volume, pulmonary reserve and compromised cardiac function => **symptoms of RP** weeks to months after the exposure
Phenotypic transformation of fibroblasts
Up-regulated ECM gene transcription and down-regulated ECM degradation
(days to weeks)
Accumulation of collagen and other fibrils in the interstitium, chronic parenchymal inflammation (months)
Fibrotic obliteration of alveolar spaces, chronic inflammatory infiltration and persistent cytokine stimulation. Arterio-capillary sclerosis. Pulmonary hypertension.
Depending on the affected volume, pulmonary reserve and compromised cardiac function => **symptoms of RF** months to years after the exposure

alveolar tissue (excluding the large vessels and airways) and available pulmonary reserve capacity. This capacity seemed to be largest during the *early* and *late* post-irradiation periods, when either the inflammatory process had only focal character, leaving portion of the irradiated tissue optically intact and, possibly still functional (the *early* phase), or when the well constituted, less cellular chronic fibrosis shrunk into mere rudiments and cleared the space for compensatory hyperinflation of healthy parts of the lungs (the *late* phase). Additionally, during the *early* and *late* post-irradiation periods, extrapulmonary factor of an incidental heart irradiation became a co-determining force in manifestation of respiratory dysfunction. Our findings supported by mounting evidence in the literature suggest that fibrosis, although elicited by a similar dose range, is not a direct consequence of pneumonitis but rather that these two are parallel processes launched simultaneously by immediate molecular events following absorption of radiation energy in a different cell types. However, albeit parallel, those processes are not independent of each other. Inflammation with its sustained cytokine production is believed to stimulate and accelerate the development of fibrosis what agrees well with our observation of the early symptomatic parenchymal inflammation almost invariably ending up in late symptomatic fibrosis.

From the perspective of these results, low radiation doses spread over large lung volumes (the dose distribution typically associated with IMRT) may be safe in terms of chronic sequelae, but their risk lies in unexpected acute toxicity linked to the haemodynamic consequences of pulmonary irradiation. This conclusion seems to be validated by limited clinical data on IMRT outcomes in NSCLC patients (32). Conversely, concentration of high radiation doses in minimal healthy lung volumes just adjacent to the targeted tumour (the distribution achievable by high precision proton radiotherapy) appears well tolerated in terms of pulmonary complications, both early and late.

7.9 Summary and perspectives

Our work provides novel insights into the pathogenesis of radiation induced lung injury. Up to present, the clinically tested models for prediction of risk of pulmonary complications resulting from radiation therapy presumed that all lung regions had identical functional importance, that radiation pneumonitis was one pathogenetic unit with uniform dose-volume-response parameters and that no

extrapulmonary interaction could have an influence on the global functional outcome. The predictive power of these dose-volume histogram based models has never been satisfactory and a consensus exists that incorporating additional biological information is crucial for improved reliability of risk prediction. Topics featured in the current thesis, i.e. the analysis of principles underlying the hypersensitivity of certain lung regions, the description of two distinct types of early damage with different dose-volume thresholds for clinical expression and different outcomes in terms of late damage, and the identification of heart co-irradiation as an enhancing factor for symptomatic radiation induced lung injury may potentially revolutionize the way predictive modeling is done. Incorporation of these findings into multi-parameter predictive models and testing of their applicability against clinical datasets are highly warranted especially with the advance of more precise and more powerful radiation techniques like IMRT and proton therapy that bring about more extreme dose distributions in the treated tissue.

References

1. Adams, M.J., Hardenbergh, P.H., Constine, L.S., and Lipshultz, S.E. Radiation-associated cardiovascular disease. Crit Rev Oncol Hematol 2003; 45: 55-75.
2. Anscher, M.S., Kong, F.M., Andrews, K., Clough, R., Marks, L.B., Bentel, G., and Jirtle, R.L. Plasma transforming growth factor beta1 as a predictor of radiation pneumonitis. Int J Radiat Oncol Biol Phys 1998; 41: 1029-1035.
3. Anscher, M.S., Kong, F.M., Marks, L.B., Bentel, G.C., and Jirtle, R.L. Changes in plasma transforming growth factor beta during radiotherapy and the risk of symptomatic radiation-induced pneumonitis. Int J Radiat Oncol Biol Phys 1997; 37: 253-258.
4. Anscher, M.S., Marks, L.B., Shafman, T.D., Clough, R., Huang, H., Tisch, A., Munley, M., Herndon, J.E., Garst, J., Crawford, J., and Jirtle, R.L. Using plasma transforming growth factor beta-1 during radiotherapy to select patients for dose escalation. J Clin Oncol 2001; 19: 3758-3765.
5. Anscher, M.S., Marks, L.B., Shafman, T.D., Clough, R., Huang, H., Tisch, A., Munley, M., Herndon, J.E., Garst, J., Crawford, J., and Jirtle, R.L. Risk of long-term complications after TFG-beta1-guided very-high-dose thoracic radiotherapy. Int J Radiat Oncol Biol Phys 2003; 56: 988-995.
6. Bivin, W.S., Crawford, M.P., and Brewer, N.R. Morphophysiology. In: Baker, H.J., Lindsey, J.R., Weisbroth, S.H., editors. The laboratory rat; New York 1979.
7. Boerma, M., Zurcher, C., Esveldt, I., Schutte-Bart, C.I., and Wondergem, J. Histopathology of ventricles, coronary arteries and mast cell accumulation in transverse and longitudinal sections of the rat heart after irradiation. Oncol Rep 2004; 12: 213-219.
8. Boivin, J.F., Hutchison, G.B., Lubin, J.H., and Mauch, P. Coronary artery disease mortality in patients treated for Hodgkin's disease. Cancer 1992; 69: 1241-1247.
9. Chang, J.Y., Liu, H.H., and Komaki, R. Intensity modulated radiation therapy and proton radiotherapy for non-small cell lung cancer. Curr Oncol Rep 2005; 7: 255-259.
10. Chang, J.Y., Zhang, X., Wang, X., Kang, Y., Riley, B., Bilton, S., Mohan, R., Komaki, R., and Cox, J.D. Significant reduction of normal tissue dose by proton radiotherapy compared with three-dimensional conformal or intensity-modulated radiation therapy in Stage I or Stage III non-small-cell lung cancer. Int J Radiat Oncol Biol Phys 2006; 65: 1087-1096.
11. Chen, Y., Williams, J., Ding, I., Hernady, E., Liu, W., Smudzin, T., Finkelstein, J.N., Rubin, P., and Okunieff, P. Radiation pneumonitis and early circulatory cytokine markers. Semin Radiat Oncol 2002; 12: 26-33.
12. Cilliers, G.D., Harper, I.S., and Lochner, A. Radiation-induced changes in the ultrastructure and mechanical function of the rat heart. Radiother Oncol 1989; 16: 311-326.
13. Cook, M.J. The anatomy of the laboratory mouse. London 1965.
14. De Jaeger, K., Seppenwoolde, Y., Kampinga, H.H., Boersma, L.J., Belderbos, J.S., and Lebesque, J.V. Significance of plasma transforming growth factor-

beta levels in radiotherapy for non-small-cell lung cancer. Int J Radiat Oncol Biol Phys 2004; 58: 1378-1387.
15. Deasy, J.O., Trovo, M., Huang, E.X., Mu, Y., El, N., I, and Bradley, J.D. High-dose heart irradiation is a statistically significant risk factor for radiation pneumonitis within logistic-multivariate modeling. Int J Radiat Oncol Biol Phys 2008; 72 (Suppl.1): S119-S119.
16. el Khatib, E. and Lehnert, S. Lung density changes observed in vivo in rat lungs after irradiation: variations among and within individual lungs. Int J Radiat Oncol Biol Phys 1989; 16: 745-754.
17. Evans, E.S., Kocak, Z., Huang, H., Zhou, S., Light, K., Folz, R., Anscher, M.S., and Marks, L.B. The role of TGF-beta in predicting radiation-induced pneumonitis. Int J Radiat Oncol Biol Phys 2004; 60 (Suppl.): S328-S329.
18. Evans, E.S., Kocak, Z., Zhou, S.M., Kahn, D.A., Huang, H., Hollis, D.R., Light, K.L., Anscher, M.S., and Marks, L.B. Does transforming growth factor-beta1 predict for radiation-induced pneumonitis in patients treated for lung cancer? Cytokine 2006; 35: 186-192.
19. Fajardo, L.F. and Stewart, J.R. Experimental radiation-induced heart disease. I. Light microscopic studies. Am J Pathol 1970; 59: 299-316.
20. Fajardo, L.F. and Stewart, J.R. Capillary injury preceding radiation-induced myocardial fibrosis. Radiology 1971; 101: 429-433.
21. Fajardo, L.F. and Stewart, J.R. Pathogenesis of radiation-induced myocardial fibrosis. Lab Invest 1973; 29: 244-257.
22. Fajardo, L.F., Stewart, J.R., and Cohn, K.E. Morphology of radiation-induced heart disease. Arch Pathol 1968; 86: 512-519.
23. Franken, N.A., Camps, J.A., van Ravels, F.J., van der, L.A., Pauwels, E.K., and Wondergem, J. Comparison of in vivo cardiac function with ex vivo cardiac performance of the rat heart after thoracic irradiation. Br J Radiol 1997; 70: 1004-1009.
24. Franken, N.A., van der, L.A., Bosker, F.J., Reynart, I.W., van Ravels, F.J., Strootman, E., and Wondergem, J. Time dependent changes in myocardial norepinephrine concentration and adrenergic receptor density following X-irradiation of the rat heart. Int J Radiat Oncol Biol Phys 1992; 24: 721-727.
25. Fu, X.L., Huang, H., Bentel, G., Clough, R., Jirtle, R.L., Kong, F.M., Marks, L.B., and Anscher, M.S. Predicting the risk of symptomatic radiation-induced lung injury using both the physical and biologic parameters V(30) and transforming growth factor beta. Int J Radiat Oncol Biol Phys 2001; 50: 899-908.
26. Gagliardi, G., Lax, I., and Rutqvist, L.E. Partial irradiation of the heart. Semin Radiat Oncol 2001; 11: 224-233.
27. Geist, B.J., Lauk, S., Bornhausen, M., and Trott, K.R. Physiologic consequences of local heart irradiation in rats. Int J Radiat Oncol Biol Phys 1990; 18: 1107-1113.
28. Gillette, S.M., Powers, B.E., Orton, E.C., and Gillette, E.L. Early radiation response of the canine heart and lung. Radiat Res 1991; 125: 34-40.
29. Graham, M.V., Purdy, J.A., Emami, B., Harms, W., Bosch, W., Lockett, M.A., and Perez, C.A. Clinical dose-volume histogram analysis for pneumonitis after 3D treatment for non-small cell lung cancer (NSCLC). Int J Radiat Oncol Biol Phys 1999; 45: 323-329.

30. Hancock, S.L., Donaldson, S.S., and Hoppe, R.T. Cardiac disease following treatment of Hodgkin's disease in children and adolescents. J Clin Oncol 1993; 11: 1208-1215.
31. Hardenbergh, P.H., Munley, M.T., Bentel, G.C., Kedem, R., Borges-Neto, S., Hollis, D., Prosnitz, L.R., and Marks, L.B. Cardiac perfusion changes in patients treated for breast cancer with radiation therapy and doxorubicin: preliminary results. Int J Radiat Oncol Biol Phys 2001; 49: 1023-1028.
32. Holloway, C.L., Robinson, D., Murray, B., Amanie, J., Butts, C., Smylie, M., Chu, K., McEwan, A.J., Halperin, R., and Roa, W.H. Results of a phase I study to dose escalate using intensity modulated radiotherapy guided by combined PET/CT imaging with induction chemotherapy for patients with non-small cell lung cancer. Radiother Oncol 2004; 73: 285-287.
33. Hope, A.J., Lindsay, P.E., El, N., I, Alaly, J.R., Vicic, M., Bradley, J.D., and Deasy, J.O. Modeling radiation pneumonitis risk with clinical, dosimetric, and spatial parameters. Int J Radiat Oncol Biol Phys 2006; 65: 112-124.
34. Ikaheimo, M.J., Niemela, K.O., Linnaluoto, M.M., Jakobsson, M.J., Takkunen, J.T., and Taskinen, P.J. Early cardiac changes related to radiation therapy. Am J Cardiol 1985; 56: 943-946.
35. Joiner, M.C. and van der Kogel, A.J. The linear-quadratic approach to fractionation and calculation of isoeffect relationships. In: Steel, G.G., editor. Basic clinical radiobiology; London 1997: 106-122.
36. Keane, T.J., Van Dyk, J., and Rider, W.D. Idiopathic interstitial pneumonia following bone marrow transplantation: the relationship with total body irradiation. Int J Radiat Oncol Biol Phys 1981; 7: 1365-1370.
37. Kocak, Z., Borst, G.R., Zeng, J., Zhou, S., Hollis, D.R., Zhang, J., Evans, E.S., Folz, R.J., Wong, T., Kahn, D., Belderbos, J.S., Lebesque, J.V., and Marks, L.B. Prospective assessment of dosimetric/physiologic-based models for predicting radiation pneumonitis. Int J Radiat Oncol Biol Phys 2007; 67: 178-186.
38. Lagrange, J.L., Darcourt, J., Benoliel, J., Bensadoun, R.J., and Migneco, O. Acute cardiac effects of mediastinal irradiation: assessment by radionuclide angiography. Int J Radiat Oncol Biol Phys 1992; 22: 897-903.
39. Lauk, S. Strain differences in the radiation response of the rat heart. Radiother Oncol 1986; 5: 333-335.
40. Lauk, S. Endothelial alkaline phosphatase activity loss as an early stage in the development of radiation-induced heart disease in rats. Radiat Res 1987; 110: 118-128.
41. Lauk, S., Bohm, M., Feiler, G., Geist, B.J., and Erdmann, E. Increased number of cardiac adrenergic receptors following local heart irradiation. Radiat Res 1989; 119: 157-165.
42. Lauk, S., Kiszel, Z., Buschmann, J., and Trott, K.R. Radiation-induced heart disease in rats. Int J Radiat Oncol Biol Phys 1985; 11: 801-808.
43. Lee, C.B., Stinchcombe, T.E., Rosenman, J.G., and Socinski, M.A. Therapeutic advances in local-regional therapy for stage III non-small-cell lung cancer: evolving role of dose-escalated conformal (3-dimensional) radiation therapy. Clin Lung Cancer 2006; 8: 195-202.
44. Lehnert, S. and el Khatib, E. The use of CT densitometry in the assessment of radiation-induced damage to the rat lung: a comparison with other endpoints. Int J Radiat Oncol Biol Phys 1989; 16: 117-124.

45. Liao, Z.X., Travis, E.L., and Tucker, S.L. Damage and morbidity from pneumonitis after irradiation of partial volumes of mouse lung. Int J Radiat Oncol Biol Phys 1995; 32: 1359-1370.
46. Libshitz, H.I. and Shuman, L.S. Radiation-induced pulmonary change: CT findings. J Comput Assist Tomogr 1984; 8: 15-19.
47. Lind, P.A., Marks, L.B., Hollis, D., Fan, M., Zhou, S.M., Munley, M.T., Shafman, T.D., Jaszczak, R.J., and Coleman, R.E. Receiver operating characteristic curves to assess predictors of radiation-induced symptomatic lung injury. Int J Radiat Oncol Biol Phys 2002; 54: 340-347.
48. Mah, K., Van Dyk, J., Keane, T., and Poon, P.Y. Acute radiation-induced pulmonary damage: a clinical study on the response to fractionated radiation therapy. Int J Radiat Oncol Biol Phys 1987; 13: 179-188.
49. Marks, L.B. The impact of organ structure on radiation response. Int J Radiat Oncol Biol Phys 1996; 34: 1165-1171.
50. Marks, L.B. Dosimetric predictors of radiation-induced lung injury. Int J Radiat Oncol Biol Phys 2002; 54: 313-316.
51. Marks, L.B., Fan, M., Clough, R., Munley, M., Bentel, G., Coleman, R.E., Jaszczak, R., Hollis, D., and Anscher, M. Radiation-induced pulmonary injury: symptomatic versus subclinical endpoints. Int J Radiat Biol 2000; 76: 469-475.
52. Marks, L.B., Kocak, Z., Zhou, S., Yu, X., Light, K., Anscher, M.S., Kahn, D., Wong, T., Folz, R.J., and Hollis, D. The association between the mean heart dose, mean lung dose, tumor location and RT-associated heart and lung toxicity. Int J Radiat Oncol Biol Phys 2005; 63 (Suppl.): S42-S42.
53. Marks, L.B., Munley, M.T., Bentel, G.C., Zhou, S.M., Hollis, D., Scarfone, C., Sibley, G.S., Kong, F.M., Jirtle, R., Jaszczak, R., Coleman, R.E., Tapson, V., and Anscher, M. Physical and biological predictors of changes in whole-lung function following thoracic irradiation. Int J Radiat Oncol Biol Phys 1997; 39: 563-570.
54. Marks, L.B., Yu, X., Prosnitz, R.G., Zhou, S.M., Hardenbergh, P.H., Blazing, M., Hollis, D., Lind, P., Tisch, A., Wong, T.Z., and Borges-Neto, S. The incidence and functional consequences of RT-associated cardiac perfusion defects. Int J Radiat Oncol Biol Phys 2005; 63: 214-223.
55. Marks, L.B., Yu, X., Vujaskovic, Z., Small, W., Jr., Folz, R., and Anscher, M.S. Radiation-induced lung injury. Semin Radiat Oncol 2003; 13: 333-345.
56. McChesney, S.L., Gillette, E.L., and Orton, E.C. Canine cardiomyopathy after whole heart and partial lung irradiation. Int J Radiat Oncol Biol Phys 1988; 14: 1169-1174.
57. McChesney, S.L., Gillette, E.L., and Powers, B.E. Radiation-induced cardiomyopathy in the dog. Radiat Res 1988; 113: 120-132.
58. McDonald, S., Rubin, P., Phillips, T.L., and Marks, L.B. Injury to the lung from cancer therapy: clinical syndromes, measurable endpoints, and potential scoring systems. Int J Radiat Oncol Biol Phys 1995; 31: 1187-1203.
59. Mehta, V. Radiation pneumonitis and pulmonary fibrosis in non-small-cell lung cancer: pulmonary function, prediction, and prevention. Int J Radiat Oncol Biol Phys 2005; 63: 5-24.
60. Murshed, H., Liu, H.H., Liao, Z., Barker, J.L., Wang, X., Tucker, S.L., Chandra, A., Guerrero, T., Stevens, C., Chang, J.Y., Jeter, M., Cox, J.D., Komaki, R., and Mohan, R. Dose and volume reduction for normal lung using

intensity-modulated radiotherapy for advanced-stage non-small-cell lung cancer. Int J Radiat Oncol Biol Phys 2004; 58: 1258-1267.
61. Newcomb, C.H., Van Dyk, J., and Hill, R.P. Evaluation of isoeffect formulae for predicting radiation-induced lung damage. Radiother Oncol 1993; 26: 51-63.
62. Prosnitz, R.G., Chen, Y.H., and Marks, L.B. Cardiac toxicity following thoracic radiation. Semin Oncol 2005; 32: S71-S80.
63. Rubin, P., Constine, L.S., and Nelson, D.F. Late effects of cancer treatment: radiation and drug toxicity. In: Perez, C.A., Brady, L.W., editors. Principles and practice of radiation oncology; Philadelphia 1992: 124-161.
64. Rutqvist, L.E., Lax, I., Fornander, T., and Johansson, H. Cardiovascular mortality in a randomized trial of adjuvant radiation therapy versus surgery alone in primary breast cancer. Int J Radiat Oncol Biol Phys 1992; 22: 887-896.
65. Schultz-Hector, S. Radiation-induced heart disease: review of experimental data on dose response and pathogenesis. Int J Radiat Biol 1992; 61: 149-160.
66. Schultz-Hector, S., Bohm, M., Blochel, A., Dominiak, P., Erdmann, E., Muller-Schauenburg, W., and Weber, A. Radiation-induced heart disease: morphology, changes in catecholamine synthesis and content, beta-adrenoceptor density, and hemodynamic function in an experimental model. Radiat Res 1992; 129: 281-289.
67. Seppenwoolde, Y., De Jaeger, K., Boersma, L.J., Belderbos, J.S., and Lebesque, J.V. Regional differences in lung radiosensitivity after radiotherapy for non-small-cell lung cancer. Int J Radiat Oncol Biol Phys 2004; 60: 748-758.
68. Seppenwoolde, Y., Lebesque, J.V., De Jaeger, K., Belderbos, J.S., Boersma, L.J., Schilstra, C., Henning, G.T., Hayman, J.A., Martel, M.K., and Ten Haken, R.K. Comparing different NTCP models that predict the incidence of radiation pneumonitis. Normal tissue complication probability. Int J Radiat Oncol Biol Phys 2003; 55: 724-735.
69. Skoczylas, J.Z., Bentzen, S.M., Overgaard, M., and Overgaard, J. Time course of radiological lung density changes after postmastectomy radiotherapy. Acta Oncol 2000; 39: 181-187.
70. Stewart, J.R. and Fajardo, L.F. Radiation-induced heart disease: an update. Prog Cardiovasc Dis 1984; 27: 173-194.
71. Stewart, J.R., Fajardo, L.F., Gillette, S.M., and Constine, L.S. Radiation injury to the heart. Int J Radiat Oncol Biol Phys 1995; 31: 1205-1211.
72. Stinchcombe, T.E., Fried, D., Morris, D.E., and Socinski, M.A. Combined modality therapy for stage III non-small cell lung cancer. Oncologist 2006; 11: 809-823.
73. Theuws, J.C., Kwa, S.L., Wagenaar, A.C., Boersma, L.J., Damen, E.M., Muller, S.H., Baas, P., and Lebesque, J.V. Dose-effect relations for early local pulmonary injury after irradiation for malignant lymphoma and breast cancer. Radiother Oncol 1998; 48: 33-43.
74. Theuws, J.C., Kwa, S.L., Wagenaar, A.C., Seppenwoolde, Y., Boersma, L.J., Damen, E.M., Muller, S.H., Baas, P., and Lebesque, J.V. Prediction of overall pulmonary function loss in relation to the 3-D dose distribution for patients with breast cancer and malignant lymphoma. Radiother Oncol 1998; 49: 233-243.

75. Theuws, J.C., Seppenwoolde, Y., Kwa, S.L., Boersma, L.J., Damen, E.M., Baas, P., Muller, S.H., and Lebesque, J.V. Changes in local pulmonary injury up to 48 months after irradiation for lymphoma and breast cancer. Int J Radiat Oncol Biol Phys 2000; 47: 1201-1208.
76. Travis, E.L., Liao, Z.X., and Tucker, S.L. Spatial heterogeneity of the volume effect for radiation pneumonitis in mouse lung. Int J Radiat Oncol Biol Phys 1997; 38: 1045-1054.
77. Tucker, S.L., Liao, Z.X., and Travis, E.L. Estimation of the spatial distribution of target cells for radiation pneumonitis in mouse lung. Int J Radiat Oncol Biol Phys 1997; 38: 1055-1066.
78. van Luijk, P., Faber, H., Meertens, H., Schippers, J.M., Langendijk, J.A., Brandenburg, S., Kampinga, H.H., and Coppes, R.P. The impact of heart irradiation on dose-volume effects in the rat lung. Int J Radiat Oncol Biol Phys 2007; 69: 552-559.
79. Varekamp, A.E. Interstitial pneumonitis following bone marrow transplantation: studies in the Brown Norway rat. Chapters 3.3-3.5. Thesis, Leiden, The Netherlands 1990.
80. Vujaskovic, Z. and Groen, H.J. TGF-beta, radiation-induced pulmonary injury and lung cancer. Int J Radiat Biol 2000; 76: 511-516.
81. Ward, H.E., Kemsley, L., Davies, L., Holecek, M., and Berend, N. The pulmonary response to sublethal thoracic irradiation in the rat. Radiat Res 1993; 136: 15-21.
82. Wennberg, B., Gagliardi, G., Sundbom, L., Svane, G., and Lind, P. Early response of lung in breast cancer irradiation: radiologic density changes measured by CT and symptomatic radiation pneumonitis. Int J Radiat Oncol Biol Phys 2002; 52: 1196-1206.
83. Wiegman, E.M., Meertens, H., Konings, A.W., Kampinga, H.H., and Coppes, R.P. Loco-regional differences in pulmonary function and density after partial rat lung irradiation. Radiother Oncol 2003; 69: 11-19.
84. Wondergem, J., van der, L.A., van Ravels, F.J., van Wermeskerken, A.M., Verhoeve, H.R., de Graaf, B.W., and Leer, J.W. In vitro assessment of cardiac performance after irradiation using an isolated working rat heart preparation. Int J Radiat Biol 1991; 59: 1053-1068.
85. Yamada, M., Kudoh, S., Hirata, K., Nakajima, T., and Yoshikawa, J. Risk factors of pneumonitis following chemoradiotherapy for lung cancer. Eur J Cancer 1998; 34: 71-75.
86. Yeung, T.K. and Hopewell, J.W. Effects of single doses of radiation on cardiac function in the rat. Radiother Oncol 1985; 3: 339-345.
87. Yeung, T.K., Lauk, S., Simmonds, R.H., Hopewell, J.W., and Trott, K.R. Morphological and functional changes in the rat heart after X irradiation: strain differences. Radiat Res 1989; 119: 489-499.
88. Yorke, E.D., Jackson, A., Rosenzweig, K.E., Braban, L., Leibel, S.A., and Ling, C.C. Correlation of dosimetric factors and radiation pneumonitis for non-small-cell lung cancer patients in a recently completed dose escalation study. Int J Radiat Oncol Biol Phys 2005; 63: 672-682.
89. Yorke, E.D., Jackson, A., Rosenzweig, K.E., Merrick, S.A., Gabrys, D., Venkatraman, E.S., Burman, C.M., Leibel, S.A., and Ling, C.C. Dose-volume factors contributing to the incidence of radiation pneumonitis in non-small-cell lung cancer patients treated with three-dimensional conformal radiation therapy. Int J Radiat Oncol Biol Phys 2002; 54: 329-339.

Summary

Radiation is routinely used in treatment of thoracic tumours. In most cases, radiation is emitted from a source outside a body and has to penetrate through skin and other tissues to reach a tumour inside. Absorption of the energy carried by radiation damages living cells, leading to cell death or preventing further cell divisions. Although modern irradiation techniques are designed to achieve deposition of a maximum of radiation energy in the tumour volume, a certain amount of energy gets absorbed in normal tissues around. This may cause harm and may result in dangerous side effects. Very complicated is treatment of lung cancer. It is the third most common cancer in Europe and the most common cause of cancer death accounting for one fifth of total cancer mortality. Majority of lung cancers is histologically rated as *non-small cell lung cancer* (NSCLC). For patients whose tumour has grown locally to an extent precluding surgical resection, radiation therapy in conjunction with chemotherapy represents the only hope for a cure. However, the majority of them die within two years of diagnosis. This is because the radiation dose required for NSCLC tumour destruction is very high and delivery of such dose without damaging surrounding vital organs (lungs, eosophagus, spinal cord and heart) is technically difficult, often impossible.

This is especially true with regard to the pulmonary side effects. With increasing absorbed dose and volume in healthy lung, the risk of pulmonary complications goes up. At some point, this risk becomes unacceptable and limits the dose that may be given to the tumour, rendering the disease incurable. The pulmonary complications can be divided into two syndromes - an acute *radiation pneumonitis* (inflammation) occurring within 1-4 months and a chronic *pulmonary fibrosis* (scarring) progressing for years after irradiation. Both destroy the delicate structure of healthy lung tissue and hamper the gas exchange and blood circulation within. That may become apparent as shortness of breath requiring therapy, hospitalization, and may even result in death. These symptoms follow radiation treatment in as many as one fifth of patients treated with commonly used (*conventional*) radiation doses (i.e. 60 Gy delivered in daily fractions over 6 weeks) that are still insufficient for a cure.

Therefore recently, efforts have been aimed at finding ways how to safely increase (*escalate*) radiation dose to lung tumours with use of *three-dimensional conformal radiation therapy* (3D-CRT). This technique provides computerized modeling of shape and location of the tumour and surrounding organs in each individual patient. Further, it shows how much radiation energy (i.e. dose) would be absorbed in the tumour and the adjacent healthy lung if any particular radiation treatment should be used. This allows objective comparison of several treatment plans and the choice of the plan with the maximum tumour but minimum normal lung dose. Moreover, information on volume of healthy lung that receives a certain radiation dose during the treatment can be obtained. These data have been related to the frequency of pulmonary complications later observed in the same patients. Many clinical studies followed lung cancer patients after the radiotherapy to find out which doses delivered to which lung volumes were safe and which were too risky. Could we accurately predict who benefits from the increased tumour dose and who, on the contrary, suffers unacceptable toxicity? The conclusion is unfortunately "NO". Sole information on irradiated lung volume and lung dose does not allow reliable prediction of treatment safety. This continues to hinder improvement of cure rates and survival in NSCLC patients.

Therefore, the search is underway for additional factors that would help determine the risk associated with escalating radiation dose in lung cancer patients. This thesis was a part of that effort. In **Chapter 2**, we examined the possibility that certain proteins produced in human body could enhance the development of radiation-induced lung injury. These proteins called *cytokines* serve as communication messengers between cells. One of them, *transforming growth factor β* (TGF-β), is known to control inflammation, tissue healing and to promote scarring (fibrosis). It plays a major role in reaction of lung tissue to radiation insult. It also is secreted by tumour cells, often in excessive amounts, and some studies have linked high blood TGF-β levels in lung cancer patients to greater risk of severe radiation injury to their lungs. We tried to verify this effect in lung cancer patients treated at the University Medical Center Groningen. We found only a week association between the risk of subsequent pulmonary complications and the rising blood TGF-β levels in the middle of the 6-week radiotherapy course, but neither at its beginning nor at its end. We concluded this mid-treatment raise in the cytokine likely originated from the radiation-injured lung itself and reflected the degree to which this tissue was

damaged. Unfortunately, this parameter did not give accurate prediction in all patients and thus appeared inadequate for a routine hospital use.

Some reports indicated that irradiation of certain lung areas led to more severe pulmonary complications then irradiation of other areas. This would mean that irradiating the tumour from certain directions (through those *radiosensitive* lung regions) could be more dangerous than irradiating from other directions. We investigated how irradiation of various lung regions (same volume and dose, different location) influenced respiratory function in experimental animals (rats) (**Chapter 3**). We found that, indeed, irradiation of lung regions containing the most of pulmonary *parenchyma* (the spongy matter where gas exchange takes place - without large airways) and/or the regions overlapping with the heart (where the heart inevitably became irradiated, too) had the most serious impact on the animals ability to breathe. This was a little surprising because the heart was traditionally considered *radioresistant* organ showing some damage only very late (years) after the irradiation. It took an additional study with a very accurately targeted *proton* radiation beam to confirm that the heart co-irradiation was truly responsible for the increased risk of respiratory complications following combined lung and heart irradiation in the rat, not only in late stages, but already within the first 3 months after the treatment (**Chapter 4**). Excitingly, several clinical studies (i.e. dealing with real patients) have since indicated that, also in humans, the heart co-irradiation could indeed be one of the most important factors determining the likelihood of acute respiratory complications, warranting large scale testing of this parameter incorporated into multiparameter predictive models in the coming future.

The post-irradiation respiratory complications are represented by strained breathing but originate in damaged structure of thoracic organs. A tool is available that yields images of impaired lung structure without touching a patient's body – computer tomography (CT). CT uses traditional X-rays but produces much clearer 2-dimensional image of a slice in the patient's body. Almost all lung cancer patients show impaired lung structure on CT at some point after their radiotherapy treatment but only some actually feel sick due to that. In **Chapter 5**, we tried to answer the question, when do these structural defects truly signal an onset of respiratory difficulties felt by the patient, i.e. *clinical symptoms*. Again, we used rats as an experimental model, irradiating various regions in their lungs and then making lung CT and breathing rate assessments. We developed a method to objectively measure

(quantify) the severity of CT detected abnormalities. The most robust relation between the CT defects and impaired breathing existed following l*ateral* lung irradiation (on the sides of both lungs) covering maximum of lung parenchyma but no airways and no heart. In agreement with our previous findings, the damage to parenchyma had the strongest impact on respiratory function while other factors, like heart irradiation, did not play a role here. This suggests that also in humans, symptoms will likely arise from structural damage in parenchyma–rich and well ventilated lung regions that are most important for gas exchange. The usefulness of our method for CT image quantification should be assessed in clinical setting.

In **Chapter 6**, we revisited the issue of *dose-volume effects* in lung irradiation. By irradiating increasing volumes of rat lung with decreasing doses, we tried to determine the thresholds for inducing respiratory complications. We came to interesting conclusions that even very low doses were risky if spread over large volumes while irradiation of very small volumes (<25% total lung volume) had no consequences despite very high doses used. This has implications for the clinical radiotherapy because both approaches, i.e. low dose distributions over large lung volumes as well as concentration of high doses into limited areas, have been adopted in the struggle to deposit maximum radiation energy in the tumour. Remarkably, low doses in our study inflicted different kind of damage than high doses. The low dose damage appeared early and tended to resolve after 3 months while the high dose damage and its symptoms tended to progress over time. We linked the former to injured pulmonary vessels and the latter to injured cells of parenchyma. To our knowledge, this was first such categorization of acute radiation-induced lung injury into two separate units.

This thesis has contributed several new insights into the processes that control the development of respiratory symptoms after radiotherapy for thoracic tumours. These insights may potentially improve the accuracy of predicting the risk of side effects in radiotherapy patients and thus allow selection of those who will benefit from increasing the dose to their tumours. The need for reliable predictive tools gains even more urgency now when aggressive radiation techniques producing extreme dose distributions, i.e. the intensity modulated radiation therapy and proton beam radiotherapy, are being introduced.

Samenvatting

Bij de behandeling van in de thorax gelegen tumoren speelt radiotherapie een grote rol. De hiervoor gebruikte straling wordt afgegeven door een bron (een lineaire versneller) buiten het lichaam en moet vervolgens de huid en andere weefsels doordringen om de tumor te bereiken. Absorptie van de energie afgegeven door de straling zorgt voor beschadigingen in levende cellen, wat kan leiden tot celdood of het onvermogen tot celdeling. Ondanks dat moderne bestralingstechnieken ontworpen zijn om de dosis stralingsenergie optimaal in de tumor af te geven, komt er toch een hoeveelheid straling in de omliggende normale weefsels terecht. Dit kan schade veroorzaken aan deze weefsels en aanleiding geven tot gevaarlijke bijwerkingen. Vooral longkanker is hierdoor erg moeilijk te behandelen, omdat de long erg gevoelig is voor de effecten van straling. Longkanker is de derde meest voorkomende kanker in Europa en de meest voorkomende oorzaak van kankersterfte, verantwoordelijk voor 1/5 van het totale aantal overledenen. De meeste gevallen van longkanker worden histologisch geclassificeerd als niet-kleincellig longcarcinoom (NKCLC). Voor patiënten met locaal uitgebreide tumor waarbij chirurgische resectie uitgesloten is, is de behandeling met radiotherapie in combinatie met chemotherapie de enige hoop op genezing. Ondanks deze behandeling sterft de meerderheid van de patiënten binnen 2 jaar na diagnose. Dit komt doordat de dosis die nodig is om NKCLC te vernietigen erg hoog is, terwijl het geven van een dergelijke dosis zonder dat het vitale omliggende weefstel (longen, slokdarm, ruggenmerg en hart) wordt beschadigd technisch erg moeilijk zo niet onmogelijk is.

Zoals hierboven al beschreven is vooral de long is erg gevoelig voor de effecten van straling. Met een toenemende long volume en dosis in het gezonde longweefsel neemt de kans op complicaties toe. Op een gegeven moment wordt het risico op toxiciteit onacceptabel wat de dosis die gegeven kan worden aan de tumor limiteert, waardoor de ziekte incurabel wordt. Pulmonale complicaties kunnen onderverdeeld worden in 2 syndromen – een acute stralings-pneumonitis (longontsteking) welke optreedt binnen 1-4 maanden na bestraling en een chronische

pulmonale fibrose (litteken vorming) welke kan optreden jaren na de behandeling. Beide complicaties verstoren de structuur, gas uitwisseling en bloedcirculatie in de gezonde long. Dit resulteert in kortademigheid, die soms behandeling behoeft, maar ook ziekenhuisopname en zelfs de dood tot gevolg kan hebben. Een op de 5 patiënten ontwikkelt deze symptomen bij een behandeling met conventionele bestralingsdoses (b.v. 60 Gy in dagelijkse fractie over 6 weken) die overigens meestal onvoldoende zijn om de ziekte te genezen. Om die reden wordt er onderzoek verricht naar manieren om veilig een hogere (geëscaleerde) dosis straling aan long tumoren te geven, waarbij gebruik gemaakt wordt van 3 dimensionale conformal radiotherapie (3D-CRT). Deze techniek levert computer modellen van de vorm en locatie van de tumor en de omliggende weefsels van iedere individuele patiënt. Verder geeft het van elk specifiek bestralingsplan weer hoeveel energie (dosis) er in de tumor en het omliggende normale weefsel terecht komt. Hierdoor kunnen verschillende bestralingsplannen met elkaar vergeleken worden, waarna uiteindelijk gekozen kan worden voor het plan met de maximale tumor dosis maar minimale normale long dosis. Verder wordt op deze manier ook informatie verkregen over het volume van het gezonde longweefsel dat tijdens de behandeling een bepaalde dosis ontvangt. Deze gegevens worden vervolgens gerelateerd aan de mate waarin pulmonale complicaties later in de patiënt optreden. In vele studies zijn longpatiënten vervolgd na de radiotherapie om uit te zoeken welke doses op welk longvolume veilig zijn en welke te veel risico met zich meebrengen. Kunnen we nu nauwkeurig bepalen wie profiteert van een geëscaleerde dosis op de tumor en wie zal onacceptabele toxiciteit ontwikkelen? Helaas is de conclusie "NEE". Alleen de informatie over het bestraalde longvolume en longdosis geeft geen betrouwbare voorspellingen over de veiligheid van een behandeling. Dit gegeven staat de verbetering van genezingspercentages en overleving van NKCLC in de weg.

Daarom wordt er onderzoek gedaan naar additionele factoren die kunnen helpen met het bepalen van de relatie tussen risico's van stralingsdosis escalatie in longkanker patiënten. Dit proefschrift beschrijft een onderdeel van deze inspanningen. In **Hoofdstuk 2** hebben we de mogelijkheid onderzocht of bepaalde eiwitten die door het menselijk lichaam geproduceerd worden mogelijk de ontwikkeling van stralingsgeïnduceerde long schade versterken. Deze eiwitten worden cytokines genoemd en dienen als communicatie signalen tussen cellen. Een van deze cytokines, *transforming growth factor β* (TGF-β), heeft de controle over ontstekingsreacties,

wondgenezing en weefselheling en induceert litteken vorming (fibrose). Het speelt een belangrijke rol in de reactie van longweefsel na blootstelling aan straling, maar wordt ook afgegeven door tumoren, vaak in excessieve hoeveelheden. Sommige studies hebben TGF-β spiegels in longkanker patiënten gerelateerd aan een grotere kans op ernstige stralingsschade aan de long. Wij hebben geprobeerd deze effecten te bevestigen in longkanker patiënten die behandeld werden in het Universitair Medisch Centrum Groningen. Wij vonden slechts een zwakke relatie tussen pulmonale complicaties en de stijgende TGF-β spiegels midden in de 6 weken durende radiotherapie behandeling, maar niet voorafgaand of daarna. We hebben geconcludeerd dat deze stijging in het midden van de behandeling toe te schrijven is aan de productie van het cytokine door het beschadigde longweefsel en dus de mate van schade weergeeft. Helaas geeft deze waarde geen nauwkeurige voorspelling in alle patiënten en bleek dus niet voldoende duidelijk te zijn waardevol voor routine gebruik in het ziekenhuis.

Sommige studies rapporteren dat bestraling van bepaalde gebieden in de long leidt tot ernstigere complicaties dan bestraling van andere gebieden. Dit zou betekenen dat bestraling van de tumor uit bepaalde richtingen (door de stralingsgevoelige long gebieden) meer risico's met zich mee zou kunnen brengen dan bestralingen uit andere richtingen. Wij hebben onderzocht hoe de ademhalingsfunctie van ratten beïnvloed werd door bestraling van verschillende long regio's (met hetzelfde volume en dosis, andere locatie) (**Hoofdstuk 3**). We vonden inderdaad dat bestraling van longregio's die het meeste longparenchym (het sponzige gedeelte waar de gasuitwisseling plaatsvindt – zonder grote luchtwegen te bevatten) en/of de regio's waarbij het hart in het bestralingveld ligt (waarbij het hart meebestraald wordt) de grootste negatieve invloed had op de ademhaling van de dieren. Dit was verassend omdat het hart traditioneel beschouwd wordt als stralingsresistent en waarbij de schade na bestraling pas vele jaren later tot expressie komt. Een additionele studie met zeer precies gerichte bestralingen met een protonen bundel was dan ook noodzakelijk om te bevestigen dat meebestralen van het hart werkelijk verantwoordelijk was het verhoogde risico of ademhalingsproblemen na een gecombineerde hart/long bestraling in de rat, niet alleen in de late fase maar ook al binnen de eerste 3 maanden na behandeling (**Hoofdstuk 4**). Interessant genoeg hebben verschillende klinische studies sindsdien aangegeven dat ook in de mens meebestralen van het hart inderdaad een van de meest belangrijke factoren is die de kans op acute complicaties bepaalt.

Dit gegeven zou op grote schaal getest moeten worden om in de nabije toekomst geïncorporeerd te worden in multiparameter voorspellende modellen.

Straling-geïnduceerde ademhalingsproblemen komen voort uit beschadigingen aan de structuren van in de thorax gelegen organen. Computer tomografie (CT) is een middel dat ons in staat stelt om afbeeldingen te maken van niet beschadigde longstructuren. CT maakt gebruik van traditionele röntgenstralen, maar produceert 2-dimensionale beelden van een plak in het lichaam van de patiënt. In bijna alle patiënten worden op enig moment na radiotherapie beschadigde longstructuren gezien, maar slechts enkelen worden daar ook werkelijk ziek van. In **Hoofdstuk 5** hebben we geprobeerd om een antwoord te krijgen op de vraag, wanneer deze structurele beschadigingen werkelijk het signaal geven voor het optreden van klinische symptomen, zijnde ademhalingsmoeilijkheden bij de patiënt. Weer gebruikten we hiervoor ratten als een experimenteel model, waarbij verschillende regio's van de long bestraald werden en vervolgens CT-scans gemaakt werden en ademhalingsfrequenties gemeten. We ontwikkelden een methode om objectieve meting (kwantificering) te verrichten van de op de CT-scan zichtbare afwijkingen. De meest robuuste relatie tussen in de CT-scan getoonde afwijkingen en de verminderde ademhaling werden gevonden na laterale long bestralingen (van beide zijkanten van de long) met een maximale hoeveelheid longparenchym, maar geen luchtwegen of hart in het veld. In overeenstemming met onze eerdere bevindingen bleek dat schade aan het parenchym de grootste invloed had op de respiratoire functie, terwijl andere factoren zoals hart bestraling geen rol speelden. Dit suggereert dat ook in mensen, de symptomen voortkomen uit structurele veranderingen in parenchym-rijk en goed geventileerde long regio's die het belangrijkst zijn voor de gas uitwisseling. De bruikbaarheid van onze methode om CT beelden te kwantificeren zou getest moeten worden in een klinische setting.

In **Hoofdstuk 6**, zijn we verder gegaan met het onderzoek aan *dosis-volume effecten* van longbestralingen. Door steeds grotere volumes van de rattenlong te bestralen met steeds lagere doses, hebben we geprobeerd om te bepalen wat de drempel waarde voor het induceren van respiratoire complicaties is. Hierbij kwamen we tot de interessante conclusie dat zelfs een erg lage dosis gespreid over een groot volume een risico op complicaties met zich meebracht, terwijl bestraling van een klein volume (<25% van het totale long volume) geen enkele consequentie had ondanks de gebruikte zeer hoge doses. Deze bevinding heeft mogelijk implicaties

voor de klinische radiotherapie aangezien beide manieren van bestraling, zijnde een lage dosis op een groot volume zowel als een hoge dosis op een beperkt gebied, gebruikt worden om een maximale dosis stralingsenergie in de tumor te krijgen. Opmerkelijk genoeg veroorzaakten lage doses op een groot long volume een ander soort schade dan hoge doses. De schade bij lage doses kwam vroeg tot expressie, , en leek na 3 maanden te verdwijnen, terwijl bij hoge doses de schade en bijkomende symptomen juist toenamen in de tijd. De eerste kon in verband gebracht worden met schade aan de pulmonale bloedvaten en de laatste met schade aan cellen van het longparenchym. Tot voor zover onze kennis strekt is dit de eerste categorisatie van acute stralingsgeïnduceerde schade in twee verschillende fenomenen.

Dit proefschrift heeft verschillende nieuwe inzichten voortgebracht in de processen betrokken bij de ontwikkeling van respiratoire symptomen na radiotherapie van in de thorax gelegen tumoren. Deze inzichten zouden kunnen bijdragen aan het verbeteren van de nauwkeurigheid van de voorspelling op het risico van bijwerkingen in met radiotherapie behandelde patiënten. Ook zouden deze inzichten het mogelijk kunnen maken om patiënten te selecteren die het meest profiteren van dosis-escalatie. De noodzaak om betrouwbaar voorspellende modellen verder te ontwikkelen is des te meer van belang omdat op dit moment agressieve bestralingstechnieken geïntroduceerd worden zoals intensiteit gemoduleerde radiotherapie en radiotherapie met protonen.

Acknowledgements

My thesis is written and I can look back on the years of my professional carrier that led me to this point. During those years, I encountered a number of people that introduced me to the principles of clinical work and/or research, who formed my opinions and channeled my efforts, and to whom credit belongs for my today's achievement. Chronologically, I first have to thank Prof. Jitka Abrahámová, MD, PhD, who inspired me, a medical student, to become a radiation oncologist. Later, when I worked under her leadership, she toughed me the fundaments of both the clinical work and clinical research and greatly supported my academic growth and aspirations. I am also thankful for meeting the Nestor of Czech Radiation Therapy and Biology, Prof. Jiří Zámečník, MD, PhD, during my postgraduate training in Prague. He introduced me to the realm of radiation biology, the discipline I fell for. This passion was further expanded thanks to Prof. Klaus-Rudiger Trott, MD, PhD, who trusted in me and gave me the chance to attend a MSc course in radiation biology at the University of London. This course, supported by the European Commission and headed by Prof. Trott, was one of the most exciting and electrifying experiences in my life. During the course, I was also able to test my potential for laboratory research in practice. This was in Dresden, Germany, under a leadership of Prof. Michael Baumann, MD, PhD, whose scientific excellence and friendly approach became a great example to me. I was lucky to meet these same qualities also in my next bosses, Prof. Harm H. Kampinga, PhD and Rob P. Coppes, PhD, at the University of Groningen, the Netherlands. The content of this thesis was created under their leadership. I thank them both for their scientific guidance, humane understanding and unrelenting support during those hard years of work that have changed me from a clinician to a lab researcher.

But my work would likely have been much harder and frustrating without the colleagues at the labs of Radiation and Stress Cell Biology and Stem Cell Biology, University Medical Center Groningen. Their selfless advice and help and disarmingly honest, caring personal attitude formed the greatest impressions I carry in me forever. I would like to remember some in particular: Willy Lemstra, Maria van Waarde, Hette Faber, Bart Kanon, Femmy Cotteleer, Isabelle Lombaert, Annet Vos, Ody Sibon, Jeanette Brunsting, Bianca Brundel, Ria Hut, Jurre Hageman, Maria Rujano, Leonie Kamminga and, most of all, my friends and paranimfen Martha Ritsema and

Rita Setroikromo. I never before, and never since, met people so open-minded and open-hearted like you. You made me feel at home and I shall never forget it.

I was lucky to meet good friends outside the lab, too. We had such good times with Mark Tuijl, Joanna Rejman, Luc Wasungu, Jan Daciuk, Marjan Boerma, and the "Dutch class bunch" Lucia Nicola, Cristiano Vezzoni and Gregor Socan, that the illusion of student life (going back in time) was almost "real". What a treat when one is over 30...

Regarding my work, I also want to acknowledge the substantial help I got from other Departments in the University Medical Center Groningen (UMCG). I am very grateful to members of the Department of Radiotherapy, UMCG, namely Paul Leferink, Peter van der Hulst, Erwin Wiegman, Haarm Meertens, Mieke van Gameren and Alof Canrinus for their professional help with dosimetry, methodology, collimator design and data collection that was absolutely crucial for successful outcome of our project. From the same Department came also the co-author of most of my articles, Peter van Luijk. His shrewdness in exact sciences compensated my weaknesses. We made up a great team! (I hope he feels the same way...). Histological procedures in our experiments would not be possible without generous help of Harry van Goor, MD, PhD, Department of Pathology, UMCG. Harry provided advice, manpower (dank je, Inge!!!) and an "unlimited" (night-time) access to the essential technology. I cannot thank him enough for having trust in me and the project. I would also like to mention the indispensable guidance I received from the head of the Department of Medical Statistics, Dr. Václav Fidler, regarding the statistical analysis of the data (when those threaten to drown me). Finally, I would like to thank the staff in the computed tomography room of the Radiology Department, UMCG, namely Wim Tukker, for calmly putting up with our regular evening intrusions into their emergency operations (the smell of rats notwithstanding).

Last but not least, I want to thank to both our grandmothers, Nea and Hana, who did not hesitate to repeatedly fly from Czech Republic, across the ocean, to our temporary home in the U.S., to baby-sit Filip and Líza. Without them, this thesis would never been written.

Thanks to all!

Alena April 2009

Curriculum Vitae

Name: Alena Nováková (maiden name: Jirešová)
Date and Place of Birth: June 4, 1969, Prague, Czech Republic

Education and Training:

1987-1994	1st Medical Faculty of Charles University, Prague, Czech Republic
1994	graduation with **Doctor of General Medicine** Diploma
1995-1998	postgradual training in radiation oncology, Postgraduate Medical School in Prague, Czech Republic
1997	Postgradual Diploma in Radiation Therapy
1995	ESTRO Teaching Course: Principles of Radiotherapy and Clinical Research, Prague, Czech Republic
1996	ESO Advanced Course: Medical Oncology, Milano, Italy
1998-1999	Master of Science Course in Radiation Biology, St. Bartholomew's and the Royal London School of Medicine, University of London, U.K. (including a 3-months laboratory research project at the Department of Radiation Oncology, University Hospital Dresden, Germany)
1999	graduation with **Master of Science in Radiation Biology** Degree
2002	ESTRO Teaching Course: Technological Advances in Radiation Oncology, Prague, Czech Republic
1999 – 2003	postgradual courses provided by University Medical Centre Groningen, Institute for Drug Exploration, The Netherlands: Laboratory Animal Science, Publishing in English, Microbiological Safety, Good Manufacturing / Clinical / Laboratory Practice, Techniques of Molecular Biology, Medical Statistics, Modern Analytical Methods in Life Sciences.

Professional Experience:

1994 - 1997	resident and radiation oncologist in training, the Department of Oncology and Radiotherapy, Thomayer Memorial Hospital, Prague, Czech Republic
1997 – 1999	radiation oncologist, the Department of Oncology and Radiotherapy, Thomayer Memorial Hospital, Prague, Czech Republic
1999 – 2003	PhD student at the Department of Radiation and Stress Cell Biology, University Medical Centre Groningen, The Netherlands

Publications:

Jiresova et al: Postnatal neuronal plasticity of the pyramidal cells of CA1 area of the hippocampus as a reaction to neurotoxic damage. Physiol. Res. 1991; 40: 585-593.

Jiresova et al: Dose-region effects in partial irradiation of rat lung. Radiother. Oncol. 2002; 64, Suppl.1: S192 / 626.

Jiresova et al: Loco-regional differences in radiosensitivity of the rat lung. Int. J. Radiat. Oncol. Biol. Phys. 2003; 55: p.490, abstract nr. 117.

Novakova-Jiresova et al: Transforming growth factor-β plasma dynamics and post-irradiation lung injury in lung cancer patients. Radiother. Oncol. 2004; 71:183-189.

Novakova-Jiresova et al: Pulmonary radiation injury: Identification of risk factors associated with regional hypersensitivity. Cancer Res. 2005; 65 (9): 3568-3576.

van Luijk, Novakova-Jiresova et al: Radiation damage to the heart enhances early radiation-induced lung function loss. Cancer Res. 2005; 65 (15): 6509-6511.

van Luijk, Novakova-Jiresova et al: Relation between radiation-induced whole lung functional loss and regional structural changes in partial irradiated rat lung. Int. J. Radiation Oncology Biol. Phys. 2006; 64 (5): 1495-1502.

Novakova-Jiresova et al: Changes in expression of injury after irradiation of increasing volumes in rat lung. Int. J. Radiation Oncology Biol. Phys. 2007; 67 (5): 1510-1518.

Presentations:

Jiresova et al: Ifosfamid in the treatment of advanced or relapsed germ cell tumors. Paclitaxel in the treatment of the advanced testicular tumors. Presented at the Uro-Oncological Symposias, Prague, Czech Republic 1997.

Jiresova et al: Taxanes in the treatment of breast cancer. Presented at the Oncological Symposias, Prague, Czech Republic 1998.

Jiresova et al: Multiparametric assay of tumour microvasculature, perfusion and hypoxia during conventional, hyperfractionated and accelerated radiotherapy in nude mice. Poster presentation at 10. Symposium Experimentelle Strahlentherapie und Klinische Strahlenbiologie, Hamburg, Germany 2001.

Jiresova et al: Volume-region-dose effects in lung irradiation. Presented at the Netherlands Radiobiological Society meeting, Amsterdam, The Netherlands 2002.

Jiresova et al: Dose-volume-region effects in partial irradiation of rat lung. Presented at the 49th Annual Meeting of the Radiation Research Society (abstract P11-103), Reno, USA 2002.

Jiresova et al: Dose-region effects in partial irradiation of rat lung. Presented at the Netherlands Radiobiological Society meeting, The Netherlands, February 2003.

Jiresova et al: Dose-region effects in partial irradiation of rat lung. Poster presentation at the Gordon Research Conference on Radiation Oncology, Ventura, USA, 2003.

Jiresova et al: Dose-volume-region effects in partial irradiation of rat lung. Poster presentation at the 12th International Congress of Radiation Research (abstract P08/1613), Brisbane, Australia 2003.

Travel Grants:

RRS Young Investigator Travel Award for the RRS/NAHS Annual Scientific Meeting, Reno, USA, 2002.

RRS Young Investigator Award for the Gordon Research Conference on Radiation Oncology, Ventura, USA, 2003.

Netherlands Radiobiological Society Klaas Breur Travel Grant for the 12th ICRR, Brisbane, Australia, 2003.

Language Skills:

English - TOEFL score 630, January 1993; FCE University of Cambridge Local Examinations Syndicate, grade **A**, 1997

Russian - passive knowledge

Dutch – limited communication skills

April 24, 2009 Alena Nováková, MD, MSc